Optics and Fluid Dynamics Department annual progress report for 2000

Hanson, Steen Grüner; Johansen, Per Michael; Lynov, Jens-Peter; Skaarup, Bitten

Publication date:
2001

Document Version
Publisher's PDF, also known as Version of record

Optics and Fluid Dynamics Department
Annual Progress Report for 2000

Risø-R-1227(EN)

Edited by S.G. Hanson, P.M. Johansen, J.P. Lynov and B. Skaarup

Risø National Laboratory, Roskilde, Denmark
May 2001

Abstract The Optics and Fluid Dynamics Department performs basic and applied research within three scientific programmes: (1) optical materials, (2) optical diagnostics and information processing and (3) plasma and fluid dynamics. The department has core competences in: optical sensors, optical materials, optical storage, biooptics, numerical modelling and information processing, non-linear dynamics and fusion plasma physics. The research is supported by several EU programmes, including EURATOM, by Danish research councils and by industry. A summary of the activities in 2000 is presented.

ISBN 87-550-2794-6 (Internet)
ISSN 0106-2840; ISSN 0906-1797

Contents

1. Introduction 7

2. Optical materials 9

2.1 Introduction 9

2.2 Polymer technology 10
2.2.1 Fabrication of 3D holograms in plastic items 10
2.2.2 A new plotter for small structures - the Nanoplotter 11
2.2.3 A set-up for production of polymer films by laser ablation 12

2.3 New laser systems 13
2.3.1 A new high-power 1.5 μm laser diode system for biomedical applications 13
2.3.2 A new diode laser system for the graphic industry 15

2.4 Polymers and optical storage 16
2.4.1 Photoinduced surface modification of azobenzene polyesters 16
2.4.2 Rewritable holographic memory card system 17
2.4.3 Light induced chiral structure in azobenzene containing polymers 18
2.4.4 Molecular reorientation dynamics in dye-containing polymers 18

2.5 Nonlinear dynamics 19
2.5.1 Photorefractive critical phenomena 19

2.6 Functional materials 20
2.6.1 Fabrication of doped, transparent semiconductor films 20
2.6.2 Ion probe array diagnostics of pulsed laser plasmas 21
2.6.3 Stem thickness determination and cutting of plants by lasers 22

3. Optical diagnostics and information processing 24

3.1 Introduction 24

3.2 Medical optics 25
3.2.1 True-reflection imaging algorithm for optical coherence tomography (OCT) 25
3.2.2 Monte Carlo simulations of an OCT set-up 26
3.2.3 Coherence tomography using measurements of Wigner phase-space distributions: a theoretical analysis 28
3.2.4 Photoacoustic imaging for medical applications 28
3.2.5 A new diode laser system for photodynamic therapy 30
3.2.6 FT-IR spectrometry for biological and medical applications 31

3.3 Infrared technology 32
3.3.1 Modelling of gaseous spectra in the AEROPROFILE project 32
3.3.2 Infrared temperature calibration 33

3.4 Phase contrast techniques 34
3.4.1 Generalised phase contrast and programmable phase optics 34
3.4.2 Polarisation encoding with spatial light modulators 36
3.4.3 Polarisation encoding for high-speed optical encryption 37
3.4.4 Programmable optical tweezers 39

3.5 Optical measurement techniques 40
3.5.1 Laser anemometry for control and performance testing of wind turbines 40
3.5.2 The angular encoder 42
3.5.3 Partially developed speckle 43
3.5.4 Zeptor – an input device for PCs 44
3.5.5 Characterisation of light sources 45

3.6 Knowledge-based processing 47
3.6.1 Machine learning techniques 47

4. Plasma and fluid dynamics 49

4.1 Introduction 49

4.2 Fusion plasma physics 49
4.2.1 Taming drift-wave turbulence 49
4.2.2 Comparison of simulations with simple plasma experiments 51
4.2.3 Benchmarking 3D codes of drift-Alfven turbulence 51
4.2.4 Anomalous diffusion of particles and the relation to transport in vortex-dominated turbulence 52
4.2.5 Turbulent equipartition and dynamics of transport barriers in electrostatic turbulence 53
4.2.6 Shear flow stabilisation of pressure driven flute modes 55
4.2.7 Reynolds stress and shear flow generation 56
4.2.8 Upgrade of and measurements using the LOTUS diagnostic 58
4.2.9 Density fluctuation measurements in the Mega Amp Spherical Tokamak 60
4.2.10 Global perspective of Denmark's energy research 61
4.2.11 Pellet injectors 62

4.3 Fluid dynamics 62
4.3.1 Formation of large-scale flows in rotating fluids by forced homogenisation of potential vorticity 62
4.3.2 Finite time singularities in a class of hydrodynamic models 64
4.3.3 Bathtub vortices 64
4.3.4 Two-dimensional turbulence in bounded flows 65
4.3.5 Comparison between finite difference and spectral schemes 66
4.3.6 Evolution of the vorticity-area density 67
4.3.7 Numerical and experimental studies of particle dynamics in flow channels 68
4.3.8 Periodically driven shear flows 69
4.3.9 Turbulent shell models 70
4.3.10 Fractal induced turbulence 70

4.4 Optics and acoustics 71
4.4.1 Modulational instability and collapse dynamics in media with nonlocal nonlinearities 71
4.4.2 Nonlinearity and disorder: classification and stability of nonlinear impurity modes 71
4.4.3 Collapse dynamics of attractive Bose-Einstein condensates 72
4.4.4 Classical and quantum properties of spatio-temporal structures in optical second-harmonic generation 73
4.4.5 Experimental observation of self-pulsing in singly resonant optical second-harmonic generation 74
4.4.6 Three-dimensional analysis of diffractive optical elements 76
4.4.7 Fast and accurate analysis of waveguide grating couplers using a boundary variation method 77
4.4.8 Numerical investigations of wavelength division multiplexing components 78
4.4.9 Pseudospectral modelling of ultrasonic wave propagation 79
4.4.10 Laser-ultrasonic monitoring of industrial processes 81

5. Publications and educational activities 82

5.1 Optical materials 82
5.1.1 International publications 82
5.1.2 Danish publications 83
5.1.3 Conference lectures 83
5.1.4 Publications for a broader readership 83
5.1.5 Unpublished Danish lectures 84
5.1.6 Unpublished international lectures 84
5.1.7 I nternal reports, including patent applications 86

5.2 Optical diagnostics and information processing 86
5.2.1 International publications 86
5.2.2 Danish publications 87
5.2.3 Conference lectures 87
5.2.4 Publications for a broader readership 89
5.2.5 Unpublished Danish lectures 89
5.2.6 Unpublished international lectures 90
5.2.7 Internal reports, including patent applications 91

5.3 Plasma and fluid dynamics 92
5.3.1 International publications 92
5.3.2 Danish publications 92
5.3.3 Conference lectures 93
5.3.4 Publications for a broader readership 93
5.3.5 Unpublished Danish lectures 93
5.3.6 Unpublished international lectures 94
5.3.7 Internal reports 96

6. Personnel 97

1. Introduction

J. P. Lynov
E-mail: jens-peter.lynov@risoe.dk

The Optics and Fluid Dynamics Department performs basic and applied research in optical sensors and optical materials as well as in plasma and fluid dynamics. The research is conducted as a combination of science and technology with the following core competences:

- Optical sensors
    - Light propagation in complex systems
    - Laser-based sensors
    - Diffractive optical components
    - Phase contrast methods
- Optical materials
    - Polymers
    - Laser ablation
- Optical storage
    - Holographic techniques
    - Optical encryption
- Biooptics
    - Light/tissue interaction
    - Diode laser systems
    - Biosensors
    - Optical tweezers
    - IR spectroscopy
- Numerical modelling and information processing
    - Plasma and fluid dynamics, optics, ultrasound
    - Knowledge-based processing
    - Image processing ("data mining")
- Non-linear dynamics
    - Turbulence
    - Vortex dynamics
    - Parametric processes
    - Photorefractive materials
- Fusion plasma physics
    - Theoretical plasma physics
    - Laser diagnostics

The output from the research activities is new knowledge and technology. The users are within industry, research communities and government, and the department is responsible for the Danish participation in EURATOM's fusion energy programme.

For the solution of many of the scientific and technological problems the department employs the following key technologies:

- Microtechnology for optical systems
    - Analogue and digital laser recording of holograms
    - Injection moulding of diffractive optical elements
- Optical characterisation
    - Determination of material surfaces
    - Phase contrast measurements
- Temperature calibration and IR measurement techniques
    - Accredited temperature calibration
    - Fourier transform infrared (FTIR) measurements

The department is organised in three scientific programmes:

- Optical materials
- Optical diagnostics and information processing
- Plasma and fluid dynamics

In the following sections, the scientific and technical achievements during 2000 for each of these programmes are described in more detail.

2. Optical materials

2.1 Introduction

P. M. Johansen
E-mail: per.michael.johansen@risoe.dk

The development towards more technologically driven research has continued during the year 2000 and has resulted in the establishment of a technological platform that is capable of evolving diffractive optical elements as an alternative to classical optical systems. The same technique is also used to develop various holographic verification elements. The platform encompasses the entire range of techniques needed for injection moulding of optical elements. The first part uses a computer to design the optimum set-up for recording an optical master in a light-sensitive polymer. The second step is the actual recording on the polymer. This is accomplished using either analogue recording in a conventional holographic set-up, or digital recording using a custom-built nanoplotter. Having finished the optical master, the production of a nickel shim is made via galvanisation. The nickel master is now inserted into a so-called mould to be inserted into a conventional injection-moulding machine. This technological platform has already proved its value in several industrial and international projects.

In addition to the technological polymers used to manufacture the optical elements above, we have also implemented a new deposition technique for depositing thin uniform layers of different polymers based on matrix-assisted pulsed laser evaporation.

The development in the field of new laser systems has also been successful during 2000. A high-power 1.5 μm laser diode system for biomedical applications has been produced. Moreover, a diode laser system with diffraction-limited output for the graphic industry has been fabricated. The system has been designed with a feedback system that forces the high-power laser diode to oscillate in a single transverse mode with a conversion efficiency of more than 80%.

The field of active polymers has resulted in photoinduced surface modification in azobenzene polyesters. Such surface changes have been induced using both a transmission mask and a single focused beam. In addition, the field of optical storage has obtained impressive results. The storage properties of micron-thin azobenzene side-chain polyester films have been examined using polarisation holographic measurements. The aim of the research is to fabricate a rewritable holographic memory card system using parallel object and reference beams. The work is performed in close collaboration with an industrial company. In addition, a light-induced chiral structure in azobenzene containing polymers has been studied using circularly polarised light @488 nm. The response of PMMA doped with disperse red chromophores subject to external ac and dc electric poling fields has also been investigated. The response is determined by the capability of the chromophores of reorienting in the polymer matrix, a process which is highly dependent on temperature.

Nonlinear dynamics has been concentrated on studying photorefractive critical phenomena. Such effects are found in experiments where both the material and the optical nonlinearities are at play at the same time and result in bifurcation in the gain as a function of contrast.

The work in the field of functional materials has been concentrated on fabrication of doped transparent semiconductor films, ion probe array diagnostics of pulsed laser plasmas, stem thickness determination and cutting of plants by lasers. In the first project a set-up has been

constructed which enables us to dope the semiconductor films with metals during the laser-assisted deposition. The second project is an integral part of a project funded by the EU, and it aims at making the laser plasma deposition controllable by measuring the ion current from selected components. The last project aims at understanding the process of laser cutting of plant tissue for weed control and is important to non-chemical agricultural production of crops.

The results obtained during the past year again attest to a vital research programme that undergoes rapid changes towards technologically driven research. The staff in the programme have gone beyond the limit in many cases to ensure fruitful collaboration with industry and, at the same time, maintain a very high scientific level.

2.2 Polymer technology

2.2.1 Fabrication of 3D holograms in plastic items

S. Højgaard Jensen, H. Pedersen and J. Stubager
E-mail: henrik.pedersen@risoe.dk

Recently, there has been a growing interest in fabrication of true 3D image holograms in injection moulded plastic objects. One aim is to use the holograms as a gimmick in the marketing of plastic products, another aim is to put user information into the hologram and, finally, perhaps the most important aim is to avoid counterfeiting of the product. As an initial test, we have tried to injection mould a true 3D image hologram of a toy sheep in small polycarbonate chips.

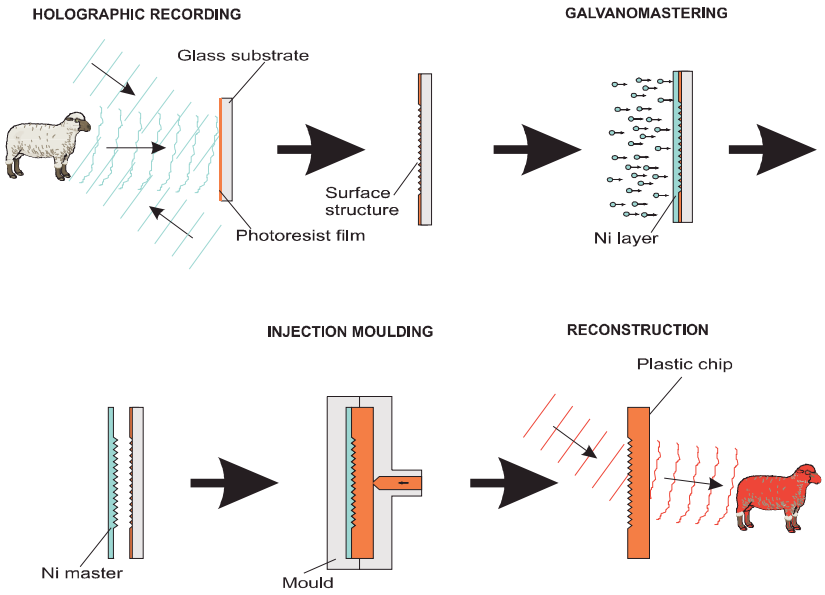

Figure 1. The manufacturing process of injection moulded 3D holograms.

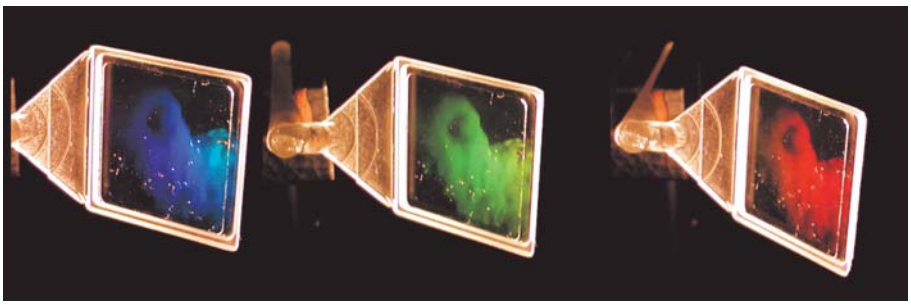

Figure 2. Pictures taken of three polycarbonate chips that show a white-light reconstructed toy sheep in three different colours.

The procedure of fabricating the holograms is shown schematically in Figure 1. The image of the sheep is first recorded in a photoresist film by letting the object beam that originates from the sheep and a plane reference beam interfere at the film. After development, the glass master is put into a galvanobath in which a thin nickel layer is formed on top of the resist. This nickel plate is then inserted into a plastic injection mould after which replication of the original hologram is formed in the moulded plastic chips. The result is given in Figure 2.

2.2.2 A new plotter for small structures - the Nanoplotter

E. Rasmussen
E-mail: erling.rasmussen@risoe.dk

Eight years ago a new laserplotter called Holoplotter capable of manufacturing diffractive structures and masks was developed[1,2]. The plotter has been used to make diffraction gratings, computer-generated holograms and diffractive optics. In general, the main objective has been to produce optical elements that cannot be made with traditional refractive optics (lenses) or diffractive optical elements that in one single element can replace several conventional optical elements.

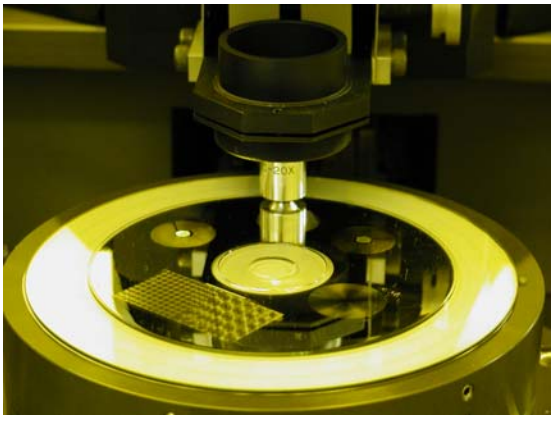

Figure 3. Writing head of the nanoplotter.

A few examples of the application areas of the nanoplotter are the manufacturing of, e.g., specifically designed optical components for two NASA projects, a number of computer-generated holograms for the English research centre DERA, test masks for a Spanish research group, and phase filters for Risø's own research in optical encryption.

The resolution of the holoplotter is down to 2.5 μm. For a number of tasks, however, this resolution is insufficient. For the last couple of years Risø has consequently been developing a

new plotter called Nanoplotter, see Figure 3 and Figure 4. The first tests performed on this plotter have just been completed and the results look quite promising.

During the tests, the following features of the nanoplotter have been observed:

- An 800 nm writing spot may be plotted in a raster with a resolution of less than 100 nm and with a degree of accuracy of less than 40 nm. Two light sources with wavelengths of 633 nm and 442 nm are available. The plotter is capable of plotting at 255 grey scale levels selected from a palette of 4096 grey levels.
- The maximum plot area is circular - Ø160 mm - or square 100 X 100 mm. The writing speed is up to 10 lines pr. sec at 20 megapixels/sec.

Figure 4. E. Rasmussen operating the nanoplotter.

See http://www.risoe.dk/ofd/products%20and%20services/nanoplotter.htm for more information.

1. Optics and Fluid Dynamics Department's Annual Progress Report for 1992, pp. 11-12. ISBN 87-550-1885-8.
2. Optics and Fluid Dynamics Department's Annual Progress Report for 1994, pg. 8. ISBN 87-550-2044-5.

2.2.3 A set-up for production of polymer films by laser ablation

B. Toftmann, A. Nordskov, J. Schou and H. C. Pedersen
E-mail: bo.toftmann.christensen@risoe.dk; j.schou@risoe.dk

The processing of polymer films is of importance to many technological applications, including non-linear optics and sensors. A new deposition technique, known as matrix assisted pulsed laser evaporation (MAPLE), has been developed at the Navel Research Laboratories, USA, for deposition of thin and uniform layers of different polymers.[1]

One of the major advantages of film production by laser ablation is the possibility of sandwiching different materials in the same fabrication process. In the Optics and Fluid Dynamics Department at Risø expertise in transparent semiconducting thin film production already exists and, recently, a set-up for polymer film production by MAPLE has been constructed, see Figure 5. The first preliminary measurements with this set-up have shown that frozen targets can be manipulated under vacuum conditions and in a background gas for many hours.

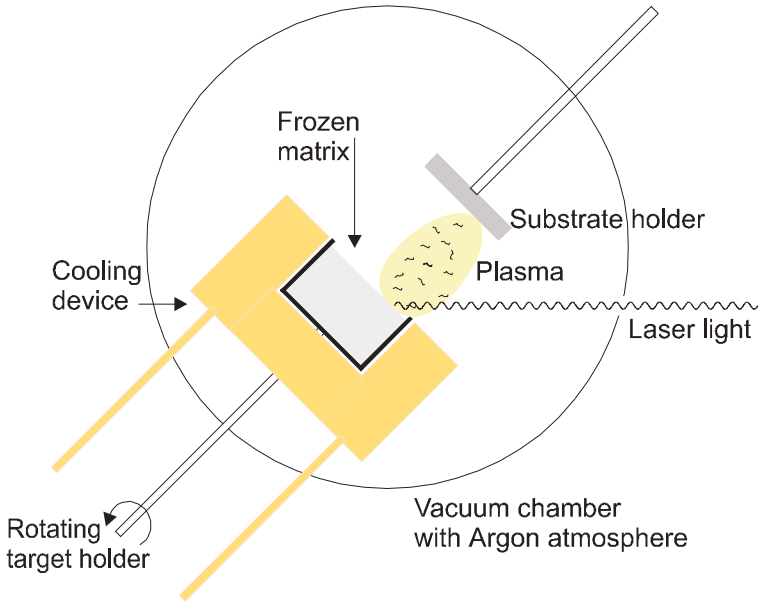

Figure 5. Schematic view of the set-up for polymer film production. The volatile component of the frozen matrix is pumped away, while the polymer molecules create a thin film on the substrate.

1. A. Piqúe, et al., Growth of organic thin films by the matrix assisted pulsed laser evaporation (MAPLE) technique, Thin solid films 355-356 (1999) 536-541.

2.3 New laser systems

2.3.1 A new high-power 1.5 μm laser diode system for biomedical applications

M. Løbel (Giga Intel A/S) and P. M. Petersen
E-mail: paul.michael.petersen@risoe.dk

A high-power 1.5 μm laser diode system for biomedical applications has been developed in an industrial project where the partner is the company GIGA located in Skovlunde, Denmark. GIGA has in-house indium phosphide semiconductor growth and processing facilities. The project is based on the knowledge obtained by Risø through its work with high-power laser diode systems and on the knowledge gathered by GIGA during its work with diodes for the telecom market. The aim of the project has been to develop a new high-power diode for system with a wavelength around 1.5 μm.

The interest in a high-power laser diode based on the InGaAsP semiconductor compound originates from two facts: firstly, the wavelength of an InGaAsP diode can be selected over a very large range (~1.1-1.6 μm); secondly, water has a strong absorption peak within this range centred at 1450 nm. Especially for human skin treatment such as resurfacing and removal of wrinkles and birthmarks is this peak of great interest since the amount of absorption determines the penetration depth in skin. In other words, by adjusting the wavelength of the light source, the penetration depth in the skin can to a large extent be controlled. The absorption and the penetration depth are vital to the efficiency of a given treatment procedure.

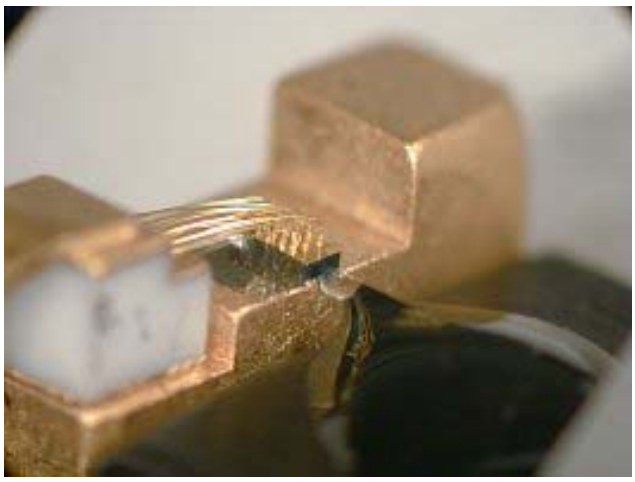

Figure 6. One watt 1480 nm laser diode array with a 100-μm wide emitting region. The diode has been flip-chip mounted on a CuW mount. The light is coupled to a multimode fibre using a simple butt-coupling geometry.

Single laser diode arrays with an emitting region of 100-200 μm have successfully been grown, processed and flip-chip mounted on a CuW heat sink for efficient thermal power dissipation. At the front and back facets, we have applied anti-reflection and high-reflection multilayer coatings, respectively. A laser diode array with an emitting region of 100 μm had a typical output of 700-900 mW at a drive current of 5 amperes. The threshold current was normally 0.5 ampere. Figure 6 shows a fibre-coupled mounted laser diode array.

Figure 7. *3-watt laser system with the lid removed (seen in the upper part of the image). The light from six laser diode arrays is coupled to six multimode fibres that are combined in a fibre bundle.*

Based on the laser diode arrays developed, a high-power laser system for clinical experiments of human skin treatment has been fabricated. Figure 7 presents the system with a fibre delivery of up to 3 watts. The light from six laser diode arrays is coupled to six multimode fibres that are combined in a fibre bundle.

Figure 8 shows the result of the removal of a brown birthmark using the fabricated high-power laser system. The removal was very efficient at even low optical power due to the high absorption coefficient in water at a wavelength of 1480 nm. The clinical experiments were performed by Professor Peter Bjerring at Marselisborg Hospital in Denmark.

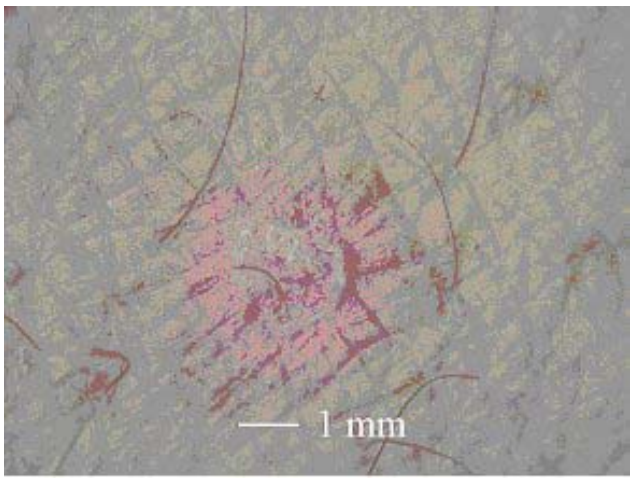

Figure 8. *An example of the removal of a brown birthmark using a 1480 nm light source. The picture was recorded one month after treatment. A 220-mW continuous wave was used for three seconds at a 500-µm large spot.*

2.3.2 A new diode laser system for the graphic industry

P. M. Petersen, S. Juul Jensen and M. Chi
E-mail: paul.michael.petersen@risoe.dk

GaAlAs semiconductor laser diode arrays with an output power exceeding 20 watts are available. These high-power laser diode systems are attractive because they can be operated with a low voltage and, moreover, because they have a lifetime of more than 10,000 hours. The laser diode arrays, however, have a multimode non-diffraction limited outputthat limits their usefulness in many practical applications.

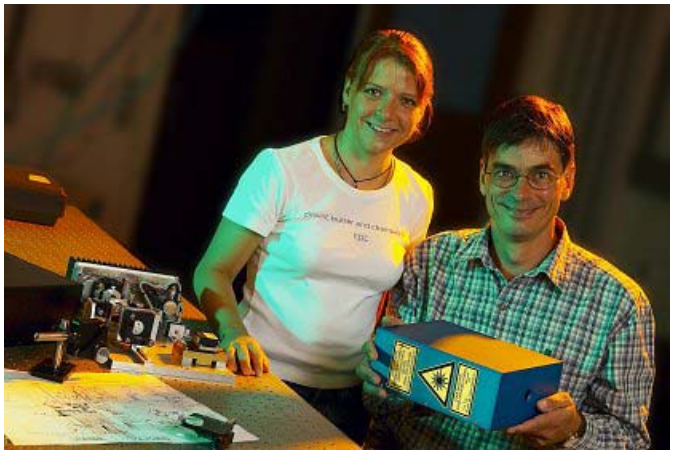

Figure 9. P. M. Petersen and S. Juul Jensen present the first high-power diode laser prototype developed for the printing industry.

In the present project a new laser diode system with a diffraction limited output beam has been developed for applications in the printing industry. The laser diode system has been designed using a new feedback system that forces the high-power laser diodes to oscillate in a single transverse mode with a conversion efficiency larger than 80 %. The strongly improved

spatial coherence properties imply that the diode laser system has an almost diffraction limited output beam that can be focused to a small spot at the size of the wavelength.

Figure 9 shows the first prototype of the laser system developed. Collaboration with the Danish company Purup-Eskofot has been established with the purpose of developing a commercial product for the printing industry based on the new laser diode technology.

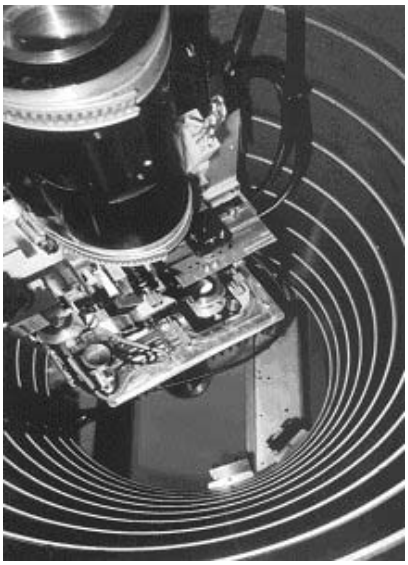

Figure 10. The new prototype laser diode system implemented in the internal drum system of a Purup-Eskofot imag setter machine

The new laser system has been implemented in the Purup-Eskofot internal drum printing system. Due to a low M^2-value of the new high-power laser diode system the output beam can be focused on a small laser spot at the offset plate. Figure 10 demonstrates the prototype of the laser system inserted (upside-down) in the internal-drum image setter machine at Purup-Eskofot. The new prototype laser system meets the requirements for the application in the printing industry in terms of output power stability, pointing stability and M^2-value. Furthermore, we have proved that it is possible to compensate for the severe astigmatism that usually exists in these high-power diode laser systems.

2.4 Polymers and optical storage

2.4.1 Photoinduced surface modification of azobenzene polyesters

P. S. Ramanujam, S. Hvilsted (Technical University of Denmark), M. Helgert, D. Bublitz*, B. Fleck* and L.Wenke* (*Friedrich-Schiller University Jena, Federal Republic of Germany)*
E-mail: p.s.ramanujam@risoe.dk

In several azobenzene polyesters light-induced surface changes have been observed using both a transmission mask and single focused beams. The polyesters differ only in the nature of the substituent on the azobenzene. We have shown that the behaviour of the surface relief is dependent on the substituents. In both the mask and the single-beam experiments, we see "peaks" in the areas irradiated with p-polarized light for the CN, CF_3, CH_3 and F substituent; for the case of Cl substituent, however, we observe valleys (see Figure 11). It is shown that

the nature of the surface relief depends on the intensity of the irradiating beam. Both s and p polarised light produce surface relief. Using a floating drop experiment, we have demonstrate[1] that the drops either expand or contract depending on the polyester architecture. We propose that a photoinduced deformation of the polymer is responsible for the surface relief phenomenon.

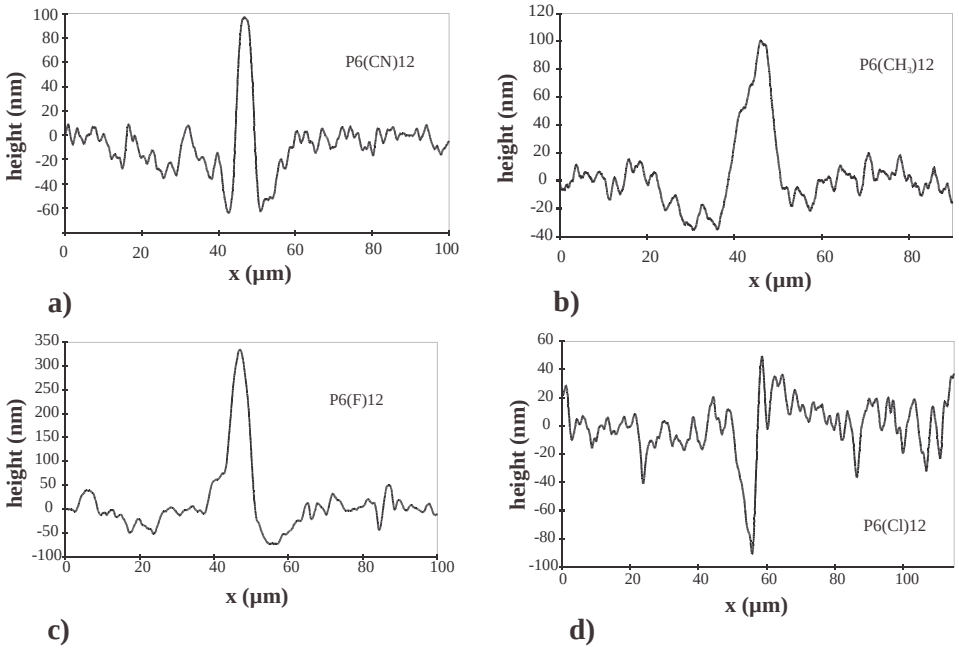

Figure 11. Atomic force microscope scans of azobenzene polyester films with different substituents. The films were irradiated with a single laser beam that was focused by a cylinder lens to a line on the film.

1. D. Bublitz, M. Helgert, B. Fleck, L. Wenke, S. Hvilsted, P. S. Ramanujam, Appl. Phys. B, 70, 863 (2000).

2.4.2 Rewritable holographic memory card system

P. S. Ramanujam, S. Hvilsted (Technical University of Denmark), E. Lörincz, P. Koppa*, F. Ujhelyi*, P. I. Richter* (*Technical University of Budapest, Hungary), G. Szarvas**, G. Erdei** and A. Süto** (Optilink Kft, Hungary, Budapest)*
E-mail: p.s.ramanujam@risoe.dk

The optical storage properties of 1-2 µm thin azobenzene side-chain polyester films on a reflective substrate have been examined by polarisation holographic measurements. The amorphous polyester film is the candidate material for the purpose of a rewritable holographic memory card system using parallel object and reference beams. This type of arrangement can be used advantageously for high-density data storage in connection with polarisation holography when recording is performed by two orthogonally, circularly polarised laser beams, and during reconstruction only one efficiently diffracted beam contains the information[1,2]. The appearance of surface relief causes undesirable higher orders in that case. We have studied temporal formation of anisotropic and topographic gratings for films with and without different types of hard protective layer and have shown that the dominant contribution to the diffraction efficiency comes from the anisotropy in case of realistic expositions well below 1 sec even for high incident intensity.

Angle dependence of diffraction efficiency has also been examined to define the applicable numerical aperture of the optics that determines hologram size and, thereby, achievable primary storage capacity of the system. Multiple writing and erasing cycles demonstrate advantageous rewritable properties of the material.

1. E. Lörincz, F. Ujhelyi, A. Süto, G. Szarvas, P. Koppa, G. Erdei, S. Hvilstged, P. S. Ramanujam, Proceedings of SPIE, vol. 4090, 185 (2000).
2. L. Gazdag, G. Szarvas, G. Erdei, A. Suto, J. Fodor, E. Lörincz, F. Ujhelyi, P. Koppa, P. I. Richter, S. Hvilsted, P. S. Ramanujam, International Symposium on Optical Memory, Technical Digest, p. 150 (2000).

2.4.3 Light induced chiral structure in azobenzene containing polymers

P. S. Ramanujam, S. Hvilsted (Technical University of Denmark), L. Nikolova, L. Nedelchev*, T. Todorov*, Tz. Petrova*, N. Tomova*, V. Dragostinova* (Bulgarian Academy of Science, Sofia, Bulgaria)*
E-mail: p.s.ramanujam@risoe.dk

Large circular anisotropy is induced in unoriented films of side-chain azobenzene polyesters on irradiation with circularly polarised light at a wavelength of 488 nm. The polyester has no chiral groups and is initially isotropic. The photoinduced optical activity has been measured to be $>10^4$ deg/cm, and the circular dichroism has been found to be on the order of 0.3. Experiments have been carried out in both liquid crystalline and amorphous polyesters. Very large rotation of the polarisation azimuth is induced depending on the input ellipticity. The sense of the induced rotation corresponds to the sense of the rotation of the input light electric vector. An analysis of the propagation of elliptically polarised light through the thickness of the film has been carried out.[1] It is shown that an optical axis is induced as a result of the reorientation of the azobenzene chromophores due to the trans-cis-trans isomerisation cycles. This induced optical axis influences the further propagation of polarised light through the film. It is shown that the angle of rotation

$$\theta(z) = (2e\delta/(1-e^2))z,$$

where e is the ellipticity of light, δ is the photoinduced birefringence and z is the thickness of the film.

1. L. Nikolova, L. Nedelchev, T. Todorov, Tz. Petrova, N. Tomova, V. Dragostinova, P. S. Ramanujam, S. Hvilsted, Appl. Phys. Lett. 77, 657 (2000).

2.4.4 Molecular reorientation dynamics in dye-containing polymers

K. G. Jespersen, P. M. Johansen and T. G. Pedersen *(*Aalborg University, Institute of Physics, Denmark)
E-mail: kim.g.jespersen@risoe.dk

Characterisation of the dynamics in optical polymers is crucial to the development of a variety of applications like holographic data storage, electro-optic modulation and light-emitting polymeric devices. Due to low costs, ease of fabrication and freedom in material design, optical polymers are interesting alternatives to crystalline materials. We investigate the response of PMMA doped with Disperse Red chromophores subject to external AC and DC electric poling fields (see, e.g., Figure 12). The response is determined by the reorientation capability for the chromophores in the polymer matrix. A rotational diffusion equation and an

associated diffusion time are believed partly to model the birefringent and electro-optic properties. By including a molecular field to the chromophore environment we can simulate the temperature dependence of the reorientation dynamics. Future research will address the field of active polymers in which reorientation of the active molecules ha been shown to influence the field dependence of electric conductivity and mobility as well as the dielectric frequency response to the poling fields.

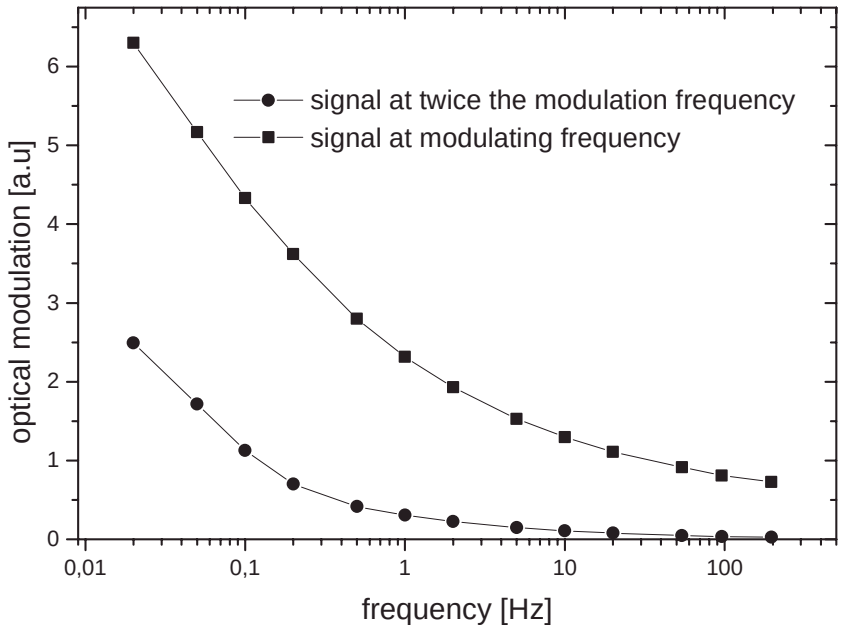

Figure 12. Modulation of an optical probe beam as an AC electric field is applied to the dye-containing polymer. The dye molecules cannot keep up with the electric field modulation at high frequencies.

2.5 Nonlinear dynamics

2.5.1 Photorefractive critical phenomena

P. M. Johansen, H. C. Pedersen, E. V. Podivilov and B. I. Sturman**
*(*Institute of Automation and Electrometry of RAS, Novosibirsk, Russia)*
E-mail: per.michael.johansen@risoe.dk

Most of the nonlinear effects in photorefractive media are caused by photorefractive optical nonlinearity; among such effects are soliton formation and periodic light pattern formation. In explaining these effects the nonlinearity in the material equations for charge separation is usually negligible or of secondary importance. When we deal with spatial subharmonics, however, the material nonlinearity is the governing mechanism in the process of generation, and the optical nonlinearity determines which spatial mode is going to be the final state. In principle this is to be classified as an optical critical effect. Above a certain threshold of contrast in the light interference pattern, $m>m_{th}$, the media response spontaneously loses its

periodicity. This causes new spatial structures to be formed, and in addition to the fundamental spatial frequency, K, and the higher spatial harmonics, $2K$, $3K$, …, new spatial frequencies arise in the Fourier spectrum of the space-charge field; the first to appear is often the $K/2$ subharmonic field. As mentioned above, the material and the optical nonlinearities operate together, and we have shown that the highly different optical and material nonlinearities are strongly hybridised near the threshold of subharmonic generation. The essence of this fact is that the optical and the low frequency eigenmodes are mutually coupled and, as a rule, cannot be separated. The threshold phenomena of the space-charge waves lead to an optical critical phenomenon that manifests itself as a singularity in the rate of spatial amplification for the light waves. In Figure 13 we show the dependence of the spatial amplification on the contrast for a grating spacing of 16 μm.

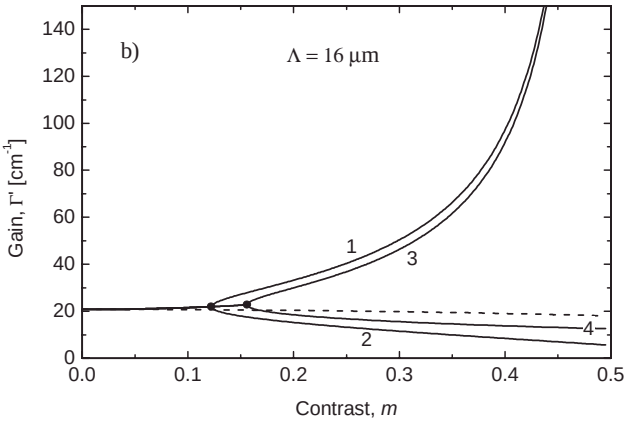

Figure 13. Dependence of the spatial amplification, Γ, on the contrast m.

2.6 Functional materials

2.6.1 Fabrication of doped, transparent semiconductor films

E. Holmelund, B. Thestrup, A. Nordskov, J. Schou, S. Tougaard (Institute of Physics, University of Southern Denmark, Odense, Denmark) and N. B. Larsen (Department of Polymers)
E-mail: j.schou@risoe.dk

Transparent semiconductors are vital materials in the optoelectronic industry because of their transparency to visible light and their relatively small electrical resistivity. Films of, for example indium tin oxide (ITO), are used extensively for liquid crystal displays. Since the supply of indium is limited, search for alternative materials has become increasingly important.

We have constructed a set-up in which it is possible to dope semiconducting films with metals during deposition of the film by pulsed laser deposition. Under normal circumstances the plume particles from intense laser impact on a target are collected on a suitable substrate. During the doping procedure a thin rod of the desired material is moved periodically into and

out of the laser beam like a metronome. The laser-ablated material from the rod is deposited as well on the substrate during normal film deposition. We have achieved concentrations of silver doped into ITO of more than 0.01; see Figure 14. The advantage of the method is that we can change the concentration of the dopant without opening the set-up; we only need to change the exposure time of the rod in the ablating laser beam.

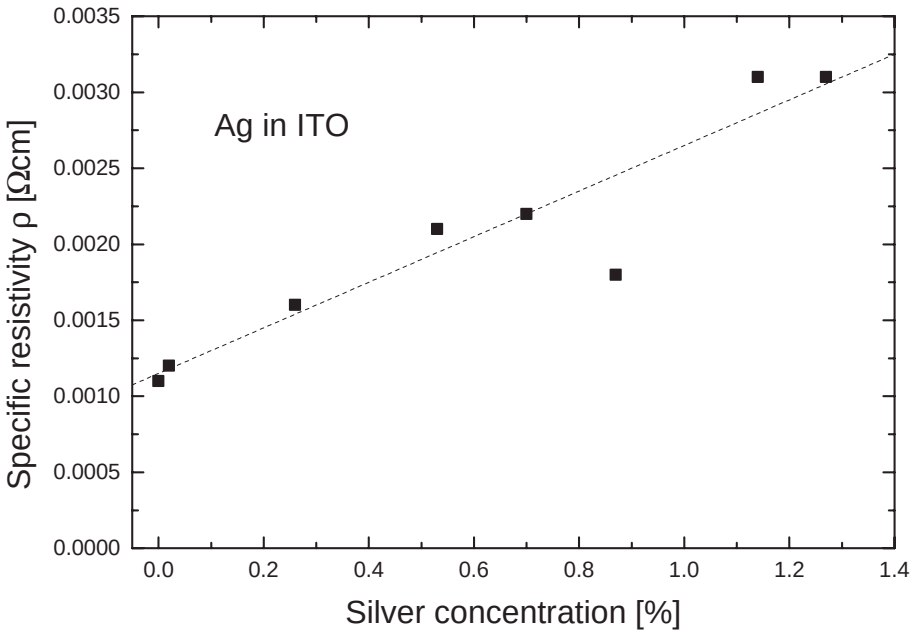

Figure 14 shows the specific resistivity of ITO films doped with silver. The resistivity increases with the concentration since the additional silver atoms lead to increased scattering of the conduction electrons in ITO.

2.6.2 Ion probe array diagnostics of pulsed laser plasmas

B. Thestrup, B. Toftmann, J. Schou, B. Doggett, J. Lunney*, T.N. Hansen* (*Trinity College, Dublin, Ireland) and Y. Shen** (**NKT Research, Copenhagen, Denmark)*
E-mail: birgitte.thestrup@risoe.dk, j.schou@risoe.dk

Thin film deposition by laser ablation has become a standard deposition technique in laboratories – especially for the production of thin films of the high-temperature superconductor YBCO. However, when used in production this technique requires a high degree of reproducibility. The composition and the quality of the deposited films strongly depend on the deposition parameters such as, e.g., the composition and the direction of the ablated plasma plume. One way to control the laser plasma is to provide information about its dynamics, in particular the angular distribution of the ion flux in the plume.

We have used an ion probe array to obtain measurements of the ion current in laser plasmas from selected components. The probe array has proved a useful tool for acquiring detailed information about the dynamics of ions in a laser plasma. The probes are placed in a semi-circular ring 8 cm from the target in the horizontal plane.

Figure 15 shows the angular distribution of the ion current from YBCO ablated in vacuum and in oxygen. The laser beam hit the target with an angle of incidence of 45°. YBCO is used to produce high-temperature superconducting thin films, and the production is typically performed in a background gas of oxygen. As can be seen in the figure, the angular distributions of the integrated current shift toward the laser beam (incident to the right) both in vacuum and at a pressure of 0.01 mbar of oxygen. In addition, introducing an oxygen pressure of 0.01 mbar into the chamber during ablation has a significant effect on the ion plume shape. Such information is important as it may be used as, e.g., an indicator for the position of the substrate during YBCO film deposition.

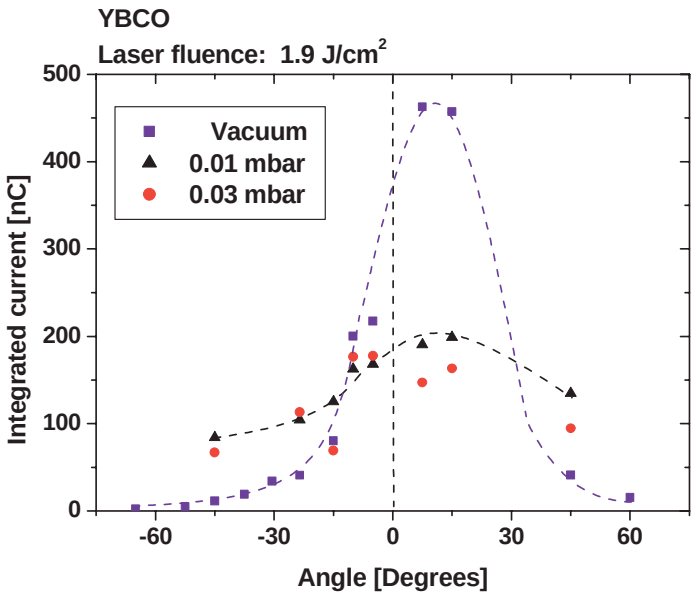

Figure 15. Angular distrubutions of ion current from YBCO ablated at oblique angle of incidence in vacuum and in oxygen.

2.6.3 Stem thickness determination and cutting of plants by lasers

J. Schou, A. Nordskov, T. Heisel and S. Christensen* (*Department of Crop Protection, Research Centre Flakkebjerg)*
E-mail: j.schou@risoe.dk

Laser cutting of plant tissue for weed control is an important issue in non-chemical agricultural production of crops. With a focused laser beam, typically from a CO_2 laser at 10.6 μm, it is possible to cut a stem of the weed *solanum nigrum* L. (black nightshade) as well as of the crop *beta vulgaris* L. (sugar beet) with a scan of the beam within a few seconds. The advantages are: it is a non-contact method (no touching edges of a knife), it can be controlled by a computer system[1] and it can be easily programmed.

The efficiency of laser cutting is obviously related to the thickness of the stem of the plant. We have, therefore, accomplished a program for measuring the thickness of individual plants at different levels of growth by a non-destructive HeNe laser at the wavelength of 632 nm. The shadow of an expanded laser beam shining on a stem was determined by a light diode

system. This turned out to give the correct thickness within 100 μm. Since the stem is a soft, flexible “rod”, it cannot be measured with mechanical tools. Examples are shown in Figure 16.

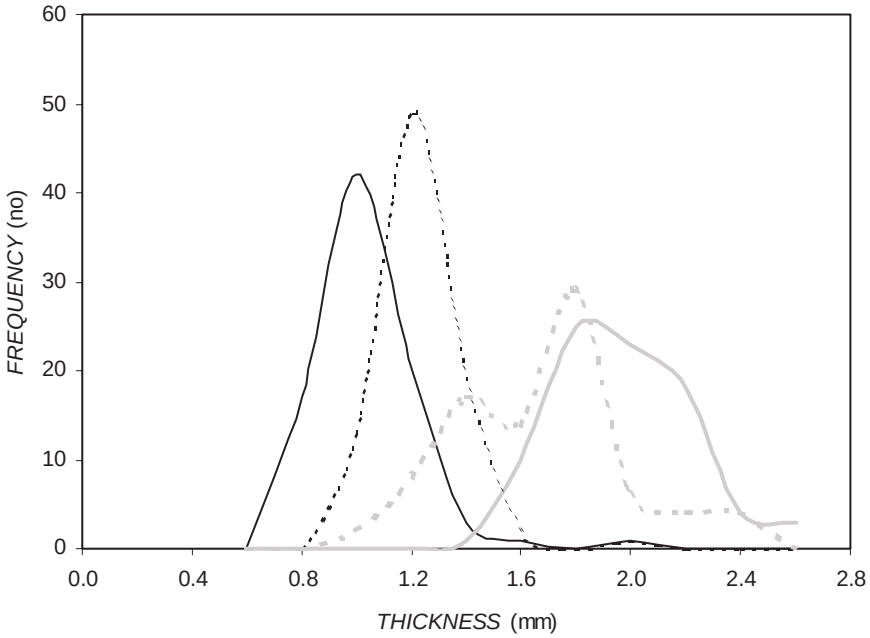

Figure 16. The thickness measurements are shown for both plants *S. nigrum* (full line) and *B. Vulgaris* (dashed line) at two different growth stages: cotyledon (black) and two-true leaf plants (grey).

1. T. Heisel, J. Schou, S. Christensen and C. Andreasen, Weed Research 41, 19 (2001).

3. Optical diagnostics and information processing

3.1 Introduction

S. G. Hanson
E-mail: steen.hanson@risoe.dk

The research conducted in the programme on Optical Diagnostics and Information Processing is centred on the common pivot point of bio-optics. This does not mean that bio-optics is the main research area for the various groups in the programme, but all the scientific groups have shares in this area. In this field, an ongoing mutual programme, Center for Biomedical Optics and New Laser Systems (BIOP), has been performed between the Research Center COM, the Department of Mathematical Modelling and the Department of Physics (Optics Group), all from the Technical University of Denmark, and the Optics and Fluid Dynamics Department at Risø. Within the framework of BIOP, a lecture programme has successfully been carried out at the Technical University of Denmark. A so-called talent project funded by the Danish Technical Research Council in bio-optics has commenced, and a basic theoretical article on optical coherence tomography has been offered to the optical community.

Two patents issued by the group working with knowledge-based processing have been acquired by the Danish company, Intellix A/S, which has by now implemented the protected algorithms in their software. This is yet another example in which knowledge acquired during basic scientific work reveals itself as being of industrial importance.

The achievements in an ongoing three-year talent project funded by the Danish Technical Research Council has been recognised by the Danish Optical Society; Jesper Glückstad was awarded the annual prize of the Danish Optical Society for outstanding performance for a young scientist. Besides, the ideas of using the phase contrast scheme for optical encryption have been included in a large project with the company Optilink within the frame of a big common project with the department. Finally, a Ph.D. project aiming at using the basic concepts has been launched. Using the basic feature that the phase contrast scheme can create practically arbitrary patterns of light dynamically almost without sacrificing the power of the laser lends itself open for use in optical tweezers. Here an arbitrary number of traps can be created and independently positioned in the observation plane. The use in fluorescence microscopy and in cell sorting is obvious.

The work on miniaturisation of optical sensors based on speckle phenomena has been sustained and two industrial developments are on the verge of being disclosed, both of which rely on protected concepts. Part of the future work will be conducted together with various national industrial academic partners within a project called MINOS (Miniaturisation of Optically Based Sensors) funded by Sensor Technology Center A/S established in connection with the sensor initiative of the Danish Agency for Trade and Industry.

The use of low-resolution, but high-speed Fourier transform infrared spectroscopy (FTIR) for analysing exhaust composition from jet engines has continued within the EU-project, AEROPROFILE. To take the field of infrared technology forward, steps have been taken to establish an accredited laboratory for infrared temperature calibration. This mission will be offered to the community in the middle of 2001 in addition to the ongoing task of performing accredited temperature calibration.

A series of measurements on furnaces and incinerators with respect to emission and control of performance parameters has been undertaken as contractual work alongside with other responsibilities.

3.2 Medical optics

3.2.1 True-reflection imaging algorithm for optical coherence tomography (OCT)

L. Thrane, T. M. Jørgensen, P. E. Andersen and H. T. Yura (Electronics and Photonics Laboratory, The Aerospace Corporation, Los Angeles, USA)
E-mail: lars.thrane@risoe.dk

The interpretation of conventional OCT images[1] like the one shown in Figure 17 is not always an easy task. One reason for this is the fact that an OCT signal, originating from a given position in a nonabsorbing scattering medium, is a result of not only the amount of light reflected at the given position, but also of the attenuation due to scattering when the light propagates through the scattering medium. Therefore, to obtain imagery, which gives a direct measure of the amount of light reflected at a given position, thereby making interpretation of OCT images easier, it is necessary to be able to separate reflection and scattering effects. Based on a new analytical OCT model[2] developed at Risø National Laboratory, a so-called true-reflection imaging algorithm has been derived. The result of using this imaging algorithm on an OCT image of a solid phantom having three discontinuities with the same value of their reflection coefficients is shown in Figure 18. As expected, the three signals are nearly equal in strength after using the algorithm. The lateral variation may be due to speckle.

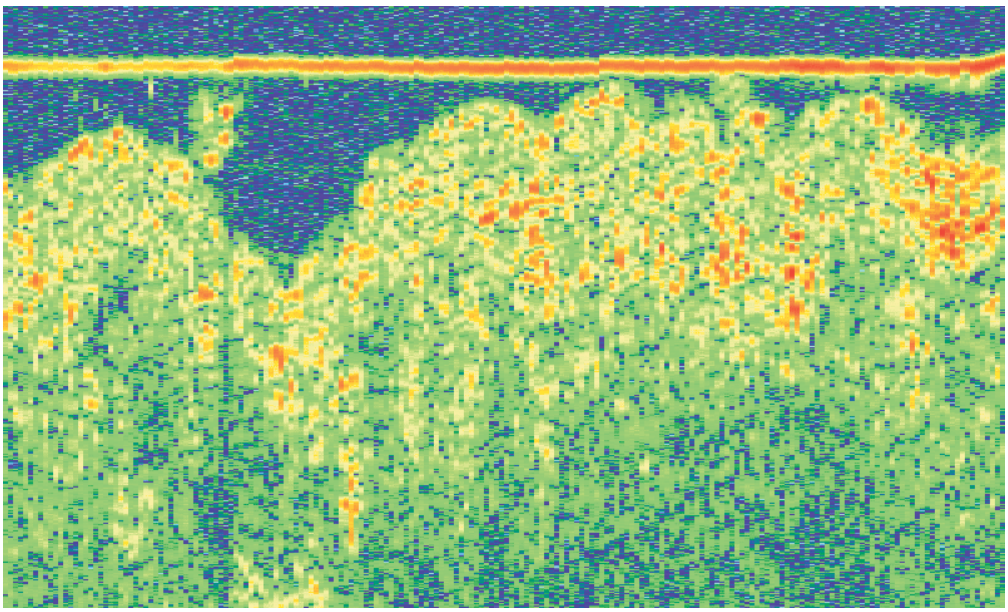

Figure 17. *In vivo* OCT image of healthy skin on the left forearm (volar side) of a human volunteer. The image was acquired with a conventional OCT system[1] (center wavelength 814 nm) developed at Risø National Laboratory.

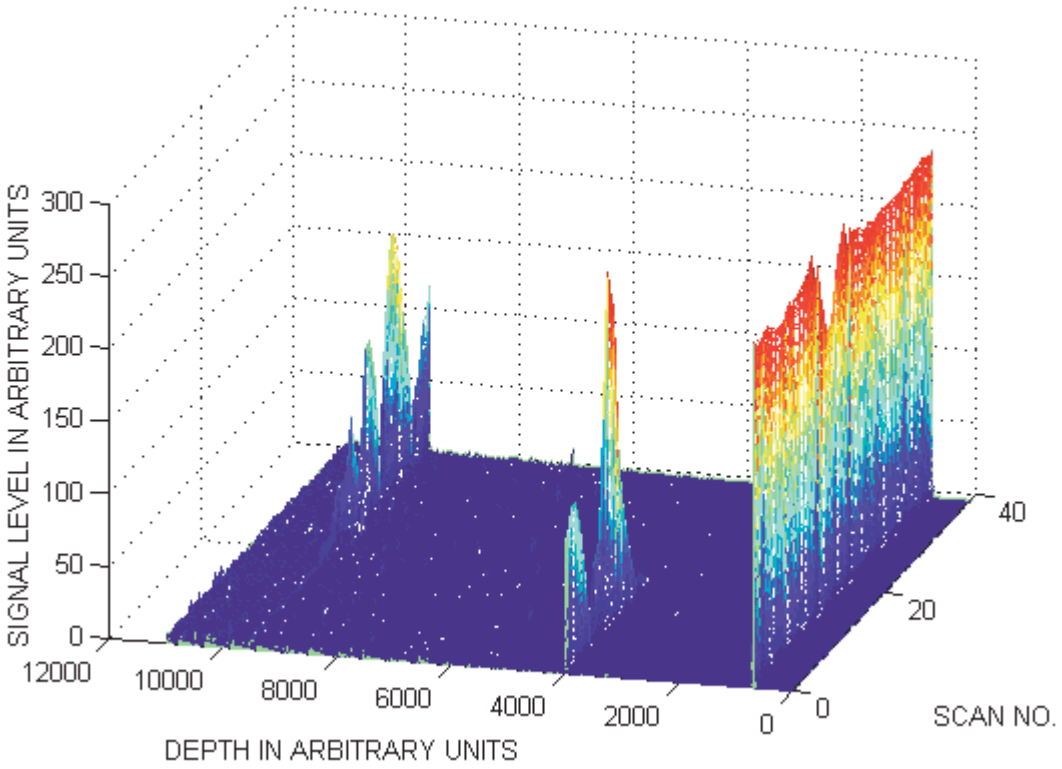

Figure 18. The result of using the true-reflection imaging algorithm on an OCT image of a solid phantom having three discontinuities with the same value of their reflection coefficients. The OCT image consists of 40 longitudinal scans. For better visualization of the effect of the true-reflection imaging algorithm, the envelopes of these scans are shown as a 3D-plot.

The present research project is supported financially by the Danish Technical Research Council under grant no. 9901433.

1. D. Huang, E. A. Swanson, C. P. Lin, J. S. Schuman, W. G. Stinson, W. Chang, M. R. Hee, T. Flotte, K. Gregory, C. A. Puliafito, and J. G. Fujimoto, "Optical coherence tomography," Science **254**, 1178-1181 (1991).

2. L. Thrane, H. T. Yura, and P. E. Andersen, "Analysis of optical coherence tomography systems based on the extended Huygens-Fresnel principle," J. Opt. Soc. Am. A **17**, 484-490 (2000).

3.2.2 Monte Carlo simulations of an OCT set-up

A. Tycho (Research Centre COM, Technical University of Denmark, Lyngby),
T.M. Jørgensen, L. Thrane, S. Hanson and P.E. Andersen
E-mail: thomas.martini@risoe.dk

Light propagation in tissue has become an increasingly important topic in recent years and has thus been extensively investigated through both analytical and numerical models in combination with experiments. Monte Carlo (MC) computer simulation is often the model of choice due to its inherent simplicity and its capability of yielding accurate results even for relatively complex geometries. Whereas an analytical model can offer faster results and a

deeper understanding of the physics, the strength of the MC simulation is that it is commonly accepted as a well-controlled substitute for experiments. An MC simulation can consequently also serve as an excellent testing of a hypothesis or support for an analytical model.

In order adequately to model an optical coherence tomography (OCT) set-up, where a focused beam is reflected from a discontinuity inside a scattering medium, it is necessary to extend the common MC implementations used for modelling scattering in turbid media. We have extended the approach to incorporate the simulation of Gaussian beam propagation in a scattering medium in combination with a heterodyne detection scheme.[1] The Gaussian beam propagation has been modelled so that its full spatial intensity distribution is obtained – i.e. both the correct beam waist and the finite spot size at focus. Excellent agreement is found between the results from a published analytical model of the OCT set-up and the results obtained by applying the proposed Monte Carlo approach (see Figure 19). The analytic model is based on the extended Huygens-Fresnel principle and has been shown to give good qualitative agreement with experiments made with an OCT set-up.[2]

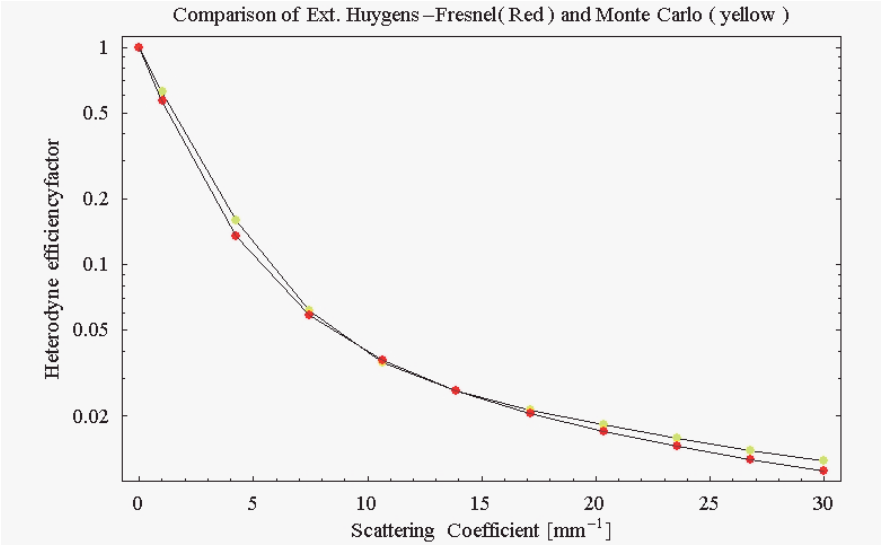

Figure 19. The so-called heterodyne efficiency factor as a function of the scattering coefficient in a tissue-like medium. The measuring configuration corresponds to an OCT set-up. The curves have been derived using the extended Huygens Fresnel principle and a Monte Carlo simulation, respectively.

1. A. Tycho, T.M. Jørgensen, L. Thrane, “Investigating the focusing problem in OCT: Comparison of Monte Carlo simulations, the extended Huygens-Fresnel principle and experiments.” In: Proceedings. Coherence domain optical methods in biomedical science and clinical applications 4, San Jose, CA (US), 24-26 Jan 2000. Tuchin, V.V.; Izatt, J.A.; Fujimoto, J.G. (eds.), (International Society for Optical Engineering, Bellingham, WA, 2000) (Proceedings of SPIE, v. 3915; Progress in biomedical optics and imaging, v. 1, no. 9) p. 25-35.

2. P.E. Andersen, L. Thrane, H.T Yura, A. Tycho, T.M. Jørgensen,, “Modeling the optical coherence tomography geometry using the extended Huygens-Fresnel principle and Monte Carlo simulations” (invited paper). In: Proceedings. Laser-tissue interaction 11: Photochemical, photothermal, and photomechanical, San Jose, CA (US), 22-27 Jan 2000. Duncan, D.D.; Hollinger, J.O.; Jacques, S.L. (eds.), (International Society for Optical Engineering, Bellingham, WA, 2000) (Proceedings of SPIE, v. 3914; Progress in biomedical optics and imaging, v. 1, no. 8) p. 394-406

3.2.3 Coherence tomography using measurements of Wigner phase-space distributions: a theoretical analysis

L. Thrane, H. T. Yura (Electronics and Photonics Laboratory, The Aerospace Corporation, Los Angeles, USA, and P. E. Andersen
E-mail: lars.thrane@risoe.dk

It has recently[1] been suggested that new venues for medical imaging may be based on coherence tomography using measurements of Wigner phase-space distributions.[2] The Wigner phase-space distribution is particularly useful for medical imaging because the phase-space approach provides maximum information about the light being used. In order to further investigate these ideas in the context of the optical coherence tomography (OCT) technique, a theoretical analysis of the Wigner phase-space distribution has been carried out for the case of diffuse reflection and small-angle scattering in the OCT geometry.[3]

The theoretical analysis, which applies to highly scattering tissue, is based on the extended Huygens-Fresnel principle for the optical field,[4] and is valid in both the single and the multiple scattering regimes simultaneously. The results are general in that they apply to both an arbitrary small-angle scattering function, and to arbitrary (real) *ABCD* optical systems.

On the basis of this theoretical analysis, a novel way of creating images based on measurements of the momentum width of the Wigner phase-space distribution has been suggested. Moreover, the advantage over conventional OCT has been specified, i.e. higher sensitivity to changes in the scattering coefficient.[3] Thus, this technique will provide the medical doctor with a new type of imagery that will contain additional information compared with conventional OCT images. Such imaging techniques may enhance diagnostic procedures.

The present research project is supported financially by the Danish Technical Research Council under grant no. 9901433.

1. S. John, G. Pang, and Y. Yang, “Optical coherence propagation and imaging in a multiple scattering medium,” J. Biomed. Opt. **1**, 180-191 (1996).
2. E. P. Wigner, “On the quantum correction for thermodynamic equilibrium,” Phys. Rev. **40**, 749-759 (1932).
3. H. T. Yura, L. Thrane, and P. E. Andersen, “Closed-form solution for the Wigner phase-space distribution function for diffuse reflection and small-angle scattering in a random medium,” J. Opt. Soc. Am. A **17**, 2464-2474 (2000).
4. R. F. Lutomirski and H. T. Yura, “Propagation of a finite optical beam in an inhomogeneous medium,” Appl. Opt. **10**, 1652-1658 (1971).

3.2.4 Photoacoustic imaging for medical applications

P. E. Andersen, S. G. Hanson, L. R. Lindvold, Bengt Hurup Hansen and S. L. Jacques (Oregon Medical Laser Center, Portland, OR, USA)
E-mails: peter.andersen@risoe.dk, sjacques@ece.ogi.edu

The term *photoacoustic imaging* describes the generation and propagation of a stress wave due to absorption of laser light.[1] Typically, the laser illumination inducing the stress wave is a short pulsed laser source, e.g. a pulsed Nd:YAG laser. Photoacoustic techniques have previously been applied to perform concentration measurements in liquids and gases.[1] Recently, the technique has been used to determine the optical properties, i.e. the mean absorption and the reduced scattering coefficients, of biological tissue.[2]

The common aspect of photoacoustic systems for imaging and for determining tissue optical properties is the use of transducers, e.g. piezo-electric transducers,[2] to detect the stress wave. There is, however, a more sensitive method of detecting the stress wave based on an all-optical detection scheme.[3] The scheme is based on a dual-beam common-path interferometer, where light from the two arms in the interferometer is directed towards the object under investigation. A change of path length in one arm due to a change of the object is detected with respect to the other part of the object; hence, a differential measurement is made. Several advantages are gained using this scheme: Firstly, it is highly sensitive of even minute path length changes, i.e. small stress wave amplitudes. Secondly, it provides a non-contact procedure, which is important from a clinical point of view. Finally, the all-optical detection scheme may be integrated into a single holographic optical element.

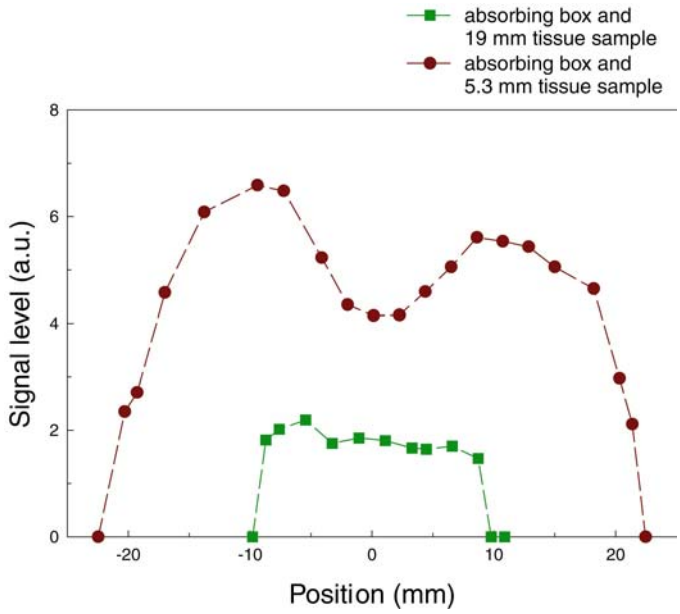

Figure 20. The photoacoustic signal as a function of position using a tissue sample, i.e. chicken breast, and an absorbing box with thickness 1 mm, width 4 mm, and length 10 mm. The absorber is scanned across the width. The circles correspond to the tissue sample thickness 5.3 mm, and the squares correspond to the tissue sample thickness 19 mm (Andersen *et al.*[5]).

We have demonstrated[4] that the all-optical detection scheme improves the photoacoustic imaging system in terms of minimum detectable signal and linear dynamic range, see Table 1. We have also demonstrated the feasibility of the all-optical detection scheme for photoacoustic imaging using gel-water phantoms[4] and *in vitro* tissue samples.[5] An example of an image profile of an absorbing object buried in tissue is shown in Figure 20. We have observed and explained the occurrence of peaks in the detected signal, see Figure 20, as the irradiating beam was scanned across the edge of the absorber.[5] The explanation involves a change in the geometrical shape of the emanated stress wave combined with scattering of the irradiating laser pulse.[5] Finally, we have observed a broadening in the imaged profile of the absorber dependent on the tissue thickness as the phantom was scanned, see Figure 20. These observations were explained by scattering of the irradiating beam and attenuation of the stress wave in the tissue.[5]

Table 1. Comparison between the optical detection scheme and piezoelectric transducers for detecting the acoustic wave. The values for the optical detection scheme have been taken from Jacques *et al.*[4] and the values for the piezoelectric transducer have been adapted from Oraevsky *et al.*[2] [*The true value is probably greater than 6 bar]

	Optical detection	Piezoelectric transducer (values adapted from Ref. 2)
Min. signal [mbar]	10 – 30	20 – 40
Linear dynamic range [bar]	0.03 – 33	0.04 – 6*

1. See, e.g., M. W. Sigrist, "Laser generation of acoustic waves in liquids and gases," *J. Appl. Phys.* **60**, R83-R121, 1986.
2. A. A. Oraevsky, S. L. Jacques, and F. K. Tittel, "Measurement of tissue optical properties by time-resolved detection of laser-induced transient stress," *Appl. Opt.* **36**, pp. 402-415, 1997.
3. S. G. Hanson, L. R. Lindvold, and B.H. Hansen, "Industrial implementation of diffractive optical elements for nondestructive testing," *SPIE Proc.* **2868**, pp. 216-224, 1996.
4. S. L. Jacques, P. E. Andersen, S. G. Hanson, L. R. Lindvold, "Non-contact detection of laser-induced acoustic waves from buried absorbing objects using a dual-beam common-path interferometer." In: Laser-tissue interaction. Jacques, S.L. (ed.), (International Society for Optical Engineering, Bellingham, WA, 2000) (Selected SPIE Papers on CD-ROM, v. 9).
5. P. E. Andersen, S. G. Hanson, S. L. Jacques, "Photoacoustic imaging of buried objects using an all-optical detection scheme." In: Laser-tissue interaction. Jacques, S.L. (ed.), (International Society for Optical Engineering, Bellingham, WA, 2000) (Selected SPIE Papers on CD-ROM, v. 9).

3.2.5 A new diode laser system for photodynamic therapy

E. Samsøe Andersen, P. M. Petersen, P. E. Andersen, S. Andersson-Engels and K. Svanberg* (*Lund Institute of Technology, Sweden)*
E-mail: eva.samsoe@risoe.dk

Photodynamic therapy (PDT)[1] is a promising alternative to existing treatment modalities of malignant and pre-malignant tumours. The treatment relies on the coexistence of light, oxygen and a photosensitive component. The photosensitizer has the capability of accumulating to a higher degree in the diseased tissue than in the surrounding healthy tissue. The treatment light excites the photosensitizer which sets off a photochemical process leading to cell necrosis. The traditionally used light source for PDT treatment has been Nd:YAG or Ar-ion laser-pumped dye laser systems. These systems are, however, inconvenient in a clinical environment due to their size, high cost and complex operation. During the past years, high-power diode lasers have become available at the required wavelengths for PDT, but diode lasers suffer from multimode non-diffraction limited output that limits their coupling efficiency to optical fibres. In PDT it is often preferable to deliver the treatment light through thinner fibres than is possible with such lasers.

For the past ten years, treatment procedures based on PDT have been developed at Lund Institute of Technology and Lund University. In order to develop the treatment further, there is a need of a compact high-power laser capable of delivering the treatment light through small diameter core optical fibres, e.g. 50 μm, with the lowest possible coupling losses.

At Risø National Laboratory, a new high-power diode laser system with unique coherence properties has been invented. The system is based on a high-power diode laser implemented in an external cavity. The external feedback system forces the multimode diode laser to exhibit a highly improved output with large coupling efficiency to optical fibres.

Figure 21. Preliminary clinical trials (animal model) carried out at Lund University using the laser system developed at Risø National Laboratory.

Recently, preliminary animal trials using the laser developed at Risø National Laboratory have been carried out in collaboration with the group in Lund with promising results. The animal models were rats with tumours inoculated into the muscles of their hind legs. These results have, however, not been completed yet. Figure 21 shows the laser output coupled through optical fibres for the procedure. Currently, the laser system is being optimised to enhance the treatment parameters further and additional clinical studies are planned in collaboration with the group in Lund.

The present project is supported financially by the Danish Technical Research Council under grant no. 9901433.

1. Q. Peng et al., ”5-aminolevulinic acid-based photodynamic therapy: clinical research and future challenges”, *Cancer* **79**, p. 2282, 1997.

3.2.6 FT-IR spectrometry for biological and medical applications

J. Bak and P. Snoer Jensen
E-mail: jimmy.bak@risoe.dk

FT-IR spectrometry has been used in our department for the last seven years to analyse various materials and processes; the technique has, e.g., been developed and used for temperature measurements, advanced gas analyses and powder analyses. Ongoing projects partly sponsored by Danish industry and the EU are dealing with temperature measurements of surfaces, characterisation of the infrared properties of various materials, and measurements of hot gases with respect to aircraft exhaust gas analysis. Recently, new activities have been initiated that focus on the application of infrared spectrometry in the biological and medical fields. The purpose of starting this activity is twofold. Firstly, infrared spectrometry holds a great potential for a variety of biological and medical applications, qualitatively, as well as quantitatively. In principle, it is possible to determine the amount and the structure of

biological molecules in many different samples including human tissue, plant material and food. Secondly, expanding the FT-IR activities into the biomedical field will support the ongoing laser-based activities in the Center for Biomedical Optics and New Laser Systems (BIOP) headed by the department.

The application of FT-IR for the determination of biological molecules in low concentrations in aqueous solutions is investigated in an ongoing Ph.D. project. Parameters such a penetration depths, detection limits and the influence of temperature are investigated. The strong background signal from water due to its presence in high concentrations limits the applicability of infrared spectrometry if this background cannot be controlled or compensated for. This work will result in basic knowledge that is important for later biological applications expanding the technique into in vitro and in vivo measurements.

Lessons treating the application of infrared spectroscopy have been given at the Danish Technical University. The lessons were part of the master course "Bio-medical Optics" arranged by BIOP. These activities will be continued in 2001.

Work is in progress for writing a centre contract proposal concerning the use of lasers and infrared spectroscopic techniques for bio-sensing. Leading partners from industry and research organisations are part of the consortium. The department will apply for funding from the Danish Ministry of Trade and Industry.

3.3 Infrared technology

3.3.1 Modelling of gaseous spectra in the AEROPROFILE project

J. Bak and S. Clausen
E-mail: jimmy.bak@risoe.dk

The AEROPROFILE project, which is partly funded by the European Commission, was initiated in December 1997 and after a short extension scheduled to end in March 2001. The scientific goal of the project is to develop software and an experimental set-up to be used for temperature and concentration profiling in an aircraft exhaust gas. Our contributions to the project have been to develop a hot gas cell facility for reference measurements, to check the quality of the developed software and methods by judging the results obtained by measurements carried out in the reference hot gas cell, to develop software which could be used to compare the performance of procedures based on high and low spectral resolution for the determination of concentration and temperatures, respectively, and, finally, to support the aircraft exhaust measurements by infrared camera recordings.

The investigation of the potential use of low resolution spectra instead of high resolution spectra for concentration and temperature profiling is driven by the foreseen applicability of low resolution, i.e. low cost and robust FT-IR spectrometers for industrial applications that are calibrated with data from commercial molecular data bases. In order to test the use of low resolution spectra, a computer program was created which could make rapid calculations of low and high resolution gas spectra for various temperatures and concentrations and compare the performance at high, intermediate and low spectral resolution. It was shown that there is no difference in the performance between the various resolution settings when line data were used. The final step in the project will be to model measured low and high resolution spectra containing gaseous interferents. Figure 22 shows a first attempt to compare measured and calculated low resolution spectra.

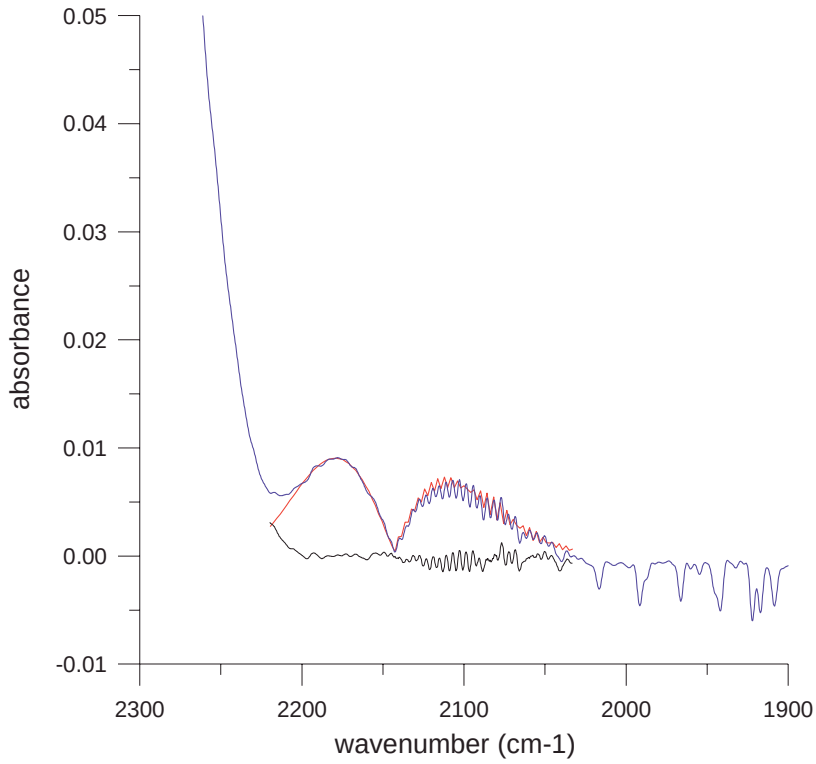

Figure 22. (blue) Measured gas spectrum (Munich 1999), (red) simulated CO spectrum, (black) the spectral residual with water vapour lines and varbon dioxide bands and non-modelled CO features.

It is well known that it is difficult to make reliable quantitative predictions of concentrations based on spectra in which overlapping spectral features from interferents and fluctuating base lines are present. Normally, in many applications it is necessary to identify the interferents in advance, and subtract these features or include them in the calibration step when chemometric methods such as PLS and PCR are used. If a non-identified interfering compound is present, an overestimated concentration value will often be the result of the analysis. It was shown that an accurate estimate of the concentration of the compound of interest can be found even if interfering spectral features are present. A computer program was used to correct the contaminated spectra. The method was demonstrated with both simulated and measured data.[1,2]

1. Bak, J., Retrieving CO concentrations from FT-IR spectra with non-modelled interferences and fluctuating baselines using PCR model parameters. Accepted for publication in Appl. Spec., 2001.
2. Bak, J., A novel approach for handling spectral data with overlapping features. Presented at the Pittcon 2000 conf., New Orleans, March 2000.

3.3.2 Infrared temperature calibration

S. Clausen
E-mail: sonnik.clausen@risoe.dk

A reference laboratory for calibration of infrared instruments was established at Risø in 1996. Traceable calibration of pyrometers and infrared thermometers is made with blackbodies in the temperature range –80°C to 1600°C. The work affects the following six main topics in order to reduce uncertainties of non-contact temperature measurements:

- Calibration service of infrared thermometers for customers
- Temperature measurements for customers
- Development of new and improved methods for infrared temperature measurements
- Measurements of spectral emissivity of samples and coatings
- Consultative service and information
- International comparisons of standards and procedures

With the aim of ensuring the traceability and the comparability of the results, comparisons between the standards and laboratories must be carried out. Risø has participated in an international comparison of radiation thermometry in 2000, i.e. the TRIRAT MT-scale covering the temperature range from 156°C to 961°C. Risø is involved in the EU project "TRIRAT" with participants from laboratories from most of Europe. The overall objective of the project is to provide improved, sub-Kelvin accuracy in infrared radiation thermometry at industrial levels in the range from –50°C to 800°C. The traceability is transferred from the highest metrological levels down to the industrial level. We work towards reaching sub-Kelvin accuracy of our calibration sources at temperatures in the range from -50°C to 250°C.

With the combination of high-accuracy traceable blackbody sources and spectral measurements, Risø has state-of-art calibration capabilities in the spectral range from 1 – 25 μm of infrared radiation with an FTIR spectrometer.[1,2]

1. Clausen, S., Berøringsløs temperaturmåling af varme gasser. In: Konferanse. Temperatur 2000, Oslo (NO), 7-8 Jun 2000. (2000) 9 p.
2. Clausen, S., Målenøjagtighed og fejlkilder ved berøringsløs temperaturmåling. In: Konferanse. Temperatur 2000, Oslo (NO), 7-8 Jun 2000. (2000) 8 p.

3.4 Phase contrast techniques

3.4.1 Generalised phase contrast and programmable phase optics

J. Glückstad, P. C. Mogensen and R. L. Eriksen
E-mail: jesper.gluckstad@risoe.dk

The imaging and visualisation of phase objects, wavefront disturbances and phase aberrations is a subject of considerable interest in optics. Different techniques are applied in such diverse fields as optical component testing, wavefront sensing and phase-contrast microscopy where a qualitative or quantitative analysis of an optical phase disturbance is required. In general, since a phase disturbance cannot be directly viewed, a method must be sought to extract the desired information indirectly, for example through the generation of fringe patterns in an interferometer. A number of such visualisation techniques are grouped under the heading of common path interferometry, in which a portion of the signal is perturbed to act as a synthetic reference for the unperturbed portion of the signal wavefront. A generic common path interferometer (CPI) for visualising a phase disturbance is shown in Figure 23.

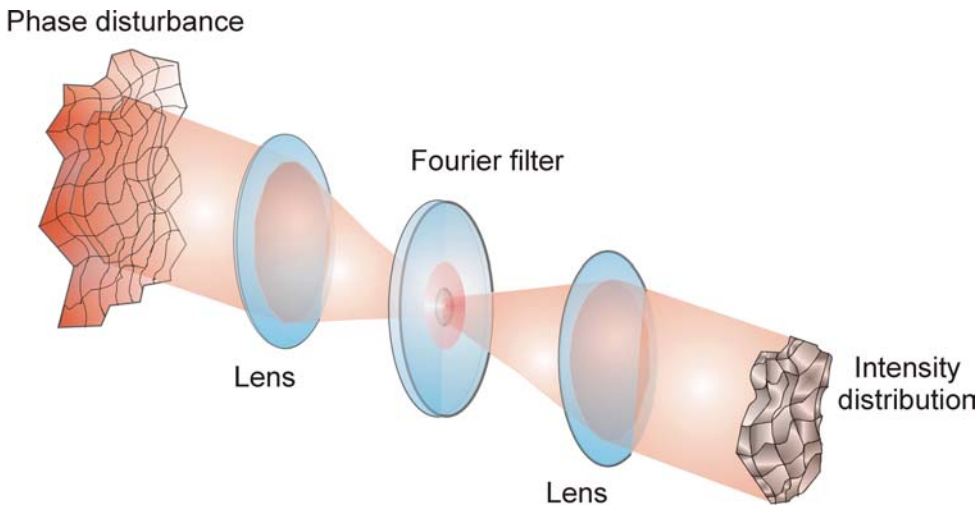

Figure 23. A schematic representation of a CPI based on a 4-f optical system. A region of a given input phase disturbance is sampled and generates an intensity distribution in the image plane of the optical system by a filtering operation in the Fourier plane. The values of the filter parameters determine the type of filtering operation. A typical versatile and efficient filter would have 100% transmission and a π phase shifting central region.

The approach we use is based on a generalisation of the phase contrast approach of Zernike[1], which is not restricted by the so-called "small-scale" phase approximation, which limits the original method. The generalised phase contrast (GPC) method can deal with a full 2π dynamic range of phase input and by a careful choice of the parameters for the Fourier filter to match the phase disturbance it is possible to convert the phase information into a high contrast intensity distribution.[2,3] The linearity of the technique has also been extended when compared with earlier work.[4]

By controlling the input phase distribution a system for visualising phase objects becomes a highly effective system for the generation of intensity distributions, where interference effects rather than an amplitude mask, are used to generate a high contrast light pattern. One particular application for the GPC technique is array generation, an example of which is shown in Figure 24. In this case, a fixed phase mask generates the controlled "phase disturbance" (see Figure 23) and from this filtered imaging operation a high contrast intensity pattern is obtained, the structure of which is determined by that of the phase mask.

It is also possible to use a phase-only spatial light modulator (SLM) as the controllable dynamic phase disturbance. An example of an irregular array generated with an SLM as input is shown in Figure 25. Such irregular arrays are extremely challenging to produce with alternative techniques such as computer-generated holography demonstrating a significant advantage of the GPC method. The role of the phase contrast filter (PCF) in generating the high contrast is emphasised by Figure 26. In this example, the PCF is not present and the resulting image shows an almost complete loss of contrast when compared with Figure 25 in which the same input phase disturbance is used.

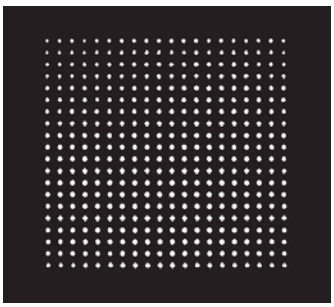

Figure 24. A 20 x 20 spot array generated using the GPC method in combination with a fixed phase mask. In this case a 60 micron PCF is used and the array dimensions are approximately 3x3mm.

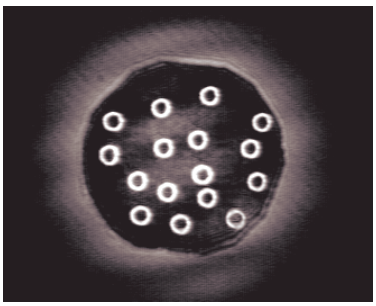

Figure 25. The GPC method with a phase-only SLM generating the input phase object, in this case a random distribution of dough-nuts. The outer aperture is due to an iris at the input of the optical system.

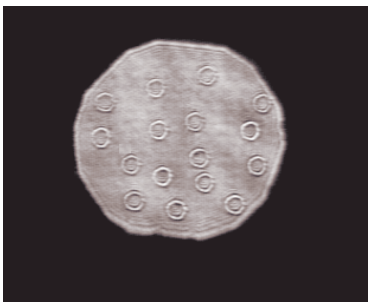

Figure 26. With the PCF removed from the optical system, contrast is lost and the input phase object is not visualised. Residual amplitude modulation in the SLM accounts for the slight visibility of the pattern.

1. F. Zernike, “How I discovered phase contrast”, Science **121,** 345-349 (1955).
2. J. Glückstad and P. C. Mogensen "Optimal phase contrast in common path interferometry" Appl. Opt.,**40**, 268-282, (2001)
3. J. Glückstad and P. C. Mogensen, “Reconfigurable ternary-phase array illuminator based on the generalised phase contrast method”, Opt. Comm. **173**, 169-175 (2000).
4. H. B. Henning, “A new scheme for viewing phase contrast images”, Electro-optical Systems Design **6,** 30-34 (1974).

3.4.2 Polarisation encoding with spatial light modulators

J. Glückstad, P. C. Mogensen and R. L. Eriksen
E-mail: jesper.gluckstad@risoe.dk

We have developed a system for optical two-dimensional encoding of the polarisation state of light using two optically addressed phase-only liquid crystal spatial light modulators (LC-SLMs). This system simultaneously combines previous techniques for generating and rotating polarised light.[1] We are thus able to generate a wavefront having a precisely controlled variation of the spatial state of polarisation. We can generate arbitrary elliptically polarised light with independent control of both the ellipticity and the rotation angle of the major axis of the ellipse by combining two LC-SLMs and two quarter-wave plates, as shown in Figure 27. The input light is incident on SLM-1, which together with the linear polarisor converts the input light to elliptically polarised light (the elliptical generator). The second SLM, SLM-2, is placed between two crossed quarter-wave plates ($\lambda/4$) and rotates the major axis of the elliptically polarised light generated by SLM-1 (the elliptical rotator). The output of the system is visualised with a polarisor and a CCD camera.

In Figure 28 we compare experimental results and theoretical analysis for the rotation of linearly polarised light so that the linear polarisation directions in all four quadrants of the test image are aligned parallel with the output polarisor. In Figure 29 we show the selective rotation of elliptically polarised light in a single quadrant. Note the different grey levels corresponding to the different strength polarisation components aligned with the polarisor.

1. J. A. Davis, D. E. McNamara, D. M. Cottrell and T. Sonehara “Two-dimensional polarization encoding with a phase-only liquid-crystal spatial light modulator”, Appl. Opt. **39**(10), 1549-1554 (2000).

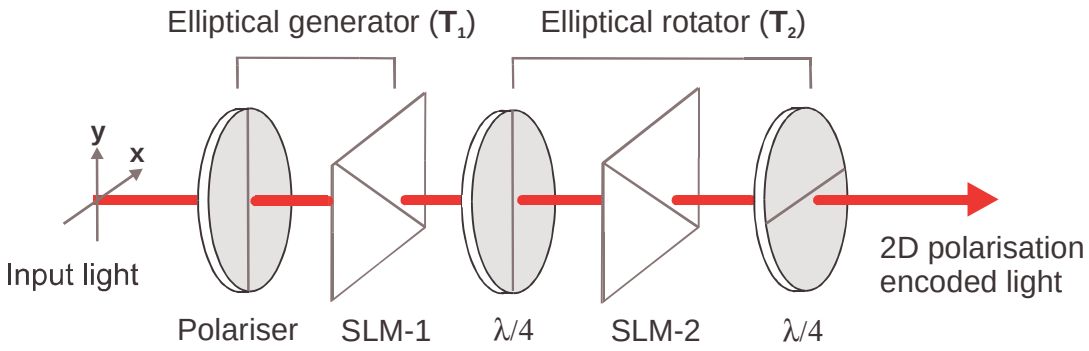

Figure 27. An optical system for converting incident polarised light into an arbitrary state of elliptically polarised light with the major axis of the elliptically polarised light rotated an arbitrary angle. The lines denote the extraordinary axis of the SLMs, the quarter-wave plates (λ/4) and the polarisation direction of the linear polarisor.

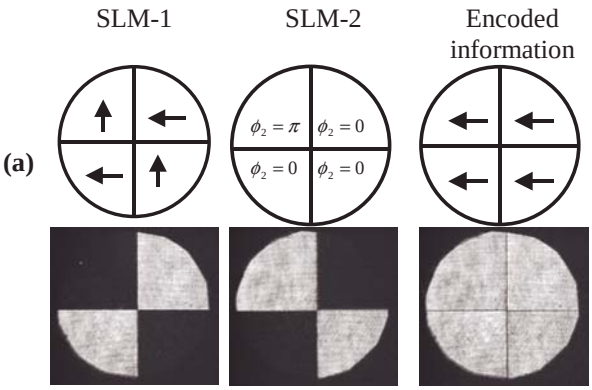

Figure 28. Experimental encoding results for the rotation of linearly polarised light. The upper half of (a) shows the linear polarisation state (indicated by arrows) and phase modulation for the four quadrants in each SLM and the resulting encoded information. The lower half of (a) shows the corresponding experimental results recorded with a CCD camera and polarisor.

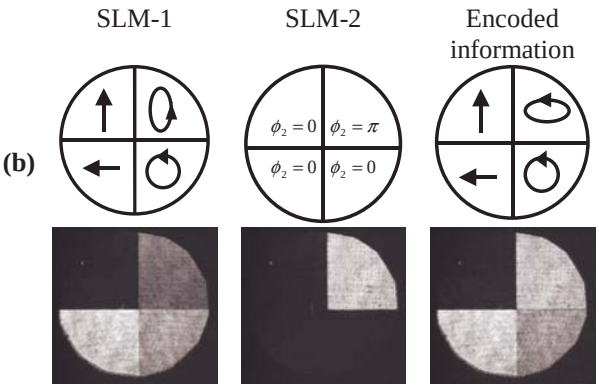

Figure 29. Experimental encoding results for the generation and selective rotation of an arbitrary two-dimensional distribution of linearly, circularly and elliptically polarised light. The upper half of (b) shows a graphical representation of the rotation and type of polarisation state and the lower half gives the corresponding experimental results as viewed with a CCD camera and polarisor.

3.4.3 Polarisation encoding for high-speed optical encryption

J. Glückstad, P. C. Mogensen and R. L. Eriksen
E-mail: jesper.gluckstad@risoe.dk

The recent expansion in Internet and data-communications traffic has raised questions regarding the optimum approach for the secure transfer of sensitive information. There is thus currently a considerable level of interest in the application of optical techniques to the encryption of data for secure transmission and storage of information.[1] This leads to a requirement for a simple, compact and high-speed optical encryption system. An attractive approach for such a high-speed optical encryption system based on a polarisation encoding technique exploits the birefringence of liquid crystal spatial light modulators.[2] The encryption and decryption operations are performed by a simple imaging operation between two spatial light modulators (SLMs).

A schematic representation of the encryption and decryption processes is shown in Figure 30. The components required for each process are identical and consist of a pair of Ferro-electric liquid crystal SLMs (FLC-SLMs) aligned so that the two fast axes corresponding to their binary states are parallel. These SLMs are placed between a pair of polarisors with a detector array at the output to convert the optical signal to a digital signal. The original information is consequently transferred from electronic to optical format by FLC-SLM 1 and is then encrypted optically by FLC-SLM 2. The detector array reconverts the encrypted optical information back to electronic format for secure transmission. At the receiving end of the network a similar decryption system repeats the electronic to optical conversion and applies the decrypting key to recover the original information. In short, the information encryption and decryption is undertaken in the optical domain and the transmission of the encrypted data takes place across a standard network in the electrical domain.

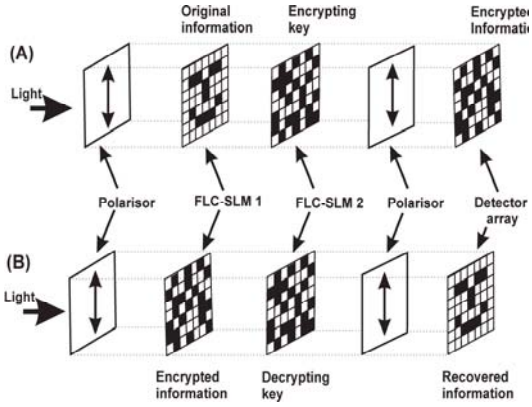

Figure 30. Schematic diagrams showing (a) the encryption operation and (b) the decryption operation. The components required for each process are identical and consist of a pair of pixelated FLC-SLMs aligned with their pixel edges parallel and placed between a pair of polarisors. The encrypted information (a) and the recovered information (b) are converted to a digital signal using a detector array.

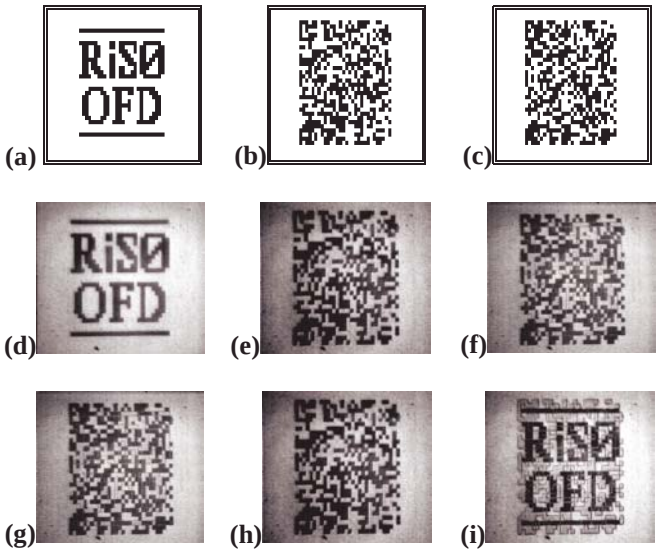

Figure 31. A set of 30x30 pixel test images for the encryption sequence of a single frame showing (a) the information we wish to encrypt, (b) the encrypting key and (c) the encrypted information which is the result of an XOR operation between (a) and (b). Experimental results for a complete encryption and decryption sequence are shown in figures (d)-(f). Here (d) is the original information, written on FLC-SLM 1 (e) is the encrypting key written on FLC-SLM 2 and (f) shows the optically encrypted information. For decryption (g) is the encrypted information, (h) is the decrypting key written on FLC-SLM 2 and (i) is the recovered information.

In Figure 31 the stages for the encryption and decryption of a 30x30-pixel test pattern are shown, with the theoretical and experimental results comparing well. In this case there are $2^{(30x30)}$ possible decrypting keys and since the FLC-SLMs have maximum frame rates of 3kHz, an encryption rate of 2.7Mbs^{-1} with a 900-bit key is possible. Utilising the full 256x256 pixel capacity of the SLM increases the key length to 65 kb and the encryption rate to approximately 200 Mbs^{-1}.

1. B. Javidi “Securing information with optical technologies” Physics Today, 50(3), 27-32 (1997)

2. P. C. Mogensen and J. Glückstad, "A phase based optical encryption system with polarization encoding", Opt. Comm. **173**, 177-183 (2000).

3.4.4 Programmable optical tweezers

J. Glückstad, P. C. Mogensen and R. L. Eriksen
E-mail: jesper.gluckstad@risoe.dk

The recent development of optical tweezers represents an extremely interesting and useful application of optics to the field of cell biology. Optical tweezers use the radiation pressure effect from a highly focussed laser beam to trap and manipulate micron-sized cells and particles with pico-newton sized forces. This technique offers a hitherto unprecedented level of control and has been extensively applied in the study of the dynamics of biological systems. We wish to apply the generalised phase contrast technique (as described section 3.4.1) in conjunction with a phase-only spatial light modulator to generate a dynamic, reconfigurable and computer controlled multiple-beam tweezer system. In such a system, the number, shape and position of tweezer beams could be modified to best suit the trapping task at hand. The first step of this project is the construction of a conventional single-beam tweezer system.[1]

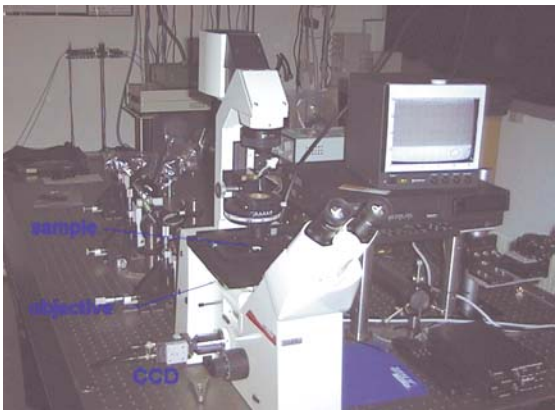

Figure 33. Photograph of the optical tweezer system showing the inverted microscope with the objective beneath the sample stage. The laser system and focussing optics can be seen directly behind the microscope, and the trapping and manipulation of samples is observed with a CCD camera.

A basic single-beam optical tweezer system has been set up, a photograph of which is seen in Figure 33. This is based around an 830 nm laser diode, and a high-resolution microscope. The output beam profile of the laser diode is circularised to have a Gaussian beam profile. Light is coupled through the objective lens onto the sample focussing the trapping beam in the focal plane of the microscope. In this basic tweezer system, beam steering is achieved by displacing a lens in the beam steering optics.

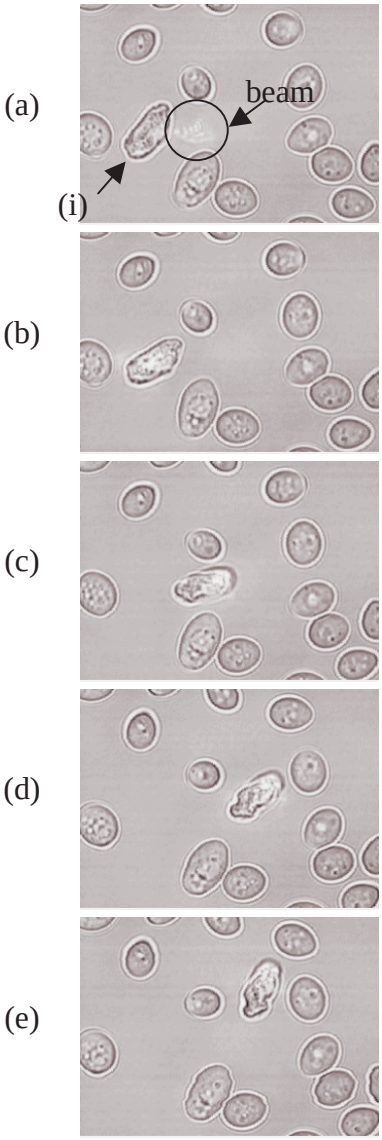

Figure 32. A set of images showing the trapping and manipulation of an individual yeast cell. (a) shows the introduction laser beam into the sample; it is initially moved to the left (b) where it traps an irregularly shaped yeast cell (i), this is then manipulated (c)-(e). As the trapped cell is manipulated, it twists and moves in the trap changing the cross section of the cell that is in focus. The typical size variation of the cells of approximately 5-10 μm

The image sequence in Figure 32 shows that trapping and manipulation of biological object, in this case a single yeast cell, is carried out relatively easily with laser powers in the 5-20 mW range. The laser light is reflected and scattered from both the cover slip and the yeast cell during the trapping process. When the plane of focus is away from the glass interfaces and nothing is held in the trap, the beam cannot be seen.

1. P. C. Mogensen and J. Glückstad, "Dynamic array generation and pattern formation for optical tweezers", Opt. Comm. **175**, 75-81 (2000).

3.5 Optical measurement techniques

3.5.1 Laser anemometry for control and performance testing of wind turbines

R. Skov Hansen
E-mail: rene.skov.hansen@risoe.dk

The research is funded in part by the European Commission in the framework of the non-nuclear energy programme, JOULE III.

The general objective of the project is to improve the market position of wind power by enhancing the credibility by more accurate performance assessment of wind turbines.

The work carried out in the Optics and Fluid Dynamics Department deals with the construction of an anemometer to measure wind velocities in front of a wind turbine. Instead of using a cup anemometer mounted on a tower, a laser anemometer is found to constitute a more flexible instrument for performing remote measurements of the wind velocities.

The laser anemometer shall be mounted on top of the nacelle and shall focus a single laser beam in front of the wind turbine. The velocity of the wind is determined by measuring the introduced Doppler shift of the laser light, scattered backwards from the aerosols in the remote beam waist. The measurement should be performed so far away that the measured wind is unobstructed by the turbine, but close enough to have a correlation between the measured wind velocity and the actual wind hitting the turbine. These requirements have led to a target measuring distance of 150 m. Based on the properties of available lasers a CO_2 laser with an optical wavelength of 10.6 μm has been selected. The laser is a sealed waveguide laser, and has been specially designed for the laser anemometer in cooperation with Ferranti Photonics. The laser yields an output power of 5 Watt with a Gaussian intensity distribution of the laser beam. The coherence length is more than two times the measuring distance.

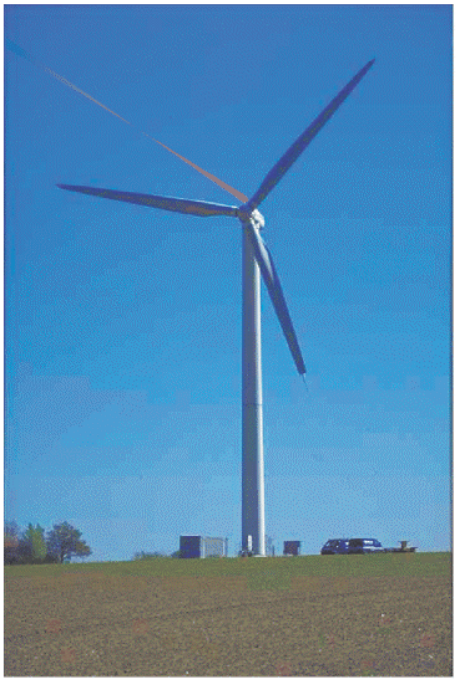

The Doppler shift is measured by using a heterodyne principle, see Figure 34 and Figure 35, where the collected backscattered light interferes with a local oscillator. In order to reduce the number of optical components in the instrument, the local oscillator is established by reflecting a small fraction of the laser output beam off a partially reflecting window.

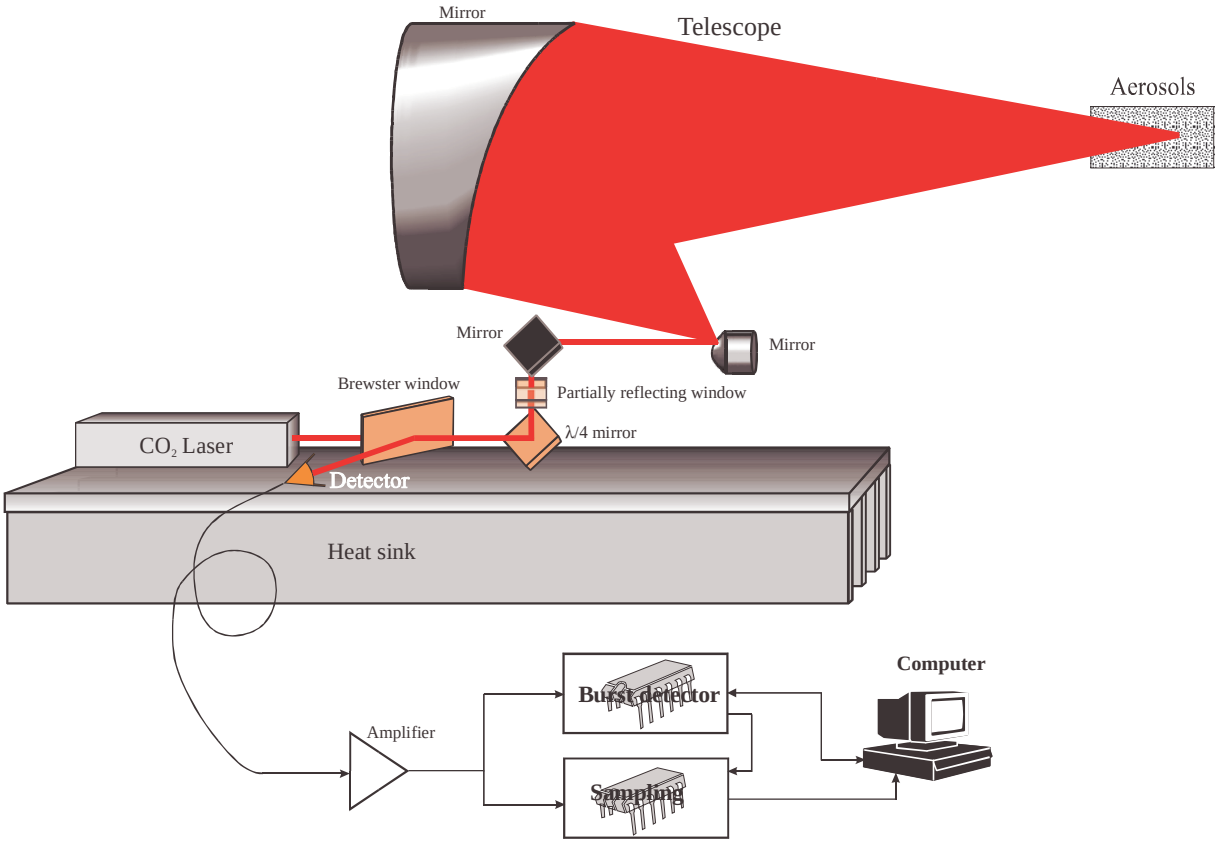

Figure 34. Heterodyne detection with simplified local oscillator.

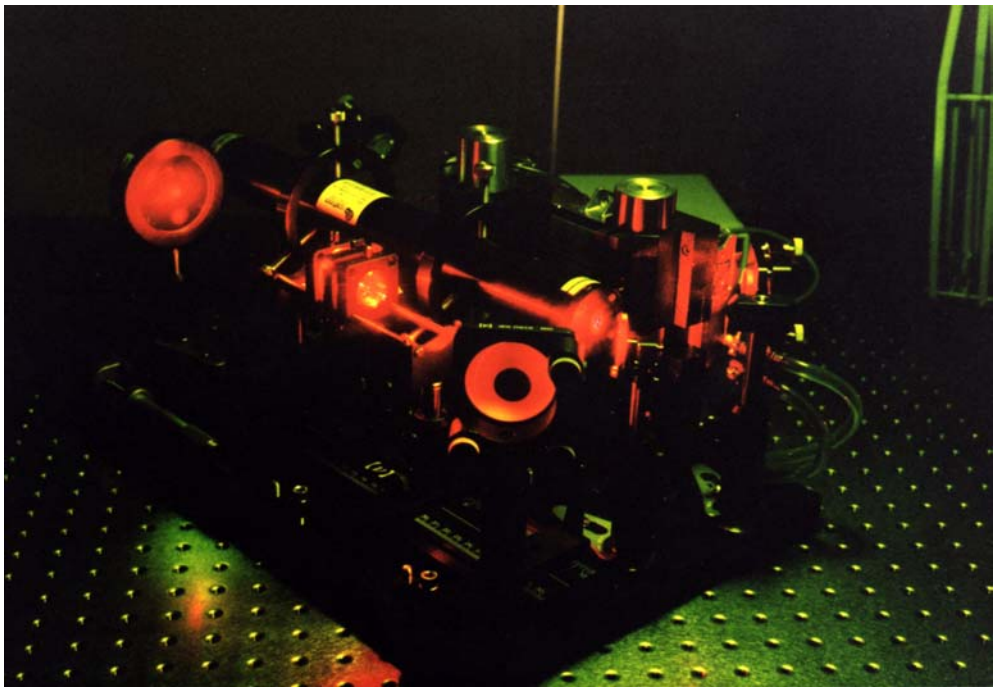

Figure 35. The laboratory test set-up for the laser anemometer. The laser beam from the CO_2 laser is invisible for the human eye. In this figure, a red HeNe laser beam is used as a guide for setting up the optics.

An important issue for the laser anemometer is the minimum required backscattering coefficient of the aerosols in the measuring volume. In heterodyne systems, the weak backscattered light is collected, whereafter it interferes with the local oscillator at the detector. The sensitivity of the laser anemometer is a function of the intensity of the local oscillator. Saturation phenomena of the detector put an upper limit on the allowable intensity of the local oscillator and, thereby, limit the instrument sensitivity to the backscattered light. For the present detector, the lowest acceptable backscattering coefficient is approximately $\beta = 1*10^{-6}$ $m^{-1}sr^{-1}$, which gives a total reflection coefficient of the aerosols in the measuring volume of $1*10^{-11}$.

3.5.2 The angular encoder

S. G. Hanson, S. Peo Petersen and B. Rose (ADC Danmark ApS)
E-mail: steen.hanson@risoe.dk

A project has been initiated by the Danish Company, JJ Measurement ApS (http://www.catscience.dk/dk_default.asp), in which the design and fabrication of a patented high-precision angular encoder has been investigated in collaboration with ADC Danmark ApS. The functional principle has previously been presented.[1] The basic system relies on recording the unique and very detailed speckle pattern that arises when coherent light is scattered off a surface, which is not fully reflective as shown in Figure 36.

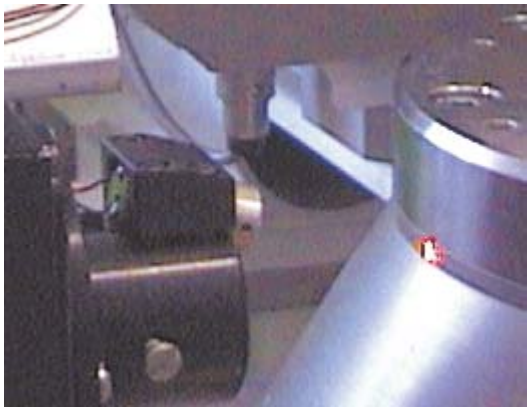

Figure 36. Optical encoder system used at a high-precision scientific stage.

To achieve a measurement that only relies on the angular displacement and is insensitive to any linear translation of the object, the image sensor is placed in the Fourier plane with respect to the object. Doing this, the measurement has been shown to be independent of the radius of rotation, the illumination wavelength and the distance to the object. No direct contact with the object is needed which means that large standoff distances can be employed without relying on having to place special markings on the object.

A series of measurements was performed where the speckle pattern from the entire circumference of a rotary stage was recorded and stored, and the various speckle patterns were “stitched” together to provide a full map of the speckle pattern covering the entire 360 degrees. Having done this, the angular position at an arbitrary position of the rotary stage can be established by correlating the present speckle pattern with the map. This has been performed where the measurements are referred to the control system associated with the rotary stage, called “TASCOM”. Figure 37 presents two independent measurements that show excellent agreement thereby merely depicting the inaccuracy of the TASCOM-system.

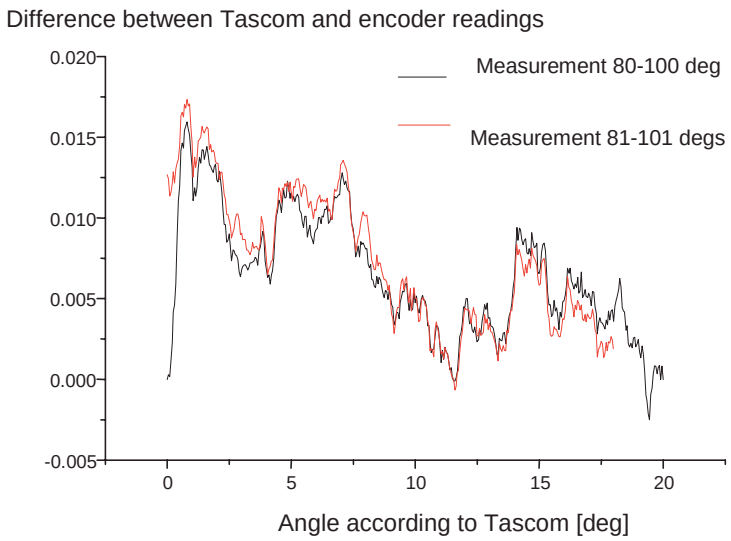

Figure 37. Absolute measurements from 80-100 deg (black) and 81-101 deg (red.).

The repeatability of the developed encoder system corresponds to an accuracy of approximately 3 μrad, and the absolute accuracy over the entire 360 degrees of rotation is approximately 60 μrad.

1. Rose, B.; Imam, H.; Hanson, S.G.; Yura, H.T.; Hansen, R.S., Laser-speckle angular-displacement sensor: Theoretical and experimental study. Appl. Opt. (1998) **37**, 2119-2129.

3.5.3 Partially developed speckle

H. T. Yura (The Aerospace Corporation, Los Angeles, USA) and S. G. Hanson
E-mail: steen.hanson@risoe.dk

The statistical properties of scattered coherent light have been extensively treated when coherent light, i.e. laser light, is scattered off a rough surface. In this case it is tacitly assumed that the phase of the scattered field is randomly distributed from one position on the surface to the next. In case of a perfect mirror, the phase of the scattered light is constant from one spatial position to the next, again resulting in a simple relation for the statistical description of the scattered field.

In the intermediate case where the surface is partly specularly and partly diffusely reflective, the statistics of the scattered field(s) become less trivial. Especially, analytical expressions are hardly achievable. We have applied a previously developed mathematical method, based on the so-called *ABCD*-method,[1] to derive analytical expressions for various statistical properties of interest, specifically with respect to speckle-based sensors.[2] In many cases such sensor systems will rely on the scattered light from metallic surfaces, which neither possess the properties of a rough surface, nor act as a perfect mirror. Thus, an analytical description of the scattered field will facilitate the optimisation of the optical sensor system. In our investigations we have assumed a Gaussian height distribution for the object and a Gaussian transverse height autocorrelation function with a smallest scale, r_h, introduced as a variable.

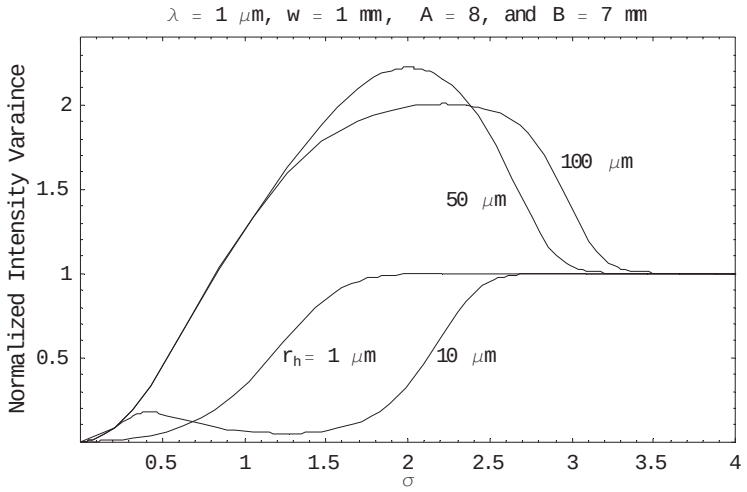

Figure 38. Normalised intensity variance as a function of the phase variance of the scattered field (rms. roughness) for various values of the lateral correlation length of the surface roughness.

Of major interest to speckle-based systems is the strength of the speckle signal, i.e. the variance of the intensity. Figure 38 shows the normalised standard deviation of the on-axis scattered light as a function of the phase fluctuation for three different values of the lateral scale of the height fluctuations, i.e. r_h = 1, 10, 35 and 50 μm, where the normalisation is performed with respect to the on-axis intensity. The scattering set-up is a 4 mm diameter ball illuminated with a plane wave of radius 1 mm and wavelength 1 μm observed at a distance of 7 mm. The figure clearly shows that an optimum exists for a certain surface roughness. This indicates that for a certain surface roughness the specularly scattered light will mix coherently with the diffusely scattered light to produce a very strong speckle pattern. If the surface roughness is increased further, the diffusely scattered light will increase in strength, but the specularly scattered light (i.e. the local oscillator) will disappear and the intensity variance decreases. On the other hand, the investigations have shown that the area over which the speckles appear will be broadened.

[1]. Yura, H.T.; Hanson, S.G., Optical Beam Wave Propagation through Complex Optical Systems. J. Opt. Soc. Am. A (1987) v. 4 p. 1931-1948.

2. Yura, H.T.; Hanson, S.G., Variance of Intensity for Partially Developed Speckle: A Physically Based Analytic Analysis., submitted for publication.

3.5.4 Zeptor – an input device for PCs

S. G. Hanson and R. Skov Hansen
E-mail: steen.hanson@risoe.dk

The Danish company Kanitech International, www.kanitech.com, has developed an input device primarily for cursor control in connection with personal computers, see Figure 39. The rotation of a reflective ball placed in the tip of the pen is probed by an optical system based on a low-cost laser and a series of detectors that records the speckle pattern arising from scattering off the surface of the ball. Needless to say, the optical system has to be cheap in high-volume production and to have low power consumption, yet being reliable and easy to align.

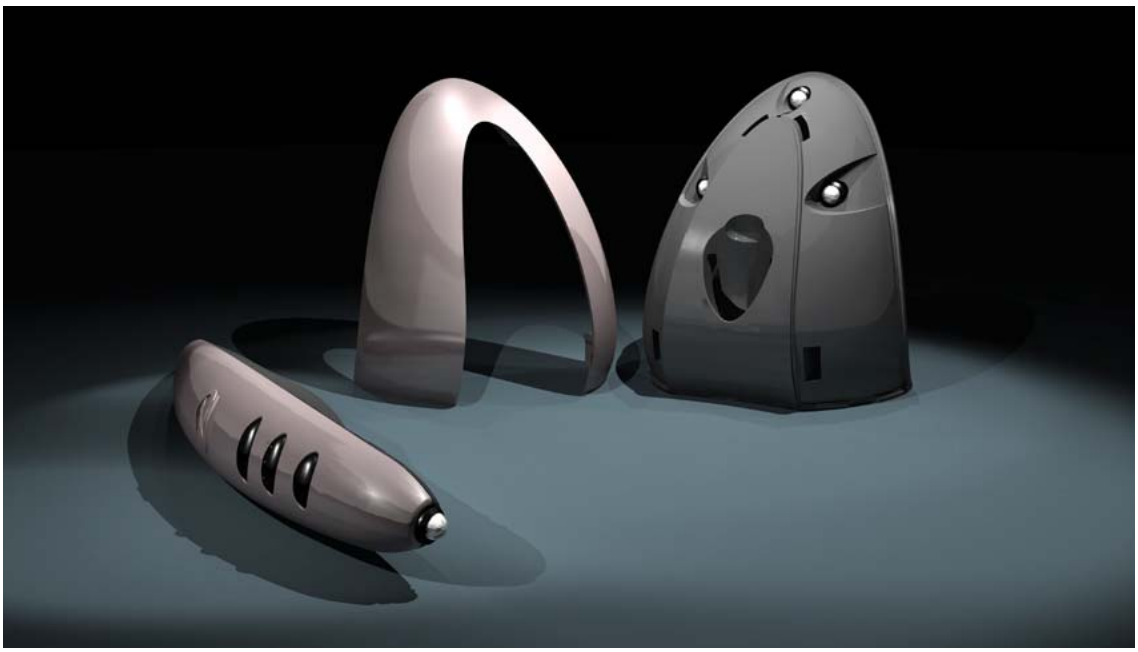

Figure 39. *Zeptor*, a pen-based input device for PCs shown to the left and the radio receiver exposed to the right.

The detector signals are digitised into one bit and the digital signals fed into a dedicated ASIC. This infers the cursor movements transmitted to the PC by a second ASIC placed in the pen, as well. These control signals are sent to a receiver connected to the USB-port of the PC.

The optical system merely relies on high-pass filtering of the detector signals with subsequent digital processing to deduce up-down and left-right commands. Thus, a series of investigations on the zero-crossing statistics had to be conducted in order fully to benefit from the statistical behaviour of these signals.

3.5.5 Characterisation of light sources

F. Pedersen and M. L. Jakobsen
E-mail: michael.linde.jakobsen@risoe.dk

As a part of the Centre for Miniaturizing of Optical Sensors, MINOS (http://www.sensortec.dk/stc.htm), we are investigating the potential of using miniature and low-cost light sources for the next generation of optical sensors. The need for sensors and particularly non-contact optical sensors is increasing rapidly these years as conditional monitoring in more traditional manufacturing becomes important and, further, as the end products themselves are expected by the consumers to be more intelligent and automated. Thus, low-cost, miniaturisation, and high reliability are necessary demands for the sensor technology in the future. Within the MINOS project the concept of micro-optical sensor systems is studied, including miniature light sources, detectors, diffractive gratings, refractive miniature structures and their replication in plastic, as well as technologies for packing these micro-optical components.

This year our main contribution has been a market analysis of commercially available semiconductor-based light sources and a detailed characteristic of a minor selection of some of these that are particularly interesting for MINOS. The light sources, which have been selected for characterisation, range from near UV to near infrared wavelengths and include both incoherent and coherent devices such as light-emitting diodes (LEDs), edge-mitting lasers (EELs) and vertical-cavity-surface-emitting lasers (VCSELs). VCSELS are particularly

attractive for this programme due to their low power consumption, low cost, extreme compactness and low sensitivity to temperature and handling.

MINOS has interest in incoherent light sources for illumination of spectroscopic samples. The demand for this type of light source is a stable spectrum within the maximum rated operating temperature range and within a given time interval during pulsed operation. Coherence is important for all the other types of micro-optical sensors that are developed in MINOS. Thus, line spectra, coherence length, interference modulation depth and capability of generating speckles are investigated on the laser diode candidates. In many cases the combination of laser diodes and optical diffractive elements requires precise control of the optical wavelength within, e.g., the maximum rated operating temperature range and, particularly, mode hopping could impose a serious problem.

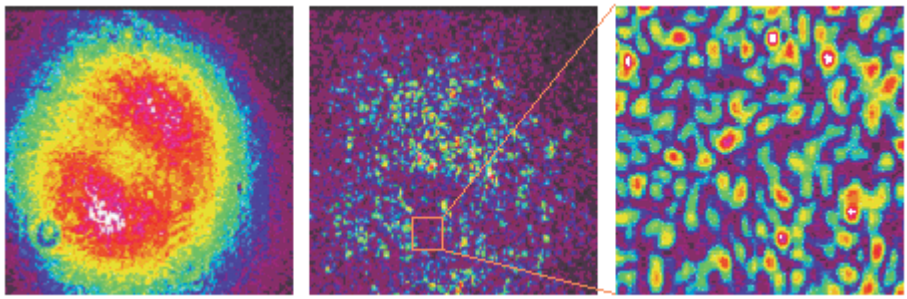

a. b. c.

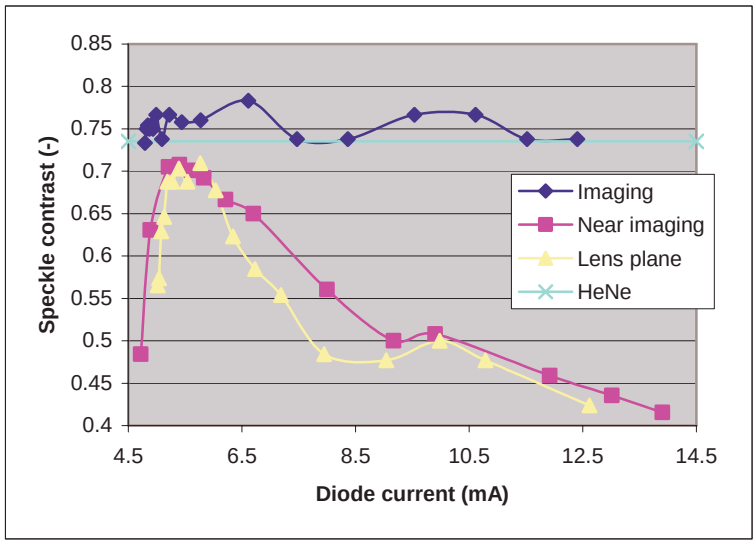

Figure 40. Speckle contrast for a VCSEL as a function of the injection current.

Generally, a VCSEL operates in a single longitudinal mode, while it supports several transversal modes, and competition among these are likely to occur. The optical geometry of the VCSEL is isotropic; consequently, the polarisation of emitted light will depend on the active modes and introduces another parameter to be considered in the optical design. In Figure 40 the speckle contrast for a VCSEL has been plotted versus the injection current. The speckle is formed by imaging a diffuse glass plate (sand blown) onto a CCD camera (Figure 40 b), and by illuminating the glass plate with light from e.g. the VCSEL (Figure 40 a). The area of spatial coherence for the source is only a fraction of the beam profile; as a result, probably only a single transversal mode is generating these speckles (Figure 40 c) – and the speckle contrast is similar for the speckle formed by using, e.g., a HeNe laser for illumination.

By moving the glass plate out of focus, several modes start to contribute to the speckles and the contrast decreases. In the extreme case where the glass plate is moved to the lens plane, the speckle contrast becomes a clear function of the total number of transversal modes emitted by the VCSEL – and thereby the diode current. When the speckle contrast reaches its maximum just beyond the threshold current, the VCSEL is presumably operating in only one or two transversal modes.

The investigation of the commercial market for these light sources has resulted in a database with more than 350 different laser diodes. A report will be written in the beginning of next year where the potential of using today's commercially available semiconductor-based light sources for miniaturised optical sensors will be evaluated

3.6 Knowledge-based processing

3.6.1 Machine learning techniques

T. M Jørgensen and C. Linneberg
E-mail: thomas.martini@risoe.dk

The area of machine learning deals with the problem of determining from a large space of potential hypotheses the one(s) that with the use of any prior knowledge can best explain a set of experimental data. Machine learning algorithms come to play in situations where the assumptions underlying traditional statistical methods do not apply. With respect to classification problems the available data correspond to a number of examples generated from a real world phenomenon, and each example can be categorised as belonging to a specific class. Based on the available data one must generate a model that correctly predicts the labels of previously unseen data generated from the same phenomenon. Accordingly, the aim of a machine-learning algorithm is to minimise the so-called generalisation error. An example would be to predict from a number of conditional parameters whether a patient suffers a given disease or not.

Variable selection

When the data/examples are described by a large number of variables relative to the number of examples, it is of utmost importance to have algorithms (data mining tools) that can extract informative features and relations from the high-dimensional input space. Significant features might be described by individual variables, but will in general be hidden in combinations of variables. Finding discriminative features corresponds to finding transformations of, and directions within, the input space, which are capable of separating examples having different class labels.[1] By transforming the original data representation into a suitable feature space, it is more likely for the classification algorithm to be successful. It is common to use some kind of singular value decompositions, e.g. principal component analysis (PCA), to form sensible data representations. However, algorithms like PCA, which is normally applied on the full-dimensional input space, do not take advantage of the fact that the class labels of the training examples are known. We have developed a feature selection strategy based on performing linear discriminant analysis within a number of randomly chosen subspaces of the input space.[2] By searching in a number of subspaces instead of just considering the full input space, we have the possibility of detecting discriminative features that would easily be "overlooked" if we simply considered all input variables at a time. The produced linear models are ranked and the best performing models are used to define linear transformations of the original

variables. The resulting set of variables is then used as input variables to train a classifier. The combination of our variable selection scheme and an n-tuple classification module has been successfully applied in a data mining project performed for a customer and in a benchmarking competition comparing a range of classification/regression models.

Ensemble of classifiers

By combining a number of weak, but uncorrelated classifiers it is in general possible to build a voting committee that performs better than a single strong classifier. Ideally, the individual classifiers should each be fairly accurate and make their errors in different parts of the input space. Given a specific set of training examples, standard decision tree algorithms like CART and C4.5 will output a unique model due to their deterministic nature. In order to obtain a set of classifiers that are grown with the same algorithm, but have low intercorrelations, it is necessary to have different kind of randomisation methods integrated. Resampling of the training set (so-called bagging) is one way to obtain different classifiers, but it is also possible to introduce randomisation in the step of determining the decision criterion for a given node in the tree. For a classification model related to the ensemble concept, we have recently demonstrated that a modified decision scheme that improves the performance of the classifier can be achieved. Due to the close relationship between the model that we analysed and ensembles of randomised decision trees, we have proposed and investigated the use of an equivalent modification of the decision boundaries in a more general setting. In addition to broadening the usability of an ensemble of randomised classification models, the suggested technique also incorporates the capability of adequately dealing with specific losses/costs associated with different kinds of prediction errors.

1. C: Linneberg, A. Höskuldsson, Combined principal component preprocessing and n-tuple neural networks for improved classification. J. Chemometr. (2000) **14** , 573-583.
2. T.M. Jørgensen, C. Linneberg, Subspace projections - an approach to variable selection and modeling. In: Putten, P. van der; Someren, M. van (eds.), CoIL challenge 2000: The insurance company case. LIACS-TR-2000-09 (2000) Paper no. 26.

4. Plasma and fluid dynamics

4.1 Introduction

J. P. Lynov
E-mail: jens-peter.lynov@risoe.dk

A unifying theme of the research performed in the Plasma and Fluid Dynamics programme is the dynamic behaviour of continuum systems. The continuum systems under investigation cover fluids, plasmas and solids. In the case of solids, the research is carried out in the fields of optics and acoutics as well as in their borderland called opto-acoutics. Both linear and nonlinear problems are addressed in a combination of experimental, numerical and theoretical studies. Scientific computing in a broad sense plays a major part in these investigations and includes theoretical modelling of the physical phenomena, development of numerical algorithms, visualisation of the computed results and last, but not least, validation of the numerical results by detailed comparisons with carefully conducted experiments.

Due to the broad approach to the problems, the various projects are scientifically overlapping, not only inside the programme, but to a large extent also with projects in the rest of the department as well as in other departments at Risø. This overlap is considered an expression of strength since it gives rise to considerable synergy between different parts of the laboratory.

The goals of the scientific studies are two-fold: on the one hand the investigations aim at achieving a deeper understanding of the fundamental behaviour of complex physical and technical systems; on the other the acquired knowledge is sought utilised in the definition and design of solutions to specific technological problems. In the following three subsections, descriptions of the scientific projects carried out during 2000 have been collected under the headings: *fusion plasma physics*, *fluid dynamics* and *optics and acoustics*.

4.2 Fusion plasma physics

4.2.1 Taming drift-wave turbulence

C. Schröder, T. Klinger* (*Institut für Physik, Ernst-Moritz-Arndt Universität Greifswald, Germany), D. Block**, A. Piel** (**Institut für Experimentelle und Angewandte Physik, Christian-Albrechts Universität Kiel, Germany), G. Bonhomme (Laboratoire de Physique des Millieux Ionisés, Université Henri Poincaré Nancy, France) and V. Naulin*
E-mails: volker.naulin@risoe.dk, schroeder@physik.uni-greifswald.de

Drift wave turbulence is basically a spatiotemporal phenomenon and, thus, it is barely expected that a purely temporal or spatial control technique proves to be efficient and robust. A number of experiments on temporal feedback stabilisation of plasma instabilities have been reported, with often ambiguous conclusions. Recently, the suppression of several drift-type instabilities has been demonstrated in a linear device.[1] However, control was achieved by rather violent changes of global plasma parameters, which may be costly or even impossible in other cases.

An alternative approach is “control of chaos”,[2] where unstable periodic states, embedded in chaos, are stabilised by only tiny adjustments of one or more accessible parameters. The success of this conception has been demonstrated for various different plasma waves and instabilities.[3] Using a continuous, temporal feedback technique, a chaotic drift wave state has successfully been controlled by weak parameter perturbations.[4] Unfortunately, low-dimensional chaotic behaviour is rather exceptional for drift waves, since their complex dynamics tends to be of turbulent nature. A much more promising strategy to tame drift wave turbulence over a wide parameter range is open-loop synchronisation acting in both space and time.[2,5] We have conducted experiments and numerical simulations on open-loop synchronisation of drift wave turbulence in a magnetized plasma with cylindrical geometry. For the synchronization experiments an arrangement of eight stainless-steel electrodes (octupole exciters) is placed in flush-mounted geometry in the edge region of the plasma column. Using a phase shifted time-dependent bias, this enables us to imprint specific waves at specific frequencies. For the numerical simulations an extension of the Hasegawa-Wakatani model is used in 2D disk geometry, with the outer drive modelled as a parallel current. Both experiment and numerical simulation show that relatively weak exciter signals synchronise turbulent drift wave states and, thereby, establish the preselected single-drift mode if the later is in resonance with a naturally excited wave (see Figure 41 and Figure 42).

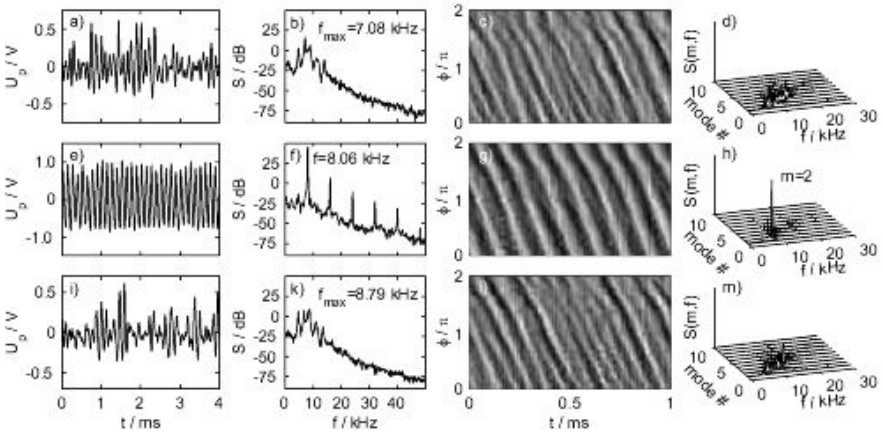

Figure 41. Temporal and spatiotemporal drift wave dynamics: experiment. The three rows correspond to the unperturbed case, active exciter with a co-rotating field and active exciter with counter-rotating field, respectively. The four columns show the density fluctuations, the frequency power spectrum, the spatiotemporal density fluctuations and the frequency mode number power spectrum. Power spectra are obtained by Fourier transformation of the temporal and spatiotemporal data.

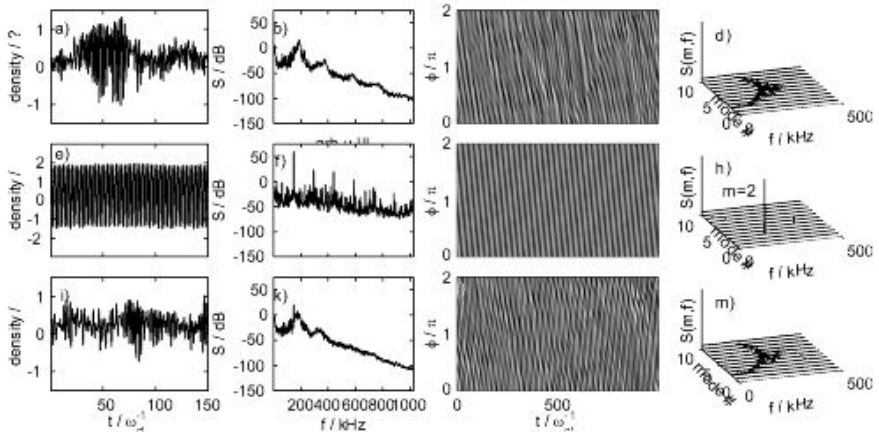

Figure 42. Temporal and spatiotemporal drift wave dynamics: simulation. The figure is arranged as in Figure 41. Excellent agreement is found between experiment and simulation.

The numerical solution allows access to the complete fields and the transport (Figure 43).

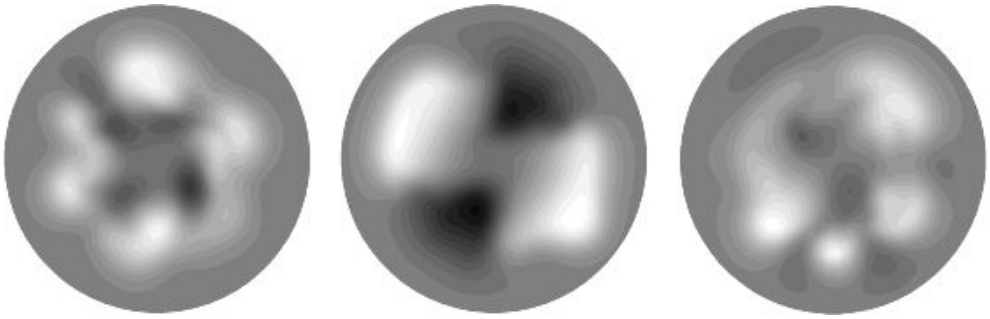

Figure 43. Snapshots of the 2D mode structure as taken from the simulations. Grey scale plots of the density fluctuations; from left to right: Unperturbed case, co- and counter-rotating current profiles.

This is an important step towards control of this kind of turbulence. 3D simulations are underway to establish the effect on transport and to better relate to experimental parameters.

1. A. K. Sen, J. S. Chiu, J. Chen, and P. Tham, Plasma Phys. Control. Fusion **39**, A333 (1997).
2. H. G. Schuster, editor, *Handbook of Chaos Control*, VCH-Wiley, Weinheim, 1999.
3. T. Klinger et al., Phys. Rev. Lett. **79**, 3913 (1997).
4. E. Gravier, X. Caron, and G. Bonhomme, Physics of Plasmas **6**, 1670 (1999).
5. T. Shinbrot, Advan. Phys. **44**, 73 (1995).

4.2.2 Comparison of simulations with simple plasma experiments

V. Naulin, D. Block, O. Grulke*, F. Greiner*, S. Niedner*, A. Piel* and U. Stroth**
*(*Christian-Albrechts Universität Kiel, Germany)*
E-mail: volker.naulin@risoe.dk

Small-sized plasma experiments with a simple geometry are an ideal playground to test various hypotheses concerning, e.g., plasma transport and the appearance of coherent structures in these nearly 2D systems. Well-developed diagnostics and good control of the experiments make it possible to verify numerical codes with these experiments. Their relatively low plasma temperatures put the relevant spatial sizes in a range where today's numerical resolution is sufficient to simulate the whole plasma cross-section. At Kiel University probe measurements of the linear experiment KIWI and the simple magnetised torus TEDDI will be compared with results from Risø's 2D and 3D codes. Information about coherent structures, turbulent transport and statistical properties of the plasma turbulence shall be obtained. Plasma properties that are difficult to access, such as three-dimensional mode structures and transient transport events, will be made available from the numerical simulations.

4.2.3 Benchmarking 3D codes of drift-Alfven turbulence

V. Naulin and B.D. Scott (Institut für Plasmaphysik, Garching, Germany)
E-mail: volker.naulin@risoe.dk

The Risø TYR code has been developed to model plasma turbulence in the edge region of large-scale fusion devices. It includes the dynamics of drift-wave turbulence and the effects of the complex equilibrium magnetic field structure of toroidal devices. The code has recently

been extended from an electrostatic 3-field model to a 5-field electromagnetic model with parallel Alfven dynamics considered. Density, electrostatic potential as well as current and parallel ion-velocity fluctuations are included. To test and verify the code and to gain insight into strengths and weaknesses of the underlying numerical schemes, the code is benchmarked against the DALF family of codes developed by Bruce Scott at the IPP Garching. Benchmarking of these kinds of codes gets more and more necessary as the code complexity increases. For plasma turbulence simulations, systematic benchmarkings have not yet been established. Thus, a large number of test runs were conducted in various regions of the parameter space. For the linear and weakly non-linear regimes excellent agreement between the codes was found. Figure 44 shows the initial linear wave structure in a sheared magnetic field, close to a resonant flux surface. In a second campaign the non-linear properties of both codes will be addressed. A focus of the benchmarking is on the electromagnetic effects, which are difficult to include into a code in a stable manner, but which have proved to be of importance to the scaling of, e.g., the transport.

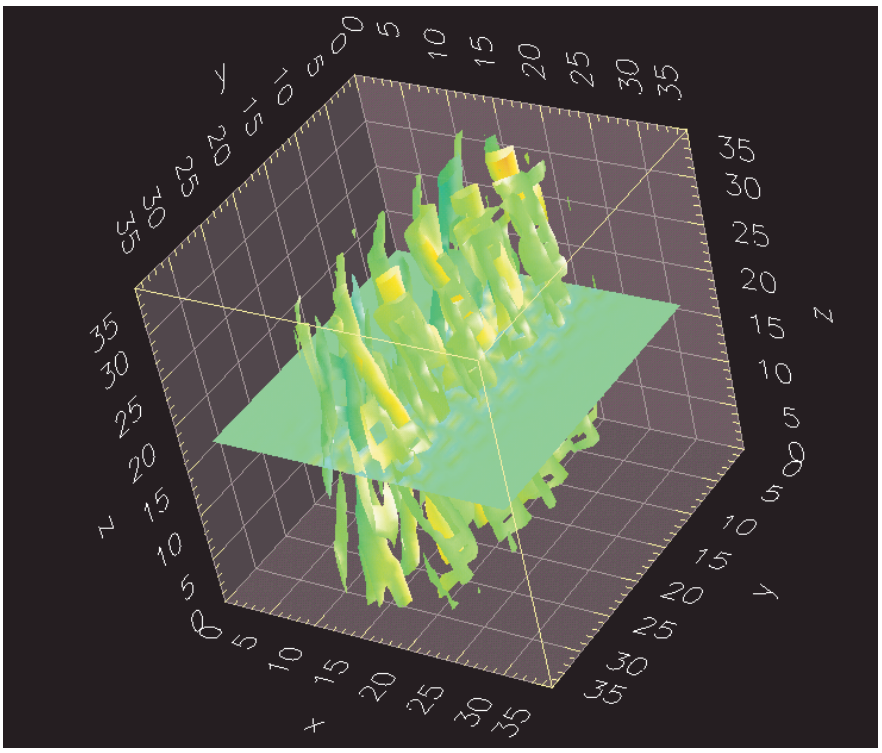

Figure 44. Density fluctuations in a sheared magnetic field. The alignment of the fluctuations with the magnetic field structure and initial localisation at the resonant flux surface can be clearly seen.

4.2.4 Anomalous diffusion of particles and the relation to transport in vortex-dominated turbulence

V. Naulin, Th. Jessen, P. Michelsen, A. H. Nielsen and J. Juul Rasmussen
E-mail: volker.naulin@risoe.dk

The turbulent diffusion in vortex-dominated 2D turbulence is found to be well described by a random-walk process with at least two different step lengths and durations in each of the two directions, parallel and perpendicular to a background density gradient. One set is given by the characteristic linear times and length scales of the wave motion, the other is determined by the

trapping times and the vortex velocities. The appearance of two different sets of scales for the Brownian motion corresponds to anomalous diffusive behaviour. For realistic drift-wave turbulence it is found to result in superdiffusion in the direction of the wave propagation and sub-diffusion along the gradient.[1]

Having determined the particle diffusion coefficient, the question arises how this compares with the anomalous ExB-flux $\Gamma = < \tilde{u} \tilde{v}_r >$ for the case of drift-wave turbulence. Using the conservation of potential vorticity a condition can be derived showing the equivalence for particle diffusion and density transport. However, we find that if the turbulence is caused by an external drive, this relation no longer holds. Then one can have finite mixing and particle diffusion due to the turbulence D > 0 and exactly zero flux. This severely limits the applications of Hasegawa-Mima type equations to describe particle diffusion and transport.

1. V. Naulin, A.H. Nielsen and J. Juul Rasmussen, Phys. Plasmas 6, 4575 (1999).

4.2.5 Turbulent equipartition and dynamics of transport barriers in electrostatic turbulence

V. Naulin, J. Nycander (FOA, Stockholm, Sweden) and J. Juul Rasmussen
E-mail: volker.naulin@risoe.dk

The generation of large-scale flows by the rectification of small-scale turbulent fluctuations is of great importance both in fluids, e.g. geophysical flows, and in magnetically confined plasmas.[1] The usually sheared flows act back on the turbulence by shearing apart and, thereby, suppressing fluctuations on all scales, thus setting up transport barriers.

In hot magnetised plasmas the main cross-field transport is anomalous and ascribed to low-frequency electrostatic fluctuations. It is generally recognised that self-consistently developing large-scale poloidal - or zonal - flows strongly reduce the radial turbulent transport by "quenching" the turbulence. This mechanism may be responsible for some forms of confinement enhancements in magnetically confined plasmas, e.g. the celebrated H-mode regime.

Since the turbulence and the associated transport cannot be avoided, it is essential to understand how the zonal flows - the transport barriers – develop and control the turbulence as well as the transport.

We investigate the evolution of turbulence and the associated formation of transport barriers – zonal flows - in a model system for 2D electrostatic pressure-driven flute modes in an inhomogeneous magnetic field. The fluctuations are flux driven and supplied via a Rayleigh-Taylor instability setting in when the pressure gradient exceeds the magnetic field strength gradient. This pressure gradient is forced by a constant temperature difference between the two sidewalls of the computational domain. The temperature difference is sustaining a thermal flux.[2]

Turbulent equipartition predicts the background profiles and gradients resulting from the homogenisation of the Lagrangian invariants due to the strong mixing by the turbulence. This is clearly revealed for large aspect ratios, $L_y/L_x > 3.8$, where x is in the direction of the gradients (“radial direction”) and y is perpendicular to the gradients (“poloidal direction”) (the confining magnetic field is in the z-direction). These profiles are flatter than the profiles that will result from classical viscous diffusion in the absence of the turbulence. For small aspect ratio, however, the numerical simulations show a strong tendency for the evolution of a poloidal shear flow that quenches the effective turbulent mixing and the transport changes from being anomalous, i.e. fluctuation driven, to being diffusive. Thus, a much steeper gradient evolves on a diffusive timescale. Subsequently, the resulting steep gradient is prone

to the Rayleigh-Taylor instability again and short burst-like destabilisation occurs locally whereby the profiles are flattened out. The transport associated with these burst-like events propagates down the background gradient and has properties of avalanche-like events. This behaviour is illustrated in Figure 45.

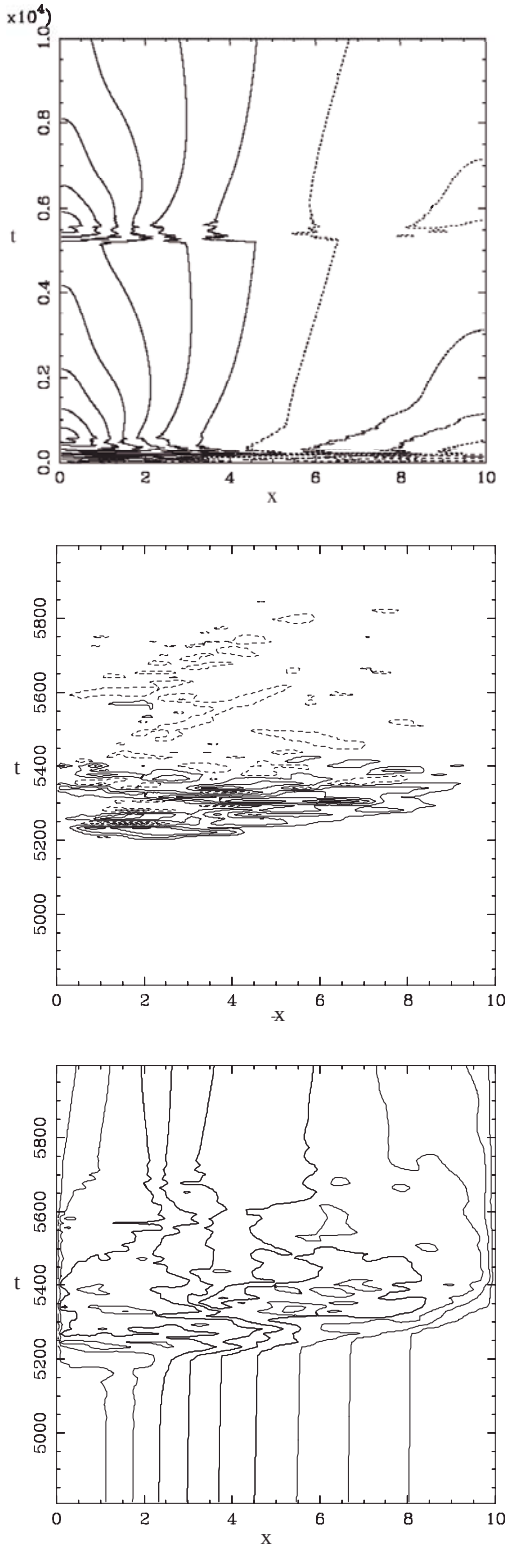

Figure 45. Upper panel: Contours of the zonal velocity, V, over time. Middle and lower panels: Enlarged with respect to time for the flux burst $\Gamma_T(t)$ plotted versus (x,t) and the temperature profile over time.

In the upper panel we show the evolution of poloidal flow by plotting the contours of the velocity V in the x-t plane. A regular zonal flow is seen to establish at around t = 100 and to dominate the evolution for a long period, where the turbulence is suppressed. The flow is slowly decaying and at t = 5200 it has become weak enough to allow the build-up of the turbulence again. This is accompanied by a strong burst in the thermal flux, as seen in the second panel, and the temperature profile is flattened out again (see the last panel).

1. P.W. Terry, Rev. Mod. Phys. **72**, 109 (2000).
2. V. Naulin, J. Nycander and J. Juul Rasmussen, Phys. Rev. Lett. **81**, 4148 (1998)

4.2.6 Shear flow stabilisation of pressure driven flute modes

E.S. Benilov (Dept. Mathematics, University of Limerick, Ireland), V. Naulin and J. Juul Rasmussen
E-mail: jens.juul.rasmussen@risoe.dk

Global flows with sheared velocity profiles are generally found to have profound influence on the evolution of a class of Rayleigh-Taylor like instabilities (RTI). This has been discussed both in the context of neutral fluids, where the RTI appears in cases with an inverted stratification so that heavier fluid is “resting” on top of lighter fluid, and in the context of magnetised plasmas, where the pressure gradient perpendicular to the magnetic field is stronger than the magnetic field gradient.

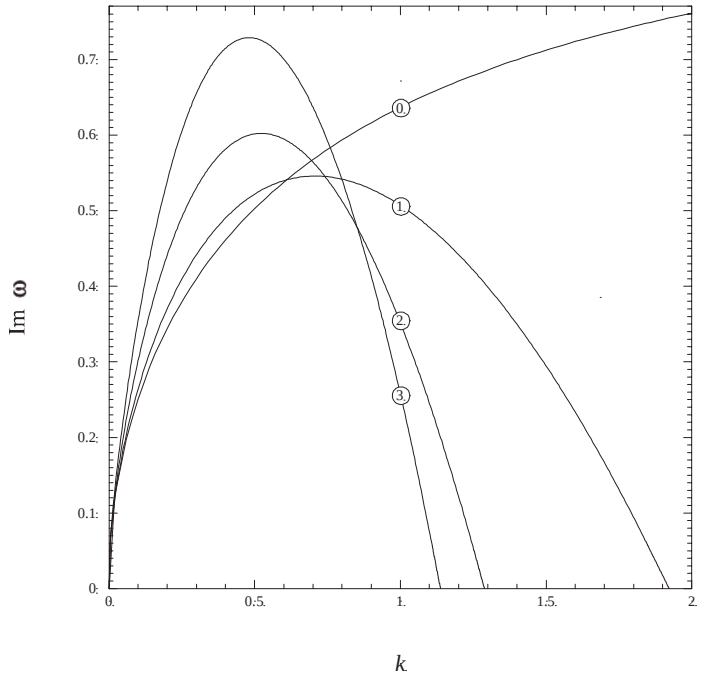

Figure 46. Growth rate of the zeroth (most unstable) mode versus wave number for an inverted stratification. The curve numbers correspond to the value of U_0.

We have considered the eigen-value problem governing the stability properties of these situations. In the long wave limit the plasma and fluid cases reduce to a similar equation. To be specific, we consider a parallel flow in a density-stratified ocean in such a way that both streamlines and surfaces of equal density are horizontal. In the plasma case this corresponds to a flow (in the y-direction) perpendicular to the pressure gradient (in the x-direction) and to the magnetic field (in the z-direction) with a gradient in the x-direction. By linearising the

governing equations we obtain an equation corresponding to the Taylor-Goldstein equation[1] for the x-variation of the stream function. Generally, it is found that the sheared flow acts destabilizingly; i.e., on an infinite domain it will extend the region of instability. We have, however, found that for realistic density/pressure profiles (*tanh*(x)) and with fixed boundaries in the x-direction sheared flows may act stabilisingly for part of the wave number spectrum. This is illustrated in Figure 46 where a shear flow with the profile $U = U_0$ *tanh(*x) is applied. The RTI is not completely suppressed, but short wavelengths (in the y-direction) are stabilised, and the shear flow has introduced a finite k_c so that perturbations with $k > k_c$ are stabilised. Similar behaviour is found for a linear shear flow $U = U_0$ x. This will imply that for a system with a finite period in the y-direction the RTI may be stabilised when the period $L < 2\pi/ k_c$.

1. J.W. Miles, J. Fluid Mech. **10,** 496 (1961) and L.N. Howard, J. Fluid Mech. **10,** 509 (1961).

4.2.7 Reynolds stress and shear flow generation

S. B. Korsholm, V. Naulin, J. Juul Rasmussen, P. K. Michelsen and L. Garcia
(Universidad Carlos III, Madrid, Spain)
E-mail: soeren.korsholm@risoe.dk

One of the major challenges in the research towards a fusion power plant is the understanding and control of the plasma turbulence leading to anomalous transport of particles and energy.

Experimentally obtained confinement schemes such as H-mode confinement regimes show a drastically reduced radial transport. The generation of H-mode confinement regimes seems to be closely related to poloidal shear flows in the edge region of the plasma. Generally, it is observed experimentally and in numerical models that shear flows in plasmas suppress turbulence and transport. The generation mechanism of these flows is thus of great interest. In this numerical work we investigate the relation between the so-called Reynolds stress[1] and the poloidal flow generation.

The model used in the numerical investigations is the three-dimensional drift wave Hasegawa-Wakatani model.[2] The simulations are performed in a slab geometry periodic in *y* and *z* (corresponding to the poloidal and toroidal directions, respectively), while we use non-permeable walls in the radial direction, $\phi(x=0) = \phi(x=L_x)=0$ and $n(x=0)=n(x=L_x)=0$, i.e. Dirichlet boundaries in *x*. ϕ is the electrostatic potential fluctuations, n is the density fluctuations and L_x is the domain length. The simulations are performed using pseudo-spectral methods.

The Reynolds stress is a measure of the anisotropy of the turbulent velocity fluctuations that produce a stress on the mean flow. This may cause acceleration of the flow in the plasma, which, e.g., could be a poloidal flow (*y*-direction). The Reynolds stress is defined as:

$$\mathrm{Re}_\phi = -\langle v_x v_y \rangle_{y,z} = \left\langle \frac{\partial \phi}{\partial y} \frac{\partial \phi}{\partial x} \right\rangle_{y,z} .$$

To determine the Reynolds stress one needs accurate measurements of the potential perturbations. However, accurate measurements of the potential perturbations are quite difficult, and nearly impossible in hot plasmas in large devices. Thus, a pseudo-Reynolds stress based on much easier obtainable density measurements is investigated. The pseudo-Reynolds stress is defined as:

$$\mathrm{Re}_n = \left\langle \frac{\partial n}{\partial y} \frac{\partial n}{\partial x} \right\rangle_{y,z} .$$

We find that the Reynolds stress Re_ϕ and the pseudo-Reynolds stress Re_n are strongly correlated with a correlation of 0.8. The reason for the strong correlation between Re_n and Re_ϕ is that the density and the potential fluctuations are strongly correlated for drift waves.

The conclusion of this work is that the pseudo-Reynolds stress may give a good estimate of the real Reynolds stress and it may therefore be possible to predict flow generation by measuring density fluctuations. In Figure 47 below we compare the poloidal flow with the flow predicted by the pseudo-Reynolds stress. The observed behaviour may, however, be specific to this particular turbulence model and more models have to be investigated.

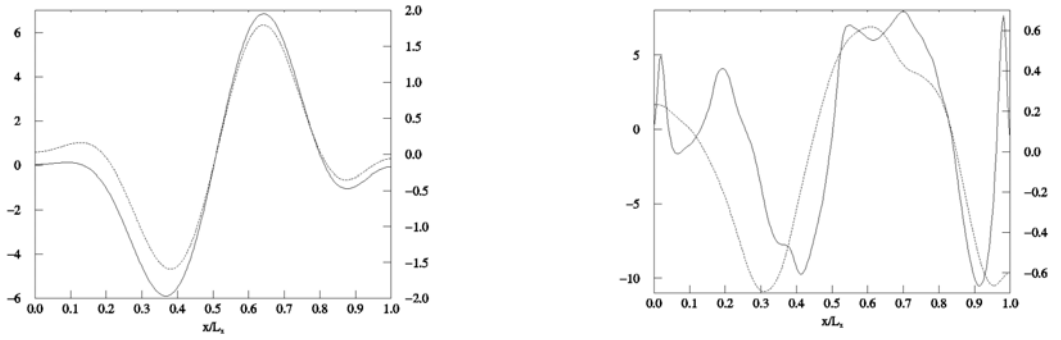

a) b)

Figure 47. The poloidal flow (dashed line) compared with the flow predicted by the drift wave pseudo-Reynolds stress (full line) at two instants in time a) t = 75 and b) t = 125.

Finally, we have looked into the effect of a misaligned probe array for determination of the Reynolds stress. It was found that the probe array in an experiment should be aligned with the magnetic field within 5-7° in order to get a good estimate of the Reynolds stress. This criterion should be possible to fulfil. In Figure 48 a schematic presentation of the probe array used in the numerical investigations is given, as well as the results of the misalignment calculations.

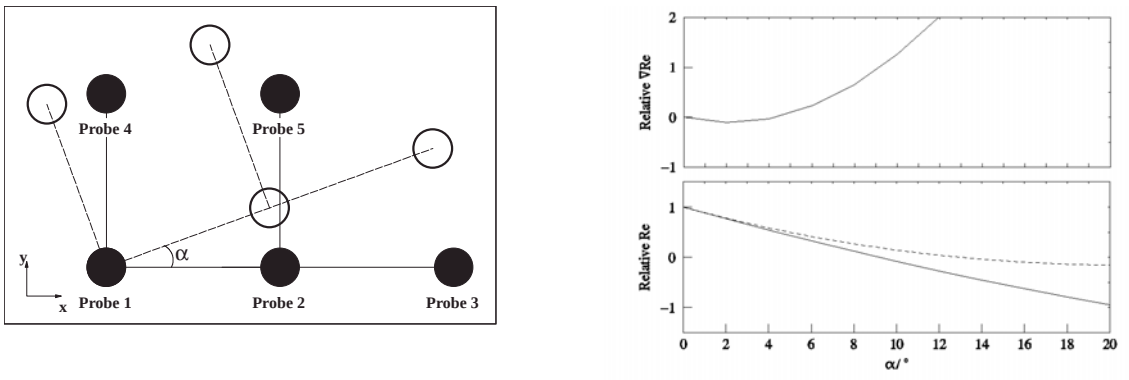

a) b)

Figure 48. a) The probe array used in the numerical investigations of the effects of misalignment. b) The upper graph shows the difference of the ”measured" divergence of the Reynolds stress and the value for perfect alignment relative to the latter as a function of the misalignment angle α. The lower graph shows the change of the Reynolds stresses measured by probes 1, 2, 4 (full line) and probes 2, 3, 5 (dashed line) relative to the Reynolds stresses for perfect alignment.

1. D. J. Triton, *Physical Fluid Dynamics*, Clarendon Press, Oxford, 2nd ed., 1988, Chapter 19.
2. A. Hasegawa and M. Wakatani, Phys. Rev. Lett. **50** (1983) 682-686.

4.2.8 Upgrade of and measurements using the LOTUS diagnostic

N. P. Basse, S. Zoletnik (*CAT-Science, Budapest, Hungary), M. Saffman***
*(**Department of Physics, University of Wisconsin, USA), M. Endler****
*(*** Max-Planck-Institut für Plasmaphysik, Teilinstitut Greifswald, Germany),*
P.K. Michelsen, B.O. Sass, J.C. Thorsen and H.E. Larsen
E-mail: nils.basse@risoe.dk

The 1999 Wendelstein 7-AS (W7-AS) campaign came to an end in August 1999. The purpose of the subsequent shutdown was to install the so-called 'island divertor' system in the machine, which is designed to be optimised for ι_a = 5/9 plasma operation (see Ref. 1 and references therein). The shutdown allowed us to make a series of improvements to the LOTUS (LOcalised TUrbulence Scattering) density fluctuation diagnostic, including:

- New acquisition rack with improved laser shutter system and other safety systems
- Upgrade of laser exciter (new high-voltage resistors, new current control card)
- New laser stabilisation system using a photovoltaic detector and modulation of the laser output mirror
- Optical rail to ease alignment on the vertical transmitting table in the W7-AS basement
- Lens holders for modified diagnostic position
- Computer upgrade

The work on these improvements predominantly took place at Risø during the autumn of 1999 and the spring of 2000.

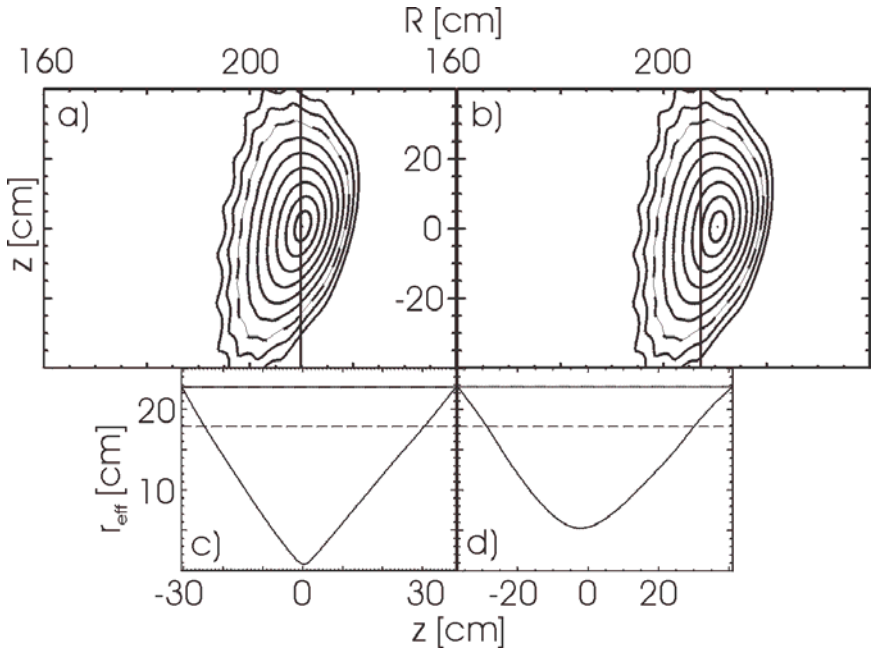

Figure 49. Comparison of measurement position relative to ι_a = 0.344 flux surfaces in 1999 (inset a, R = 209.8 cm) and 2000 (inset b, R = 207.2 cm). The vertical lines indicate the approximate measurement volume position. Insets c and d show the effective radial coordinate r_{eff} along the vertical measurement volumes. The dashed lines show the last closed flux surface, and the dotted lines show the plasma boundary.

The divertor installation meant that one of the modules was placed directly above our lower access port. In collaboration with IPP-Garching,[2] a hole was made in one of the recessed tiles to allow our four laser beams to pass through. The hole is rectangular (40 mm in the toroidal direction φ and 42 mm in the major radius direction *R*) with an addition to allow

extra flexibility. The limitation posed by the divertor (previously full access through a 200 mm diameter window) means that it is no more possible to measure with one wide measurement volume; measurements are now resticted to two narrow volumes. The centre of the hole has been displaced with respect to the centre of the window; inward along *R* by 19.5 mm, toroidally by 33.1 mm. The toroidal change is very slight compared with a machine circumference of about $2\pi R \sim 12500$ mm, but the major radius change is more significant as can be seen in Figure 49.

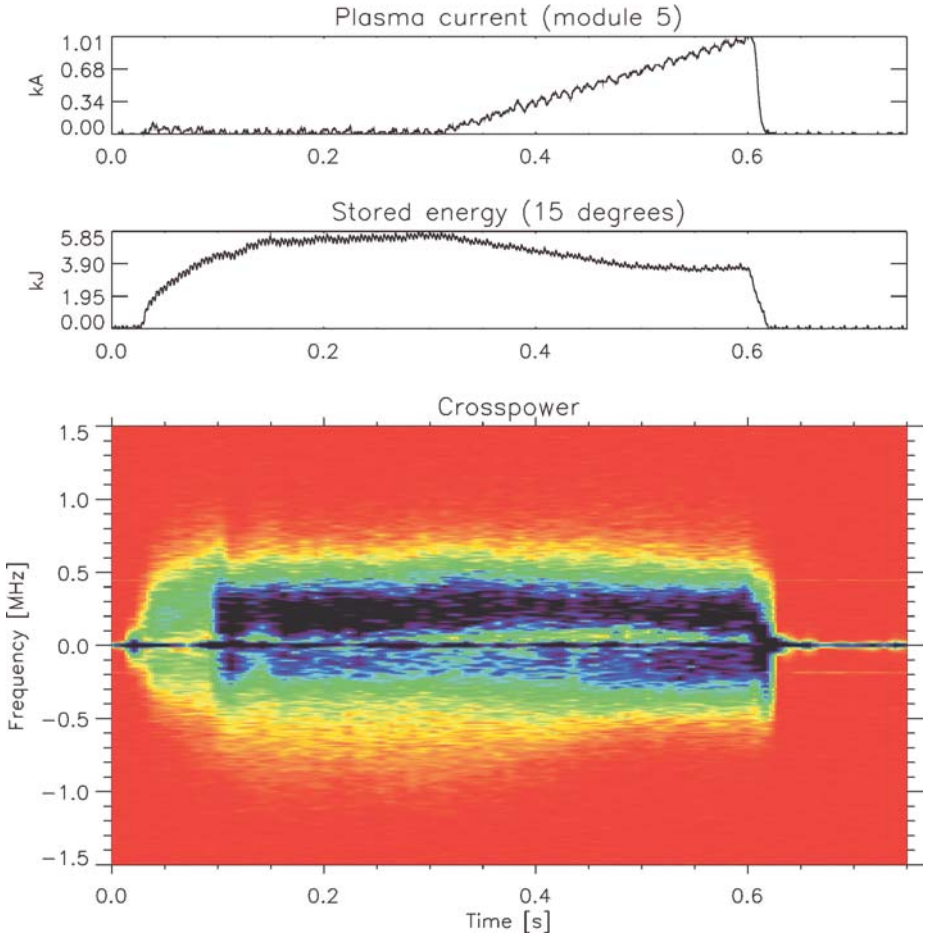

Figure 50. From top to bottom: Net plasma current, stored energy and crosspower amplitude (linear scale) versus frequency and time. The wave number of the density fluctuations measured was 20 cm^{-1}.

We now briefly discuss the dedicated experimental programme in the 2000 campaign. In 1999 we made a series of experiments to investigate the changes of density fluctuations during slow current induced confinement transitions.[3] The initial plan was to redo previous experiments with the modified set-up, but due to in-vessel diagnostics and a bad torus conditioning (boronisation was impossible because of the planned December 2000 opening) a number of plasma parameters were changed. However, it was still possible to construct discharges where a slow current ramp induces a gradual confinement degradation. The main plasma parameters were: $\iota_a = 0.350$, $B_\varphi = 2.5$ T, $B_z = 12$ mT, 450 kW central ECR heating, deuterium gas, $n(r_{eff}=0) \sim 7\times10^{19}$ m^{-3} and $T_e(0) \sim T_i(0) \sim 1.3$ keV. A series of seven similar shots (#50031-50037) was made, where we changed the relative position of the measurement volumes between each one. An example of the measurements is shown in Figure 50. We measured density fluctuations at 20 cm^{-1}; the measurement volume separation was 19 mm, and the volume diameter (two times waist) was 7 mm. The top plot shows the plasma current

in kA. This was compensated to zero for the first 300 ms of the discharge and thereafter slowly ramped up to 1 kA (at 600 ms). The centre plot shows the corresponding stored energy in kJ. The maximum confinement is reached just before the current ramp is initiated at 300 ms. From that point on, the stored energy drops slowly in response to the current induced change of ι_a. The colour contour plot shows the crosspower amplitude between the two LOTUS measurement volumes on a linear scale versus frequency and time. Positive/negative frequencies are fluctuations travelling radially outward/inward along *R*. It is clear that there is a spin-down and amplitude increase of the two features having opposite frequencies as has been reported previously.[4] However, the interpretation is difficult because too many factors have been changed compared with our baseline experimental configuration. Moreover, the plasma confinement is extremely sensitive to changes around the $\iota_a = 0.35$ 'edge' of W7-AS. During the next experimental W7-AS campaign, which is to commence in March 2001, we will redo the experiments with parameters identical to those of the 1999 experiments. This will hopefully clarify the impact of the changed diagnostic position.

1. K. McCormick et al., Plasma Phys. Control. Fusion **41** (1999) B285.

2. Bertram Brucker (2000) Private communication.

3. R.Brakel et al., Plasma Phys. Control. Fusion **39** (1997) B273. R.Brakel et al., 25th EPS, ECA **22C** (1998) 423.

4. N.P. Basse et al., 27th EPS ECA **24B** (2000) 940-943.

4.2.9 Density fluctuation measurements in the Mega Amp Spherical Tokamak

S. B. Korsholm and G. Cunningham (Culham Science Centre, Abingdon, Oxfordshire, UK)
E-mail: soeren.korsholm@risoe.dk

The control of plasma transport is essential in the development of fusion energy as a power source. Transport of energy and particles out of a plasma has experimentally been shown to be governed by turbulent transport. An understanding of the plasma turbulence is thus important.

Previously, the study of turbulence had mainly been performed analytically and numerically, but over the last decade an increasing effort has been made to investigate plasma turbulence experimentally. Ideally, these investigations would require simultaneous measurements of small-scale fluctuations in the plasma temperature, density, electric potential, ion velocities and magnetic flux as well as the individual phase relationships. Such measurements are beyond the scope of present-day technology, despite the use of many different diagnostics. The measurements of some of the plasma properties, however, are possible and this year Risø staff has been involved in running the fluctuation reflectometer at the newly built Mega Amp Spherical Tokamak (MAST) located at Culham Science Centre, UK.

The experimental set-up is illustrated in Figure 51, where the MAST vessel is seen to the left. The system proved good at detecting H-modes (high confinement modes), which is illustrated in Figure 52. Future developments will include expansion to four frequency channels, and extension of the measured frequencies up to 6 MHz.

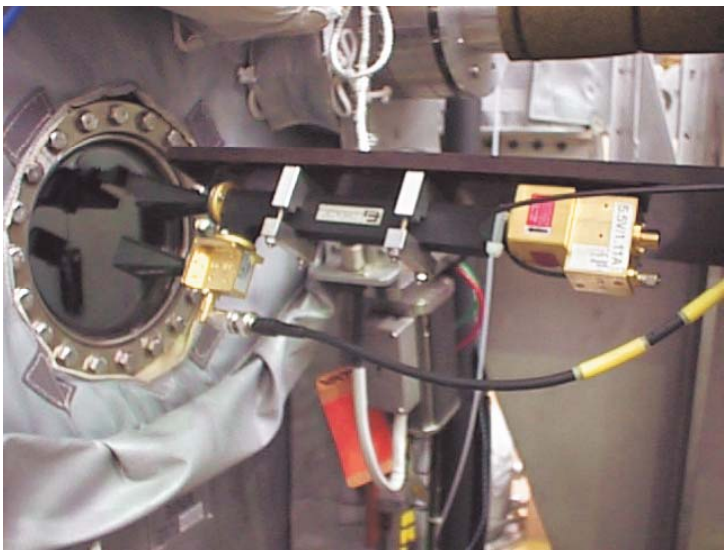

Figure 51. The MAST fluctuation reflectometer.

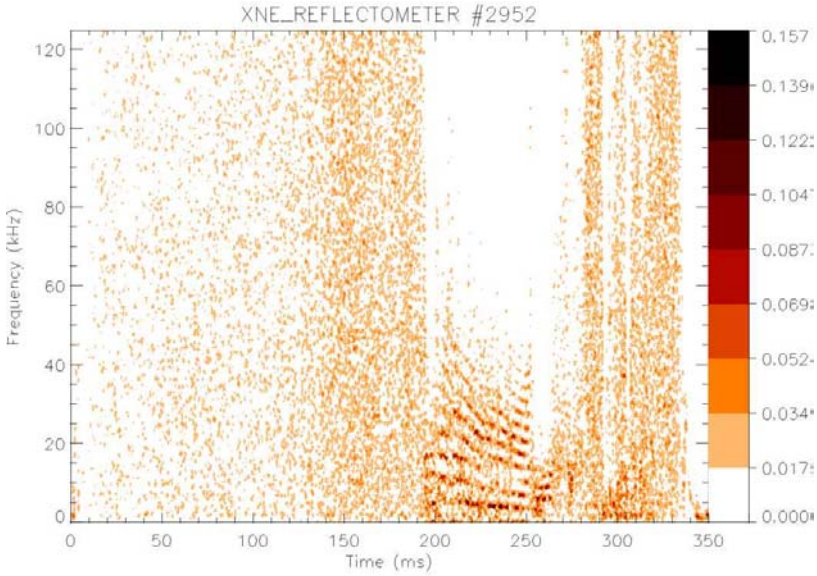

Figure 52. Spectrogram of MAST shot no. 2952 where the H-mode starts at t = 195 ms and a low frequency mode structure builds up. Data from the MAST fluctuation reflectometer.

4.2.10 Global perspective of Denmark's energy research

P. Dannemand Andersen (Systems Analysis Department), P.K. Michelsen and L. Nissen (Information Service Department)
E-mail: poul.michelsen@risoe.dk

An investigation of the international trends within Danish energy R&D was performed at the request of the Danish Energy Agency. An article describing the result of the work was used in the 1999 annual report of the Danish Energy Research Programme (ERP). The objective of the work was to put the Danish R&D activities within ERP in perspective by giving the reader (1) a short introduction to international trends of development within energy research and (2) an

overview of Denmark's strong points within energy research. The target group of the report was the general public. The new role of the research in society was described, especially for the energy research. Subjects for future energy research were estimated from key sources from WEC's, IEA's and Intergovernmental Panel on Climate Changes (IPCC) scenarios for the next century. The present research and development effort in technology was found from OECD's and IEA's statistics. Finally, some of the important energy technologies for the future were assessed.

4.2.11 Pellet injectors

P.K. Michelsen and B. Sass
E-mail: poul.michelsen@risoe.dk

Technical support to the groups that still have Risø-made pellet injectors has continued. The 8-shot pellet injector that was designed and produced at Risø more than ten years ago to the Dutch tokamak RTP at the FOM-Institute was recently transferred to MAST (Mega Amp Spherical Tokamak) at Culham Science Center, UK. After an initial test of the injector, the main injector unit was brought to Risø where all the gun barrels were changed to new ones with larger but different diameters in order to get larger pellets. A new cryostat was also installed and the whole unit was reconditioned. After returning to Culham the injector was successfully tested. The plan is to connect the injector to MAST with a very long and curved guide tube since the injector is located in a small room next to the torus hall.

4.3 Fluid dynamics

4.3.1 Formation of large-scale flows in rotating fluids by forced homogenisation of potential vorticity

J. van de Konijnenberg, V. Naulin, J. Juul Rasmussen and B. Stenum
E-mail: jens.juul.rasmussen@risoe.dk

Generation of large-scale mean flows by turbulent mixing at smaller scales is of great importance in various situations such as, e.g., geophysical flows. These so-called zonal flows will regulate the turbulence by suppressing the small-scale fluctuations and setting up transport barriers. A relatively simple description of the generation of zonal flows is provided by the idea of homogenisation of Lagrangian invariants, here the potential vorticity.

We have performed laboratory experiments in a rotating fluid with sloping bottom and numerical simulations based on the quasi-geostrophic approximation to investigating the formation of large-scale flows by mixing and homogenisation of the potential vorticity. Specifically, we consider a rotating tank with radially symmetric bottom topography and a rigid lid. The bottom has a constant slope in the radial direction, which may be either negative (the shallowest part is at the centre) or positive (the deepest part is at the centre). For this system the so-called potential vorticity $PV = \omega + \beta r$ is a Lagrangian conserved quantity. Here ω is the relative vorticity and β is proportional to the slope of the bottom. Thus, it is readily seen that an effective mixing that homogenises PV will - for $\beta < 0$ - lead to replacing the high PV near the centre with low PV from the outside, and this will appear as an anticyclonic vortex over the centre, "the pole", where ω will be lower than near the wall. For $\beta > 0$, on the other hand, a cyclonic vortex will appear.

In the experiment the mixing is forced by periodic pumping near the outer boundary of the tank at two azimuthally opposite positions. The azimuthally averaged forcing is consequently zero. The velocity field is measured by particle tracking in the horizontal plane. After a transient time of several tens of forcing periods, we observe the formation of a zonal velocity in the anti-cyclonic direction (for $\beta > 0$). The zonal velocity peaks in the region away from the forcing regime. In the forcing region a slight cyclonic flow is observed (see Figure 53). This is in agreement with the discussion above. As a control case, we checked that no zonal flow appeared in the case of a flat bottom.

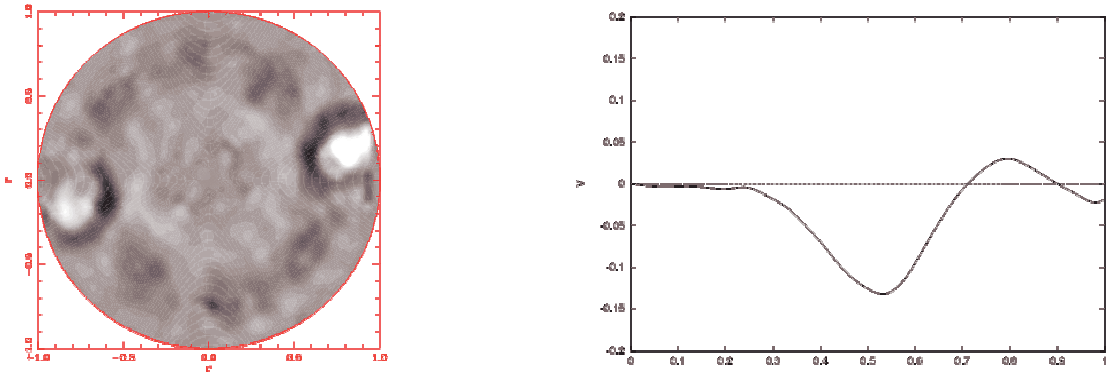

Figure 53. Left panel: Vorticity averaged over several forcing periods; the two pumping locations are seen on the left- and right-hand sides. Right panel: Averaged azimuthal velocity profile; an anticyclonic flow is clearly observed inside the pumping region.

We have numerically modelled the experiment by solving the quasi-geostrophic vorticity equation in the β-plane approximation on a disk. The forcing is modelled by localised vorticity sources. Using the parameters of the experiment, we find satisfactory agreement. In addition, we are employing the numerical model to investigate the influence of varying parameters as, e.g., the Ekman friction, on the structure of the zonal flows, their radial scale sizes and strengths. Finally, by generalising the numerical model we consider the influence of a finite radius of deformation (Rossby radius) on the formation and structure of the zonal flow. Recalling the analogy between Rossby wave dynamics on the β-plane and drift-wave dynamics in a magnetised plasma with a density gradient perpendicular to the magnetic field, a similar mechanism may apply for the formation of azimuthal flows in a cylindrical plasma. The density is here maximum in the centre and the analogous "fluid" model will have $\beta > 0$. We therefore expect the formation of a cyclonic rotation around the plasma column, resulting from the homogenisation of the PV, which is clearly revealed by the numerical investigations of drift-wave turbulence in a cylindrical plasma. The homogenisation of generalised PV is thus an effective mechanism of forming sheared azimuthal plasma flows. These flows appear to be of outmost importance to the plasma confinement.

4.3.2 Finite time singularities in a class of hydrodynamic models

V.P. Ruban, D.I. Podolsky* (*Landau Institute for Theoretical Physics, Moscow, Russia) and J. Juul Rasmussen*
E-mail: jens.juul.rasmussen@risoe.dk

The question of the possibility of spontaneous formation of a finite time singularity in solutions of the Euler equation for an ideal incompressible fluid has been discussed for a long time. At present, this fundamental problem of fluid dynamics is still far from a complete solution though some rigorous analytical results have been obtained.[1] The nature of the presumed singularity has still to be clarified although many theoretical scenarios for blow-up have been suggested until now and, moreover, extensive numerical simulations have been performed to observe the singular behaviour. In particular, the self-similar regime of singularity formation seems very probable. For this regime, all length scales decrease like $(t^*-t)^{1/2}$, the velocity increases according to $(t^*-t)^{-1/2}$, and the maximum of the vorticity behaves like $(t^*-t)^{-1}$. It is very important to note that the curvature of vortex lines in the assumed self-similar solution should tend to infinity in the vicinity of the singular point. This is consistent with recent results[1] where a blow-up of the vorticity, if it does take place, must be accompanied by a singularity in the field of the vorticity direction.

In our investigations we take the point of view that an infinite curvature of frozen-in vortex lines is in some sense a more fundamental characteristic of hydrodynamic singularity than an infinite value of the vorticity maximum. To illustrate this statement, we consider a class of models of incompressible inviscid fluids, different from Eulerian hydrodynamics, so that finite energy solutions with infinitely thin frozen-in vortex filaments of finite strengths are possible. This property allows us to study the dynamics of such filaments without the necessity of a regularisation procedure for short length scales. The linear analysis of small symmetrical deviations from a stationary solution is performed for a pair of anti-parallel vortex filaments and an analogue of the Crow instability is found at small wave numbers. A local approximate Hamiltonian is obtained for the nonlinear long-scale dynamics of this system. Self-similar solutions of the corresponding equations have been found analytically. They describe the formation of a finite time singularity, with all length scales decreasing like $(t^*-t)^{(1/(2-\alpha))}$, where t^* is the singularity time. Here α is a small parameter, "measuring" the departure from the Eulerian dynamics.

1. J.T. Beale, T. Kato and A. Majda, Commun. Math. Phys. **94**, 61 (1984); P. Constantin and C. Fefferman, Indiana Univ. Math. J. **42,** 775 (1993); P. Constantin, C. Fefferman and A. Majda, Commun. Partial Diff. Equat. **21,** 559, (1996).

4.3.3 Bathtub vortices

A. Andersen, T. Bohr (Inst. Phys., Technical University of Denmark, Lyngby), M. Ernebjerg (Oxford University, UK), J. Juul Rasmussen, and B. Stenum
E-mail: aanders@fysik.dtu.dk

Bathtub vortices, i.e. swirling flows with a free surface which may extend down to the outlet of the fluid container, are well known. The properties of such flows have, however, to our knowledge not been described in detail neither experimentally nor theoretically. The free surface appears with a very sharp tip for some parameter values, and the flow field around the tip is strongly singular. To investigate these properties we have constructed two experimental set-ups (one at the Technical University of Denmark and one at Risø) which each consists of a cylindrical container with a circular hole at the centre of the bottom. The cylinder is rotating

about a vertical axis, and using a recirculation system we obtain a steady bathtub vortex flow. Flow visualisations and measurements of the free surface shape have been carried out at the Technical University of Denmark, see Figure 54, and using the particle tracking system at Risø, we have measured velocity profiles.

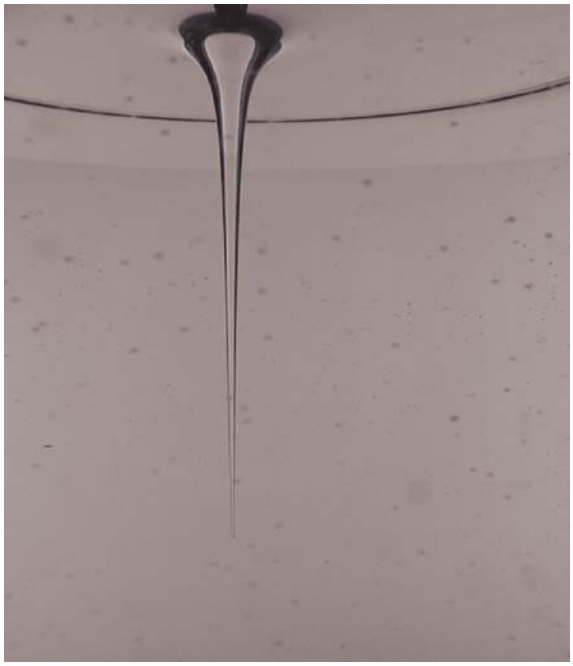

Figure 54. Recorded image of the free surface for a steady bathtub vortex. The air-filled core of the bathtub vortex ends in a sharp tip above the outlet at the centre of the container bottom.

We have obtained the free surface profile and have determined the flow field at a distance away from the vortex centre. The measured velocities have been found to agree with predictions from the boundary layer theory and the theory of rotating flows. At the moment, we focus experimentally and theoretically on the flow in the vortex region close to the axis of rotation, and we aim at extending the theoretical predictions to this region, where standard boundary layer theory is not valid.

4.3.4 Two-dimensional turbulence in bounded flows

A. H. Nielsen, J. J. Rasmussen, H. J. H. Clercx (University of Technology, Eindhoven, The Netherlands) and E. A. Coutsias (University of New Mexico, Albuquerque, USA)
E-mail: anders.h.nielsen@risoe.dk

During the last decades two-dimensional turbulence in unbounded domains (or more precisely in double periodic domains) in Navier-Stokes fluids has been investigated intensively by means of numerical simulations. The presence of an inertial range in the energy spectrum of these flows has been well documented. As two-dimensional flows exhibit an inverse cascade in the energy, coherent structures comparable with the size of the periodic domain will eventually emerge. Thus, the presence of boundaries and especially the conditions imposed on these will play a significant role in the evolution of the turbulence and the coherent structures.

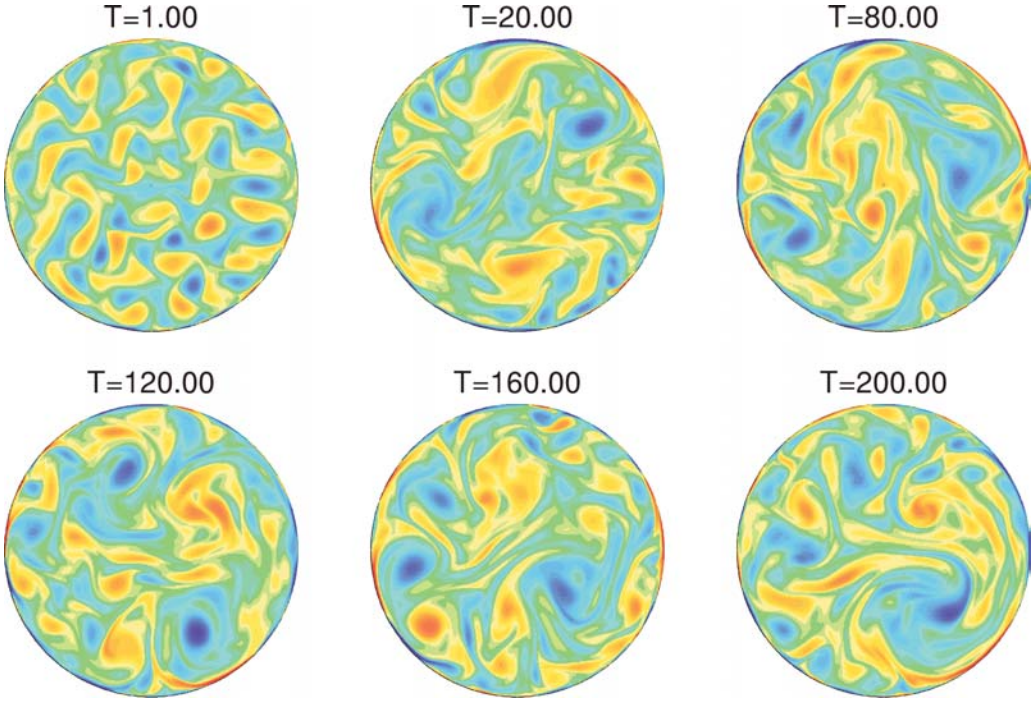

Figure 55. Time evolution of the vorticity field using random forcing in a disk with no-slip boundary. Red colours correspond to positive values, whereas blue colours correspond to negative values. Spectral evolution M = 512 (radially), N = 512 (azimuthally). The Reynolds number for T=20 to T=200 is approximately Re=2500.

Figure 55 shows the time evolution of a forced turbulent flow field contained in a disk with no-slip boundary. The model equations are the Navier-Stokes equations, which are forced at a given length scale, using random phases. Initially, we observe vortices with the same length scales as the forcing, see T=1.0, but quickly the vortices start to interact, forming larger structures. As these vortices interact with the boundary, smaller vortices are created and injected into the interior of the domain preventing the build-up of (and even destroying) larger structures. The turbulent state can therefore be maintained in a bounded domain, whereas for a computer simulation for the same parameters in unbounded (periodic) domain the inverse cascade will dominate and create domain-filling vortices.

4.3.5 Comparison between finite difference and spectral schemes

A. H. Nielsen and V. Naulin
E-mail: anders.h.nielsen@risoe.dk

Computer simulations of complex two-dimensional flows have been performed in nearly all areas of fluid dynamics and plasma physics. One of the most fundamental questions is therefore how well the different computer schemes perform compared to each other as well as compared with the real world. When solving the full Navier-Stokes equations, there are two generally different schemes that are widely used. Firstly, finite different schemes that are fast and can be applied to complex geometries; secondly, spectral schemes that are very accurate, but slow, and that can be used directly on simple geometries only.

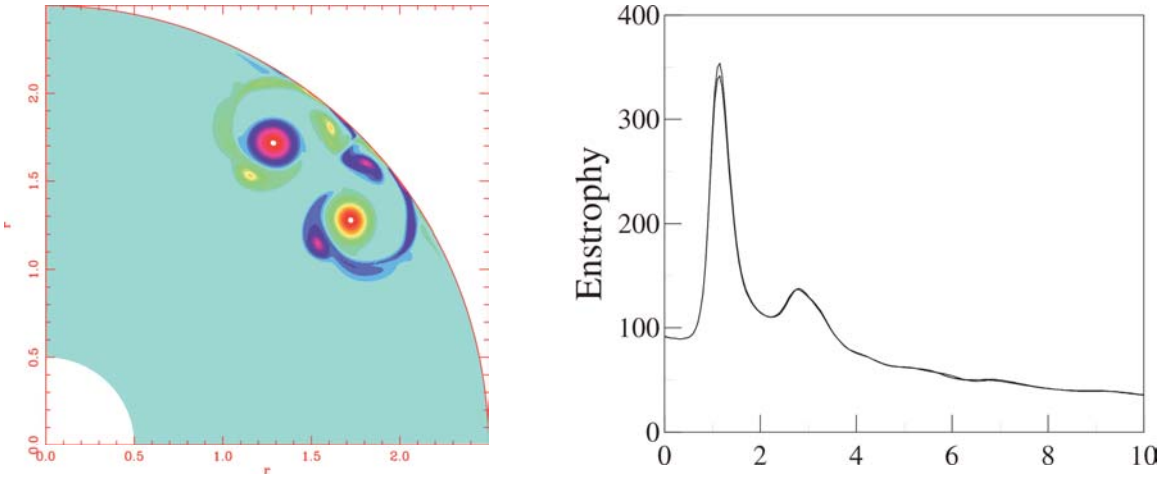

(a) (b)

Figure 56. (a) Snap-shot of a Lamb-dipole colliding with a no-slip wall. (b) Time evolution of the enstrophy using a spectral scheme and a finite different scheme. A resolution of 512x512 has been used.

In this project we study a situation where a Lamb-dipole collides with a wall enforcing no-slip boundary conditions. No-slip boundary conditions are tedious to implement numerically and, thus, pose a great challenge to code performance. For fairly high Reynolds numbers, the dipole collision with the wall generates a complex, turbulent time evolution. A strong boundary layer is created and injected into the interior of the domain creating a variety of new structures. A snapshot of this is presented in Figure 56 (a) obtained from a spectral code based on Chebyshev polynomials and Fourier modes. Very similar results are found using a finite different code. In order to show differences between the two codes we display the time evolution of the enstrophy in Figure 56 (b). The schemes are in fairly good agreement with each other. The finite different scheme, however, generates a slightly higher peak in the vorticity than does the spectral code. Our aim is to understand in detail how accurate the schemes are as the Reynolds number is increased, hereby augmenting the complexity of the flow. Further, we are interested in their scalability and how well behaved they are for increasing numerical resolution.

4.3.6 Evolution of the vorticity-area density

A. H. Nielsen, R. A. Pasmanter (KNMI, De Bilt, the Netherlands) and J. Juul Rasmussen
E-mail: anders.h.nielsen@risoe.dk

Numerical simulations of the freely decaying, incompressible Navier-Stokes equations in two dimensions have shown that under appropriate conditions after a relatively short period of chaotic mixing, the vorticity becomes strongly localised in a collection of vortices that move in a background of weak vorticity gradients. In order to quantify this evolution and the final vorticity state it was suggested to introduce the “vorticity-area density” .[1] This quantity will also facilitate the comparison of the numerical results (and experimental results) with theories based on statistical mechanics description of two-dimensional flow dynamics. The time dependent vorticity-area density is defined as:

$$G(\sigma,t) \equiv \int_A \delta\big(\sigma - \omega(x,y,t)\big)dA,$$

where A denotes the domain and ω is the vorticity. The big advantage of using the vorticity-area density to characterise the flow field is that it is a one-dimensional quantity compared with the two-dimensional vorticity flow field. Moreover, calculating the different moments of G will produce the conserved quantities of Navier-Stokes equations such as the circulation, enstrophy, etc. The aim of this project is to identify the form of G for well-defined states numerically and compare it with theoretical predictions.

1. H. W. Capel and R. A. Pasmanter, 'Evolution of the vorticity-area density during the formation of coherent structures in two-dimensional flows', Physics of Fluids, Vol. 12, no. 10, p. 2514.

4.3.7 Numerical and experimental studies of particle dynamics in flow channels

B. Stenum, S. Lomholt and M. Maxey (Department of Applied Mathematics, Brown University, Providence, USA)
E-mail: bjarne.stenum@risoe.dk

The comparative numerical and experimental studies of particle dynamics at low Reynolds numbers in a flow channel have been extended to include interactions between particles. Experimentally, the dynamics of rising particles has been studied in vertical and inclined flow channels in order to validate the results of the numerical studies. The experiments were carried out in a rectangular flow channel with a cross section of 100 mm × 10 mm and a length of 150 mm. The 2 mm polymer particles were injected from below into a resting mixture of water and glycerol. The positions of the particles were determined with subpixel accuracy by digital image processing. Numerically, similar experiments were performed by means of the force coupling method. In this model a particle is treated as a fluid volume and source terms are added to the Navier-Stokes equations in order to model the particle. The first two source terms, the force monopole and the force dipole, describe the first two levels of the multipole expansion corresponding to the external force (gravitational force) and the torque on the particle. The numerical studies were performed both with and without inclusion of the force dipole.

The studies of single particles interacting with the channel wall were performed at particle Reynolds numbers between 0.19 and 13.6, and the channel was tilted an angle of about 10 degrees while the interactions between two particles were performed in a vertical channel at particle Reynolds numbers of 1.55 and 13.5. The interactions between three particles were studied for particle Reynolds numbers of about 1.6 only.

In all cases the experimentally measured particle trajectories were well reproduced by the numerical experiments. For single particles interacting with the wall it was found that the influence by the force dipole was most significant at the lowest Reynolds numbers. This may be ascribed to the thick lubrication layer at low Reynolds numbers. For interactions between two particles the inclusion of the force dipole reduced the overlap of the particles observed in the simulations without the force dipole. The interactions between three particles were also well reproduced by the simulations and both the trajectories (Figure 57), and the velocities of the particles agreed well shoving that most of the effects are captured by the first two source terms.

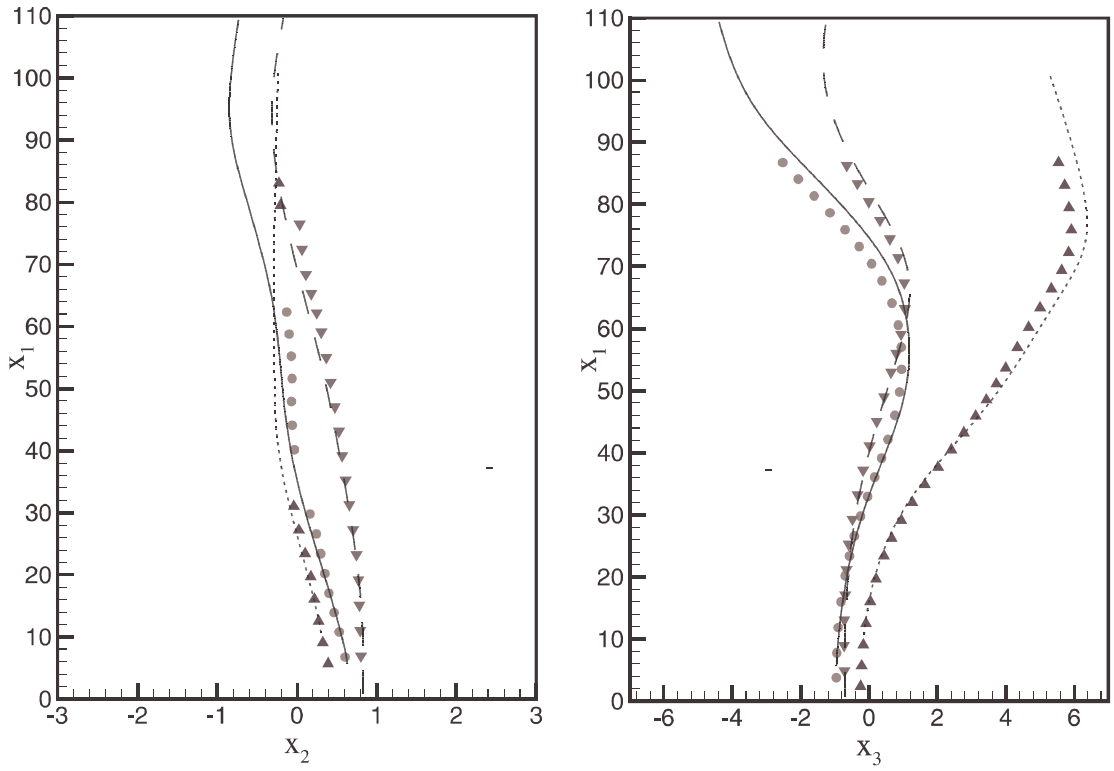

Figure 57. Measured particle trajectories (points) of three interacting particles compared with the results of the simulation (curves) with inclusion of both the force monopole and the force dipole. Left-hand side: In the plane across the channel. Right-hand side: In the plane along the broad side of the channel.

4.3.8 Periodically driven shear flows

F. Okkels, B. Stenum, J. Juul Rasmussen and A. H. Nielsen
E-mail: fridolin.okkels@risoe.dk

We have investigated the configuration and interaction of 2-dimensional vortices created by a periodically oscillating circular shear field in the rotating parabolic annulus (see last year's annual report, Risø-R-1157, for further description of the parabolic annulus). This study may be seen as a frequency response analysis of a circular shear field. Since the mean-shear is zero, the only parameters determining the state of the system are the amplitude and the frequency of the oscillations. As these parameters slowly increase, the flow undergoes the following transitions: First a stationary, radially symmetric flow becomes unstable and organises into a chain of vortices, being created within every half-period of maximum shear and then destroyed by the following chain of new vortices having the opposite sign (i.e. rotation). As the frequency increases, the unstable shear field exists for too short a period for vortices to be generated, and the radially symmetric flow is obtained again. For higher values of amplitude and frequency, the strong shear field creates 3-dimensional effects that perturb the free surface of the annulus. This perturbation produces a jet along the shear layer causing the layer to organise into a set of alternating vortices that in the end become unstable.

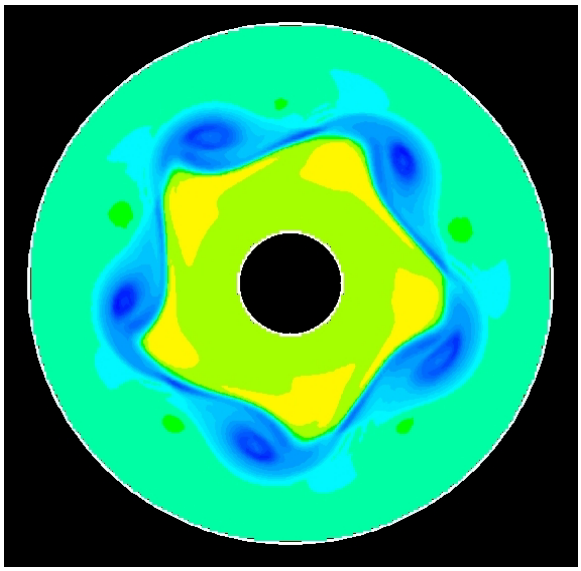

Figure 58. A typical vorticity field generated by the numerical simulations.

The flow field is measured by different techniques like particle tracking or measuring the variations in light absorption and then assuming the flow to be geostrophic.

In parallel with the experimental measurements, numerical simulations have been performed and have helped to distinguish the (expected) 2-dimensional behaviour from the (unexpected) 3-dimensional effect arising from the surface perturbations. When applying the 3-dimensional effects to the simulations, the experimental and the numerical behaviour matches nicely. A typical vorticity field generated by the numerical simulations is shown in Figure 58.

4.3.9 Turbulent shell models

F. Okkels and M. Høgh Jensen (Niels Bohr Institute, University of Copenhagen, Denmark)
E-mail: fridolin.okkels@risoe.dk

This theoretical work concerns the creation and the dynamics of temporal structures in the GOY-shell model of turbulence, simulating the cascade of energy in 3-dimensional fully developed turbulence. The strength of this simple model is that the statistics of its dynamics match very well that of experimental turbulence measurements. The evolution is dominated by strong intermittent bursts that propagate through the system, and applying dynamic system analysis to the model a simple 3-dimensional chaotic attractor is extracted from which the nature of the burst propagation can be explained.

4.3.10 Fractal induced turbulence

F. Okkels, J.C. Vassilisoc and B. Mazzi* (*University of Cambridge,*
Dept. of Applied Mathematics and Theoretical Physics, UK)
E-mail: fridolin.okkels@risoe.dk

Normally 3-dimensional generic turbulence is assumed to be forced at large length –scales, but when a fractal obstacle is placed in a wind tunnel, it excites wake turbulence on a broad range of scales. Such an experiment was performed and the experiment was simulated using a

modified version of the shell model described above. The statistical properties of the experiment were reproduced qualitatively by the model and this shows the robustness of shell models since they were originally created to be forced at the large scales as in generic 3-dimensional turbulence.

4.4 Optics and acoustics

4.4.1 Modulational instability and collapse dynamics in media with nonlocal nonlinearities

O. Bang (IMM, Technical University of Denmark, Lyngby), W. Krolikowski (Australian Photonics Cooperative Research Centre, Australian National University, Canberra, Australia), J. Juul Rasmussen and J. Wyller (Department of Mathematical Sciences, Agricultural University of Norway, Norway)
E-mail: jens.juul.rasmussen@risoe.dk

Nonlinear wave propagation in various media is characterised by a nonlocal response, and the propagation is governed by the nonlinear Schrödinger equation (NLS) with a nonlocal nonlinear term of the type $\int R(x-x')|\psi(x')|^2 dx'$, where ψ designates the complex wave envelope and R is a response function of finite extension. In case of nonlinear optics, the nonlocal NLS represents a phenomenological model for propagation of optical beams in media, where the nonlinear refractive index change, induced by the optical beam, is determined by some sort of transport process. It may include, e.g., heat conduction in materials with thermal nonlinearity or diffusion of molecules or atoms accompanying nonlinear light propagation in atomic vapours. Nonlocality also accompanies propagation of electromagnetic waves in plasma. In addition, the nonlocal response appears naturally as a results of many body interaction processes in the description of Bose-Einstein condensates.

We have studied the modulational instability of a plane wave in a non-local nonlinear Kerr medium for various types of response functions. We show that nonlocality suppresses the instability in the case of self-focusing nonlinearity while it has much weaker effect in a self-defocusing medium. For special cases of the response function, the plane wave may become unstable even in the defocusing case if the intensity exceeds a certain critical value. For higher dimensional cases where local nonlinearity will lead to a catastrophic collapse of the wave field, we show rigorously that the non-locality will always hinder the ultimate collapse.

4.4.2 Nonlinearity and disorder: classification and stability of nonlinear impurity modes

A.A. Sukhorukov, Y.S. Kivshar* (* Optical Sciences Centre, Australian National University, Canberra, Australia), O. Bang**, P. L. Christiansen** (**IMM, Technical University of Denmark, Lyngby) and J. Juul Rasmussen*
E-mail: jens.juul.rasmussen@risoe.dk

Wave scattering by localised impurities (or defects) is a fundamental problem in many branches of physics. Impurities break the translational symmetry of a physical system and lead to several effects such as wave reflection, resonant scattering and *impurity modes* - spatially localised oscillatory states excited at the impurity sites. These two kinds of problems, i.e. wave scattering in inhomogeneous media and defect-supported localised modes, appear in many different physical systems such as the scattering of surface acoustic waves by surface

defects or interfaces, excitation of defect modes in superconductors in the vicinity of the twinning planes, the dynamics of the tight-binding Holstein-type models of the electron-phonon coupling, light propagation in dielectric super-lattices with embedded defect layers, defect states and bends in photonic crystal waveguides, and light trapping and switching in non-uniform waveguide arrays. In all such cases the impurities (or defects) lead to energy trapping and localisation in the vicinity of the defects that occur in the form of spatially localised impurity modes. When nonlinearity becomes important, it may lead to self-trapping and energy localisation even in a perfect (or homogeneous) system in the form of *intrinsically localised modes*. Spatially localised modes of nonlinear systems are usually associated with *solitary waves* (or solitons) in continuous models, or *discrete breathers* in lattice models. When both nonlinearity and disorder are present simultaneously, it is expected that competition between the two different mechanisms of energy localisation (i.e. one that is due to the self-action of nonlinearity, and another one that is due to localisation induced by disorder) will lead to a complicated physical picture of localised states and their stability.

In this work we consider one of the examples of such competition, and analyse different types of nonlinear localised modes and their stability in the framework of the generalised nonlinear Schrödinger equation with point-like impurity. We present a systematic classification and stability analysis of spatially localised impurity modes of three distinct types - one- and two-hump symmetric, localised modes and asymmetric, localised modes - for both focusing and defocusing nonlinearity and two different (attractive or repulsive) types of impurity. We obtain *an analytical stability criterion* for the nonlinear localised modes and consider the case of power-law nonlinearity in detail. We discuss several scenarios of instability-induced dynamics of the nonlinear impurity modes, including mode decay or switching to a new stable state, and *collapse at the impurity site*.

Our results can be linked to different special cases of the theory of nonlinear guided waves in layered dielectric media, and they also provide a generalisation of the theory of nonlinear impurity modes in solids, together with the analysis of their stability and instability-induced dynamics, emphasising the cases where we can observe clear evidence of competition between the two physical mechanisms of energy localisation.

4.4.3 Collapse dynamics of attractive Bose-Einstein condensates

L. Bergé (CEA/Bruyéres-le-Châtel, B.P. 1,2 Bruyéres-le-Châtel, France)
and J. Juul Rasmussen
E-mail: jens.juul.rasmussen@risoe.dk

The formation of Bose-Einstein condensates (BECs) in trapped clouds of alkali atoms is now experimentally well established. Among those, ^{7}Li atoms are characterised by attractive interactions with a negative scattering length. This promotes a collapse-type instability that yields a singular increase in the BEC wave function. It occurs when the number of particles, N, exceeds a threshold value, N_c. BECs formed in ^{7}Li gas develop several sequences of collapse.[1] From the initial cooling, the condensate is first fed by the thermal cloud of uncondensed atoms. Then, once the number of atoms is above N_c, the condensate sharply concentrates with increasing density. As the density rises, inelastic collisions such as three-body molecular recombination increase whereby the collapse is arrested. The thermal cloud is next believed to refill the condensate that reaches $N > N_c$ and then collapses again. The cycle of collapses repeats many times until the gas comes to equilibrium. This scenario is supported by numerical integrations of the Gross-Pitaevskii equation that takes the form of a non-linear Schrödinger equation (NLS) with external parabolic potential.

By applying the basic knowledge[2] on the collapse in the framework of the NLS we have considered the collapse dynamics of the BECs with attractive interaction. In particular, we have employed the self-similar description of the collapse evolution. We have shown that BECs collapse with a mean radius contracting like $(t_c - t)^{1/2}$ at leading order, where t_c denotes the collapse moment. In three dimensions *the collapse is weak*: the amplitude of the wave function blows up at centre, while particles are expelled outwards with a constant density profile. Recombination losses limit the collapse, but they only damp a few percent of the atoms at each blow-up. Several blow-up events develop within one collapse sequence. The condensate is then re-confined by the trap and can further undergo more collapse cycles as long as a stable state has not been reached. Quasi-two-dimensional condensates are subject to *strong collapse*, in the sense that the number of particles remains mostly confined in the centre. In this case, recombination removes a significant fraction (up to 0.5) of particles per collapse event. The results of our analysis are found to describe experimental observations very well.

1. C.A. Sackett, J.M. Gerton, M. Welling and R.G. Hulet, Phys. Rev. Lett., **82**, 876 (1999).
2. J. Juul Rasmussen and K. Rypdal, Phys. Scr. **33**, 481 (1986); L. Bergé, Phys. Rep., **303**, 259 (1998).

4.4.4 Classical and quantum properties of spatio-temporal structures in optical second-harmonic generation

M. Bache, P. Lodahl and M. Saffman (University of Wisconsin, Madison, Wisconsin, USA)
E-mail: morten.bache@risoe.dk

Cavity enhanced $\chi^{(2)}$ nonlinearities have recently drawn much attention to the formation of patterns in the intensity of the light beam. These patterns are observed in the transverse plane perpendicular to the propagation direction of the light beam, and they are a consequence of the nonlinearity of the optical material. These materials are interesting since they have a very fast response time giving them a potential application in information processing.

Most of the studies have been concentrated on optical parametric oscillation (OPO) where photons of frequency 2ω decay into photons of frequency ω_+ and ω_-, and second-harmonic generation (SHG) where photons of frequency ω combine into photons of frequency 2ω. Our project concerns formation of spatio-temporal instabilities (patterns) in SHG where we have included that the second harmonic may decay through the OPO process into parametric fields also resonant in the cavity; for this reason the model is called the internally pumped optical parametric oscillator (IPOPO). These parametric fields turn out to have decisive influence on the pattern formation. In certain parameter areas the parametric fields completely stabilise the system so that no patterns can be observed.[1,3] Thus, these areas should be avoided if one wants to make an experimental observation of the instabilities. In other areas the pattern formation expected in SHG may be observed despite the presence of the parametric fields.[1,3] Finally, the parametric fields are responsible for completely new spatio-temporal structures not observed in optical systems before. These include spiral waves in the intensity of the light[2] and oscillating grey and bright localised structures arising due to bistability caused by the presence of the parametric fields.[3] The stability of the system with the parametric fields excited can in some cases be calculated using a linear stability analysis, and this shows that the instability is often both spatial and temporal leading to travelling waves. In the case of the spirals, travelling rolls break up to form intensity spirals; an example is shown in Figure 59 (left). In Figure 59 (right) an example of coexisting grey and bright localised structures in the transverse plane is shown.

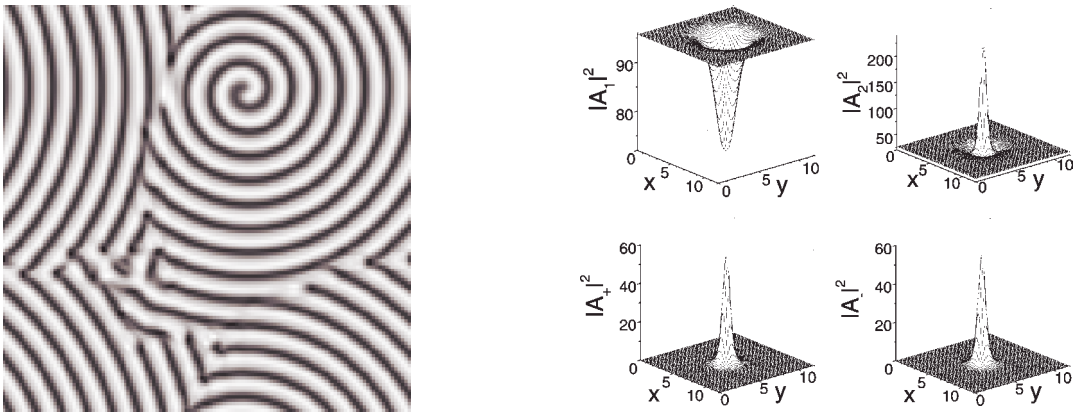

Figure 59. Left: The intensity of the fundamental showing a spiral. The formation of this structure is due to destabilization of the internally pumped optical parametric oscillator (IPOPO) above the parametric threshold, and is therefore a secondary instability. Right: Localised structures (cavity solitons) showing coexistence of a gray soliton (fundamental, upper left corner) and bright solitons (second harmonic, upper right corner, and parametric fields, lower two plots). They arise due to bistability in the IPOPO above the parametric threshold. By increasing the pump level slightly these solitons start to oscillate in time.

Moreover, the quantum properties of pattern formation in SHG have been investigated where the interest in $\chi^{(2)}$ nonlinear materials until now solely has been concerned with the OPO. It turns out that just below threshold for pattern formation even though the system in a classical sense is stable, the quantum fluctuations of the light allow for a so-called quantum pattern to be observed in the correlations between different points in space. The SHG model differs substantially from the OPO model promising new effects, and work is currently in progress both in the singly resonant set-up and the doubly resonant set-up. The nonlinear analysis carried out for the singly resonant model[4] also opens the door for investigating analytically the quantum behaviour above threshold for pattern formation.

1. P. Lodahl, M. Bache and M. Saffman, "Modification of pattern formation in doubly resonant second harmonic generation by competing parametric oscillation", Opt. Lett. **25**, 654 (2000).
2. P. Lodahl, M. Bache and M. Saffman, "Spiral intensity patterns in the internally pumped optical parametric oscillator", Phys. Rev. Lett. **85**, 4506 (2000).
3. P. Lodahl, M. Bache and M. Saffman, "Spatio-temporal structures in the internally pumped optical parametric oscillator", Phys. Rev. A. **63,** 023815 (2001).
4. P. Lodahl and M. Saffman, "Nonlinear analysis of pattern formation in singly resonant second-harmonic generation", Opt. Comm. **184**, 493 (2000).

4.4.5 Experimental observation of self-pulsing in singly resonant optical second-harmonic generation

M. Bache, P. Lodahl, A. V. Mamaev (Russian Academy of Sciences, Moscow, Russia),
M. Marcus and M. Saffman* (*University of Wisconsin, Madison, Wisconsin, USA)*
E-mail: morten.bache@risoe.dk

During the last couple of decades the cavity enhanced $\chi^{(2)}$ nonlinearities have been the subject of many studies concerning the formation of patterns in the intensity of the light beam. These patterns are observed in the transverse plane perpendicular to the propagation direction of the light beam. However large the interest, the experimental verification of these instabilities has proved to be very difficult for several reasons. First, due to weak nonlinearities of the optical

materials a high power laser source is needed, and this causes thermal problems leading to fluctuations not related to the nonlinear properties of the material. Secondly, mainly the doubly resonant cavity has been considered which is difficult to operate stably. Therefore we have considered the singly resonant cavity where only the pump field is resonant and not the generated second harmonic.[1]

One problem of the singly resonant set-up is, however, that theoretically the simplest observable instability is not present,[2] namely the self-pulsing instability where the intensity oscillates regularly in time, in this case with frequencies on the order of 100 MHz. To our surprise we observed such oscillations in the singly resonant set-up, and in order to explain this novel phenomenon we had to extend the singly resonant model. As shown before in the doubly resonant set-up,[3] by including the possibility that the generated second harmonic decays through a nondegenerate parametric process leads to new types of pattern formation, and in the singly resonant set-up we found that the presence of the parametric fields also leads to self-pulsing instability. This extended model was found to explain in great detail the experimental observations.

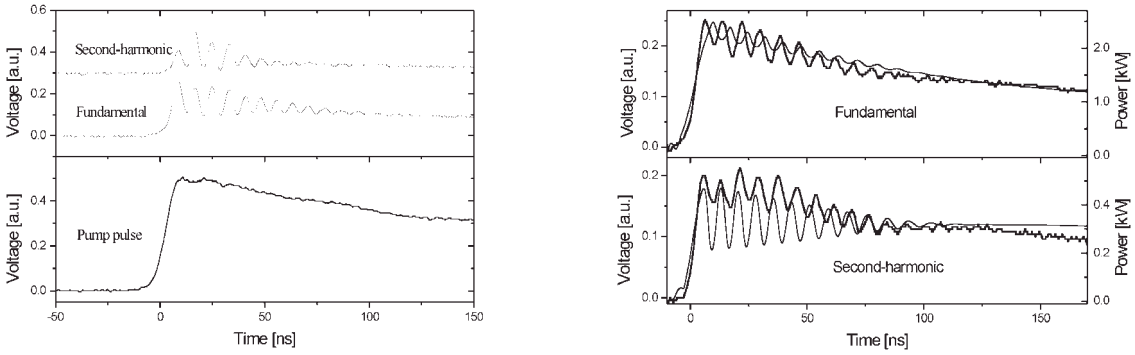

Figure 60. Left: The bottom plot shows the intensity of the pump pulse injected into the cavity at the fundamental wavelength. The upper plot shows the intensity cavity output of the fundamental and second harmonic, and the self-pulsing oscillations are observed at a frequency of around 120 MHz. After approximately 70 ns the pump pulse goes below the threshold for self-pulsing and the oscillations are damped towards a steady state. Right: Comparing experiments and numerical simulations. The full (thin) line is the experimental (numerical) traces of the intensities outside the cavity. The numerics are given in kW.

The experimental configuration used a pulsed set-up giving 200 ns pulses with 3 kW peak power. The pulse repetition rate was 5 Hz giving a very low average pump power, which may explain why thermal problems were small in this set-up. A typical time trace of the intensity is shown in Figure 60 (left), where self-pulsing with a frequency of 120 MHz is observed. The effects of a pulsed pump profile on the dynamics of pattern formation have not been addressed before and, therefore, we have performed simulations with a pump profile fitted to a typical experimental one. An example of this is shown in Figure 60 (right) where good agreement is observed confirming that the instability is in fact of a self-pulsing type and not due to thermal problems.

1. M. Bache, P. Lodahl, A. Mamaev, M. Marcus and M. Saffman, “Observation of self-pulsing in singly resonant optical second-harmonic generation”, submitted (2000).
2. P. Lodahl and M. Saffman, “Pattern formation in singly resonant second harmonic generation with competing parametric oscillation”, Phys. Rev. A **60**, 3251 (1999).

3. P. Lodahl, M. Bache and M. Saffman, “Modification of pattern formation in doubly resonant second harmonic generation by competing parametric oscillation”, Opt. Lett. **25**, 654 (2000); “Spiral intensity patterns in the internally pumped optical parametric oscillator”, Phys. Rev. Lett. **85**, 4506 (2000); “Spatio-temporal structures in the internally pumped optical parametric oscillator”, Phys. Rev. A. **63,** 023815 (2001).

4.4.6 Three-dimensional analysis of diffractive optical elements

P. G. Dinesen, J. S. Hesthaven (Brown University, Rhode Island, USA) and J. P. Lynov
E-mail: jens-peter.lynov@risoe.dk

The time-domain spectral collocation method has already proved to be very accurate and highly efficient in comparison with other rigorous numerical algorithms for the solution of Maxwell’s equations in the time domain. We have therefore used this method in the analysis of full three-dimensional focusing waveguide grating couplers used for controlled coupling from a guided wave to free-space radiation.

The main advantages of the spectral-collocation method over, e.g., the finite-difference time-domain method that solves essentially the same set of equations are the absence of numerical dispersion, the accurate resolution of complex geometries and the fact that the method is very well suited for parallel implementation.

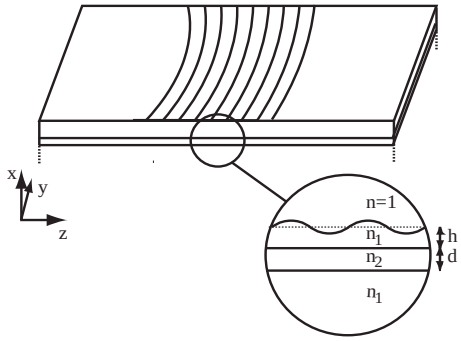

Figure 61. Schematic outline of waveguide grating coupler.

Parallel implementation of the full three-dimensional spectral-collocation method solving for all six electric and magnetic field components has been used extensively on the new Risø IBM RS/6000 parallel supercomputer in the design of focusing grating couplers with simultaneous focusing in both transverse directions. Figure 61 shows a schematic outline of a waveguide grating coupler with a surface relief for simultaneous focusing in both transverse directions. Figure 62 presents the simulated output from such a grating coupler clearly illustrating the focusing properties of the waveguide grating coupler.

The surface relief had a Gaussian truncation with a 1/e width of 8 wavelengths. The code was run in parallel on eight processors for 24 hours.

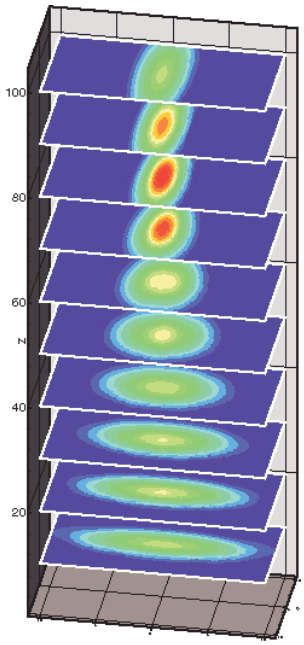

Figure 62. Simulated focused output from grating coupler.

4.4.7 Fast and accurate analysis of waveguide grating couplers using a boundary variation method

P. G. Dinesen and J. S. Hesthaven (Brown University, Rhode Island, USA)
E-mail: jens-peter.lynov@risoe.dk

The full three-dimensional modelling of diffractive optical elements (DOEs) remains a significant computational challenge. With the growing appreciation of the possibilities offered by the DOEs it becomes increasingly important to attempt the development of design tools as opposed to analysis tools. For such studies one is in need of very fast solvers to allow multiple parameter variations and, ultimately, enable the development of automated, inverse tools for optimal design.

It is with this ultimate goal in mind that we have set out to develop a new class of tools specifically designed to allow fast and accurate modelling of waveguide grating couplers used for controlling the coupling between a thin film optical waveguide and free space. We have previously discussed in detail the formulation of a two-dimensional boundary variation method suitable for the analysis of waveguide grating couplers. In this work we extend the boundary variation method to the full three-dimensional waveguide-grating problem required to model general two-dimensional surface relief gratings.

We have demonstrated that the conclusions from the two-dimensional case on accuracy and computational efficiency carries over to the general three-dimensional grating, confirming that the boundary variation method proposed offers a fast and accurate forward solver suitable for integration into an optimal design loop. Figure 63 shows an example of radiation from a focusing grating coupler computed using the boundary variation method. Our studies show that the method is in the order of 400 times faster than our rigorous spectral-collocation method and requires about 20 times less memory.

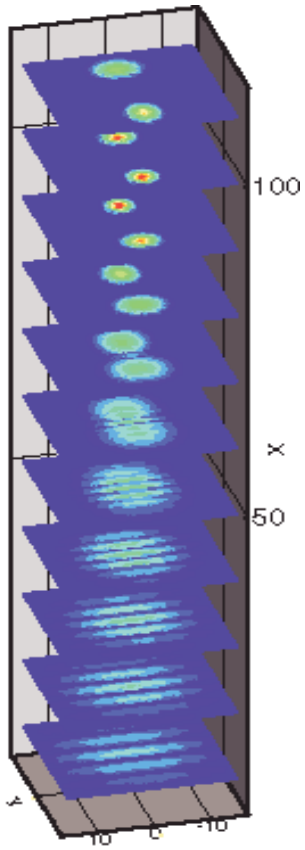

Figure 63. Multiplex grating with dual focusing simulated with boundary variation method.

4.4.8 Numerical investigations of wavelength division multiplexing components

K. Dridi
E-mail: jens-peter.lynov@risoe.dk

As at April 2000, a new industrial post doc. project sponsored by the Danish Academy of Technical Sciences was initiated with Risø and Ibsen Microstructures A/S (located in Farum, north of Copenhagen); the company was later acquired by ADC Telecommunications and changed its name to ADC Danmark ApS. During the year 2000, ADC Danmark ApS built new processing facilities for the production of phase masks, fibre Bragg gratings and future integrated optics components; this expansion will continue in the year to come. Optical communication is a business area that experiences exponential growth, and there is a tremendous interest in exploiting the full optical bandwidth of transmission fibres, the veins of the network of the information age. Any component that deals with wavelength division multiplexing (WDM) is therefore of great value, enabling greater capacity, i.e. higher transmission rates of more information (internet, e-commerce and multi-media applications). These components perform optical signal processing in such a way that the separation and recombination of signals of different wavelengths are possible. In March 2001, ADC Danmark ApS presented the first prototype of one of these WDM components, the “D-mon” (dense WDM, or DWDM monitor). The latter may be used in optical networks to measure the power in the different channels (signals of specific wavelength) carrying information. Such a component indicates whether signal regeneration/amplification is needed at a certain point in the network because of the inevitable power losses in optical signals as they propagate over

great distances in fibres. The D-mon has successfully been presented at the Optical Fiber Communication conference in Anaheim, California. The component is characterised by a smaller size and a lower power consumption than actual monitors on the market. According to telecommunications industry analyst RHK the market for these components will grow to $24 billion by 2004 (see Figure 64 (a)). A DWDM component reproducible en masse in the portfolio of ADC Danmark ApS, in the infancy of this particular market, is clearly a great advantage. Key elements of this technology are multidimensional periodic structures such as gratings in silica, and photonic crystal structures in general. As the processing and fabrication of these components are delicate, good physical understanding and modelling/design tools are essential. During the year 2000, gratings of different geometries and material composition have been designed, both polarisation-dependent and -independent.

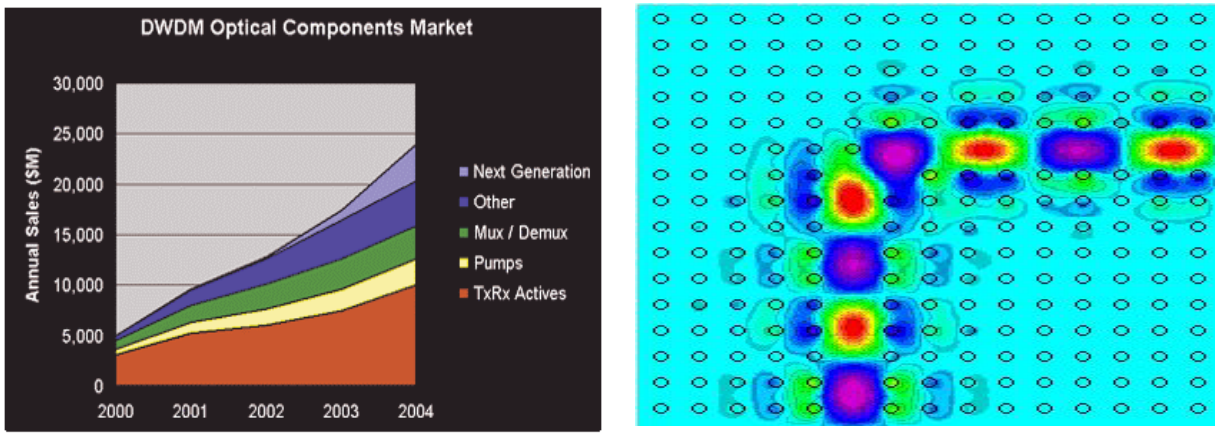

(a) (b)

Figure 64. (a) DWDM optical component market. (b) Line defect bend in a periodic lattice.

Among other activities, an evaluation of methods for the measurement of the optical constants of materials has been conducted, and a provider has been located. This resulted in the ordering of the recommended dual prism set-up, an automatised measurement system based on prism coupling. Moreover, a study of grating pulse diffraction has been conducted, clarifying the dispersion in relatively short pulse transmissions at high bitrates. Finally, efficient mathematical models for the investigation of condensed matter physics in photonic crystal structures (see Figure 64 (b)) have been implemented in the form of a software tool. Figure 64 (b) shows a periodic lattice of dielectric rods in a background of air in which a subwavelength 90 degrees line defect bend has been carved. There is no radiation loss due to the band gap of the bulk material, and transmission is close to 100%, contrary to classical optical waveguides. There is beautiful analogy between photons in periodic dielectric materials of high index contrasts and electrons in a periodic lattice of atoms in semiconductors.

4.4.9 Pseudospectral modelling of ultrasonic wave propagation

S. Arnfred Nielsen
E-mail: steen.arnfred.nielsen@risoe.dk

Due to new and stronger demands for testing procedures in industries requiring a high standard for quality assurance, mathematical modelling of ultrasonic wave propagation has become an important discipline in non-destructive testing of elastic materials.

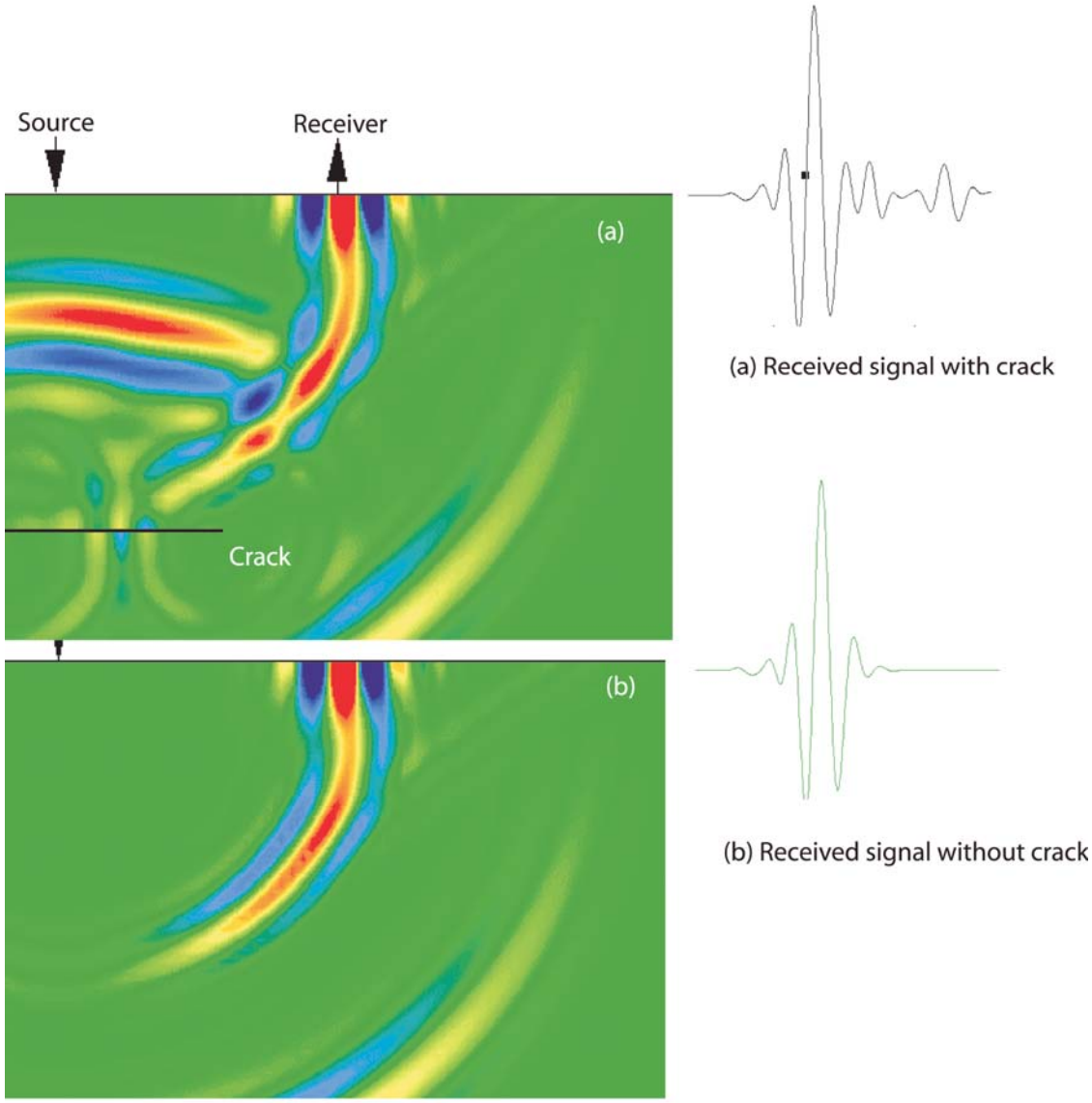

Figure 65. Velocity field in elastic media with and without crack. The field is generated by a point source on a stress-free boundary. (a) Velocity field and received time signal with a crack present and (b) velocity field and received time signal without crack. Red colours correspond to positive values while blue colours correspond to negative values. Iterations N = 700, time step dt = 0.018 s, speed of sound cl = 1.7, ct = 1.0 and normalised density.

The aim of the present work has been to develop an approach for solving the elastic wave equation in discontinuously layered materials in general complex geometries. The approach is based on a direct pseudospectral solution of the time-domain elastodynamic equations. In this approach, the global computational domain is decomposed into a number of subdomains adding the required geometrical flexibility to the method. Moreover, this decomposition allows for efficient parallel computations, hence decreasing the computational time. Every subdomain is mapped onto the unit square using transfinite blending functions. With this curvilinear mapping the elastodynamic equations can be solved to spectral accuracy and, furthermore, complex interfaces can be approximated smoothly, thus avoiding staircasing. Spatial derivatives are evaluated on Chebyshev-Gauss-Lobatto nodal points within each subdomain by means of a pseudospectral approach, and a global solution is reconstructed from the local solutions using properties of the equations of elastodynamics. Each subdomain can be prescribed with either open, physical or stress-free boundary conditions. Boundary

conditions are applied by means of characteristic variables. Finally, the global solution is advanced in time using a fourth order Runge-Kutta scheme.

Figure 65 shows the velocity field in an elastic material with and without a stress-free crack. The field is generated by a point source on a stress-free boundary. In the first material (a) a crack is present and the corresponding velocity field and received time signal are seen. In the second material (b) no crack is present and the corresponding velocity field and received time signal are seen.

4.4.10 Laser-ultrasonic monitoring of industrial processes

P. E. Andersen, P. G. Dinesen, S. A. Nielsen and B. Stenum
E-mail: steen.arnfred.nielsen@risoe.dk

Conventional ultrasonic monitoring is inherently limited by the large acoustical impedance mismatch between air and solids. The goal of this project is to overcome this limitation by using laser-generated ultrasound as well as optical detection of ultrasonic waves.

Laser generation of ultrasonic waves is accomplished by firing intense and short laser pulses at a surface of a metal or, in principle, any other solid. If the absorbed energy from the laser pulse is sufficiently high and the pulse duration is sufficiently short, the absorbed energy cannot be led away by thermal diffusion. Instead, a stress wave is generated, the properties of which depend on the laser pulse, the boundary conditions at the surface as well as the material properties.

A number of experiments have been carried out to investigate the generation and detection of ultrasonic waves by laser, using a frequency-doubled Q-switched Nd:YAG laser at 532 nm. Stress waves have been successfully generated in a number of materials ranging from a piece of rail to an animal bone and have been detected by conventional ultrasound transducers. Figure 66 shows an example of the transducer signal from a laser-generated stress wave propagating through a steel bar. The arrival of the initial P-wave is clearly indicated and the time delay is verified using the thickness of the bar and the ultrasonic velocity in steel.

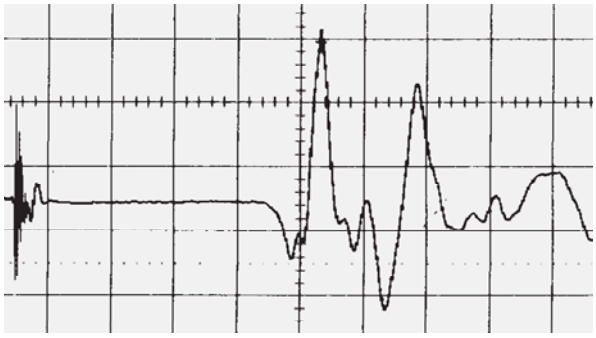

Figure 66. Time evolution of laser-generated ultrasonic wave in a steel bar.

An all-optical detection based on a differential detection scheme has been demonstrated for the detection of a laser-generated stress wave in a dielectric absorber placed in water. It is, however, anticipated that more sensitive detection schemes must be used for the detection of stress waves in metals with rough surfaces. Further work is in progress.

5. Publications and educational activities

5.1 Optical materials

5.1.1 International publications

Bublitz, D.; Fleck, B.; Wenke, L.; Ramanujam, P.S.; Hvilsted, S., Determination of the response time of photoanisotropy in azobenzene side-chain polyesters. *Opt. Commun.* (2000) v. 182 p. 155-160.

Bublitz, D.; Helgert, M.; Fleck, B.; Wenke, L.; Hvilsted, S.; Ramanujam, P.S., Photoinduced deformation of azobenzene polyester films. *Appl. Phys. B* (2000) v. 70 p. 863-865.

Ellegaard, O.; Schou, J.; Urbassek, H.M., Monte Carlo description of gas flow from laser-evaporated silver. *Appl. Phys. A* (1999) v. 69 p. S577-S581.

Fleck, B.; Wenke, L.; Ramanujam, P.S.; Hvilsted, S., Theoretical and experimental investigations on an incoherent optical correlator. *Opt. Commun.* (2000) v. 174 p. 311-315.

Hansen, T.N.; Schou, J.; Lunney, J.G., Langmuir probe study of plasma expansion in pulsed laser ablation. *Appl. Phys. A* (1999) v. 69 p. S601-S604.

Helgert, M.; Fleck, B.; Wenke, L.; Hvilsted, S.; Ramanujam, P.S., An improved method for separating the kinetics of anisotropic and topographic gratings in side-chain azobenzene polyesters. *Appl. Phys. B* (2000) v. 70 p. 803-807.

Juul Jensen, S.; Løbel, M.; Petersen, P.M., Stability of the single-mode output of a laser diode array with phase conjugate feedback. *Appl. Phys. Lett.* (2000) v. 76 p. 535-537.

Limeres, J.; Carrascosa, M.; Petersen, P.M.; Andersen, P.E., Nonlinear cross talk between gratings recorded in $BaTiO_3$ by mutually incoherent beam pairs. *J. Appl. Phys.* (2000) v. 88 p. 5527-5533.

Nikolajsen, T.; Johansen, P.M., Optical fixing using shallow traps - application to $La_3Ga_5SiO_{14}$ doped with praseodymium. *J. Opt. A* (2000) v. 2 p. 255-259.

Nikolova, L.; Nedelchev, L.; Todorov, T.; Petrova, T.; Tomova, N.; Dragostinova, V.; Ramanujam, P.S.; Hvilsted, S., Self-induced light polarization rotation in azobenzene-containing polymers. *Appl. Phys. Lett.* (2000) v. 77 p. 657-659.

Pedersen, T.G.; Johansen, P.M.; Pedersen, H.C., Particle-in-a-bos model of one-dimensional excitons in conjugated polymers. *Phys. Rev. B* (2000) v. 61 p. 10504-10510.

Pedersen, T.G.; Johansen, P.M.; Pedersen, H.C., Characterization of azobenzene chromophores for reversible optical data storage: Molecular quantum calculations. *J. Opt. A* (2000) v. 2 p. 272-278.

Pedrys, R.; Krok, F.; Leskiewicz, P.; Schou, J.; Podschaske, U.; Cleff, B., Time-of-flight study of water ice sputtered by slow xenon ions. *Nucl. Instrum. Methods Phys. Res. B* (2000) v. 164 p. 861-867.

Podivilov, E.V.; Sturman, B.I.; Pedersen, H.C.; Johansen, P.M., Critical enhancement of photorefractive beam coupling. *Phys. Rev. Lett.* (2000) v. 85 p. 1867-1870.

Sanchez, C.; Alcala, R.; Hvilsted, S.; Ramanujam, P.S., Biphotonic holographic gratings in azobenzene polyesters: Surface relief phenomena and polarization effects. *Appl. Phys. Lett.* (2000) v. 77 p. 1440-1442.

Thestrup, B.; Dam-Hansen, C.; Schou, J.; Johansen, P.M., Holographic grating formation in laser-deposited aluminium-doped zinc oxide and indium tin oxide films. *J. Opt. A* (2000) v. 2 p. 196-199.

Thestrup, B.; Schou, J., Transparent conducting AZO and ITO films produced by pulsed laser ablation at 355 nm. *Appl. Phys. A* (1999) v. 69 p. S807-S810.

Toftmann, B.; Schou, J.; Larsen, N.B., Ablation from artificial or laser-induced crater surfaces of silver by laser irradiation at 355 nm. *Appl. Phys. A* (1999) v. 69 p. S811-S814.

Toftmann, B.; Schou, J.; Hansen, T.N.; Lunney, J.G., Angular distribution of electron temperature and density in a laser-ablation plume. *Phys. Rev. Lett.* (2000) v. 84 p. 3998-4001.

Åstrand, P.-O.; Ramanujam, P.S.; Hvilsted, S.; Bak, K.L.; Sauer, S.P.A., Ab initio calculation of the electronic spectrum of azobenzene dyes and its impact on the design of optical data storage materials. *J. Am. Chem. Soc.* (2000) v. 122 p. 3482-3487.

Åstrand, P.-O.; Sommer-Larsen, P.; Hvilsted, S.; Ramanujam, P.S.; Bak, K.L.; Sauer, S.P.A., Five-membered rings as diazo components in optical data storage devices: An ab initio investigation of the lowest singlet excitation energies. *Chem. Phys. Lett.* (2000) v. 325 p. 115-119.

5.1.2 Danish publications

Thestrup, B., Deposition of ITO and AZO thin films by laser ablation at 355 nm in a background atmosphere. Risø-R-1140(EN) (2000) vp. (ph.d. thesis) www.risoe.dk/rispubl/ofd/ris-r-1140.htm.

Thestrup, B.; Doggett, B.; Schou, J., Dynamics of laser-plasma for selected components studied with electrical probes. (2000) 25 p.

Toftmann, B.; Schou, J., SmartProbe and Langmuir probe measurements, Dublin, July 2000. (2000) 15 p.

5.1.3 Conference lectures

Hvilsted, S.; Ramanujam, P.S., Polymer scaffolds bearing azobenzene - A potential for optical information storage. In: Conference proceedings. International conference on new trends in functional polymers, Huangshan (CN), 8-13 May 2000. (University of Science and Technology of China, Huangshan, 2000) p. 26-31.

Lörincz, E.; Ujhelyi, F.; Sütö, A.; Szarvas, G.; Koppa, P.; Erdei, G.; Hvilsted, S.; Ramanujam, P.S.; Richter, P.I., Rewritable holographic memory card system. In: Proceedings. Optical data storage 2000, Whistler (CA), 14-17 May 2000. (The International Society for Optical Engineering, Bellingham, WA, 2000) (SPIE proceedings series, 4090) p. 185-190.

5.1.4 Publications for a broader readership

Dam-Hansen, C.; Pedersen, H.C., Replication of microoptics. *DOPS-Nyt* (2000) v. 15 (no.4) p. 18-21.

5.1.5 Unpublished Danish lectures

Holmelund, E.; Thestrup, B.; Schou, J.; Johnson, E.; Nielsen, M.M., Crystallinity of ITO and AZO thin films produced by laser ablation. In: Programme. Abstracts. List of participants. Danish Physical Society annual meeting 2000, Nyborg (DK), 8-9 Jun 2000. (HCØ Tryk, København, 2000) FF65P.

Petersen, P.M., New diode laser architectures using phase conjugators. Endagsmøde i Dansk Optisk Selskab, Lyngby (DK), 30 Nov 2000. Unpublished. Abstract available.

Schou, J., Characterization and production of transparent conductors by pulsed laser ablation. Modern topics in surface science, University of Southern Denmark, Odense (DK), 2-3 Nov 2000. Unpublished.

Schou, J., Spredningsteori og partiklers vekselvirkning med stof. Forelæsning ved Syddansk Universitet, Odense (DK), 19 Dec 2000. Unpublished.

Toftmann, B.; Schou, J., 'Flip-over' effect of a laser ablation plume. In: Programme. Abstracts. List of participants. Danish Physical Society annual meeting 2000, Nyborg (DK), 8-9 Jun 2000. (HCØ Tryk, København, 2000) AF01P.

5.1.6 Unpublished international lectures

Gazdag, L.; Szarvas, G.; Erdei, G.; Suto, A.; Fodor, J.; Lorincz, E.; Ujhelyi, F.; Koppa, P.; Richter, P.I.; Hvilsted, S.; Ramanujam, P.S., Holographic memory card system using polarization holography. In: Technical digest. International symposium on optical memory 2000 (ISOM 2000), Hokkaido (JP), 5-8 Sep 2000. (Chitose Institute of Science and Technology, Hokkaido, 2000) p. 150-151.

Holmelund, E.; Thestrup, B.; Schou, J.; Johnson, E.; Nielsen, M.M.; Tougaard, S., Crystallinity of ITO and AZO thin films produced by laser ablation. International millennium conference on quantitative surface analysis (QSA-11), Guildford (GB), 3-7 Jul 2000. Unpublished. Abstract available.

Hvilsted, S.; Ramanujam, P.S., Polarized light the landscape gardener of azobenzene polymer films. Nordic polymer days, Helsinki (FI), 24-26 May 2000. Unpublished. Abstract available.

Johansen, P.M.; Jespersen, K.G.; Pedersen, T.G., Dynamics of the electro-optic properties of dye-containing polymers. Nonlinear Optics for the Information Society (NOIS 2000), Twente (NL), 26-28 Oct 2000. Unpublished. Abstract available.

Kitchen, S.R.; Dam-Hansen, C.; Hanson, S.G., Optical displacement sensor based on common-path interferometry for industrial purposes. In: Program and summaries of contributions. Northern optics 2000, Uppsala (SE), 6-8 Jun 2000. Biedermann, K.; Olin, U. (eds.), (Swedish Optical Society, Stockholm, 2000) p. 134.

Pedersen, T.G.; Jespersen, K.G.; Johansen, P.M., AC field modulation of the optical properties of dye-containing polymers. E-MRS 2000 Spring meeting. Symposium H - Optoelectronics II: Molecular Photonics: from Macroscopic to Nanoscopic Applications, Strasbourg (FR), 30 May - 2 Jun 2000. Unpublished. Abstract available.

Pedersen, T.G.; Jespersen, K.G.; Johansen, P.M., Rotational diffusion model of orientational enhancement in AC field biased photorefractive polymers. E-MRS 2000 Spring meeting. Symposium J - Optoelectronics IV: Photorefractive Materials: Physical Phenomena and Applications, Strasbourg (FR), 30 May - 2 Jun 2000. Unpublished. Abstract available.

Pedersen, T.G.; Johansen, P.M.; Pedersen, H.C., Optical properties of liquid-crystalline azobenzene polymers. In: Program and summaries of contributions. Northern optics 2000, Uppsala (SE), 6-8 Jun 2000. Biedermann, K.; Olin, U. (eds.), (Swedish Optical Society, Stockholm, 2000) p. 175.

Pedersen, T.G.; Johansen, P.M.; Pedersen, H.C., Optical properties of liquid-crystalline azobenzene polymers. Northern Optics 2000 and EOSAM 2000, Uppsala (SE), 6-8 Jun 2000. Unpublished. Abstract available.

Pedersen, T.G.; Johansen, P.M., Optical data storage in liquid-crystalline azobenzene side-chain polymers. CLEO/Europe-IQEC 2000, Nice (FR), 10-15 Sep 2000. Unpublished. Abstract available.

Pedrys, R.; Krok, F.; Schou, J., Ejection of molecules from heavy water ice by keV electron or slow heavy ion bombardment. 3. International conference on cryocrystals and quantum crystals, Szklarska Poreba (PL), 28 Jul - 4 Aug 2000. Unpublished. Abstract available.

Petersen, P.M., Phase conjugate high power laser diode arrays (Invited talk). International conference on applications of photonic technology (ICAPT 2000), Quebec City (CA), 12-16 Jun 2000. Unpublished.

Podivilov, E.V.; Sturman, B.I.; Pedersen, H.C.; Johansen, P.M., Enhancement of the photorefractive 2W-coupling near the threshold of subharmonic generation. E-MRS 2000 Spring meeting. Symposium J - Optoelectronics IV: Photorefractive Materials: Physical Phenomena and Applications, Strasbourg (FR), 30 May - 2 Jun 2000. Unpublished. Abstract available.

Schou, J., Panel discussion: Can laser beam compete with ion beams?. Gordon research conference in laser interactions with materials, Andover, NH (US), 11-16 Jun 2000. Unpublished.

Schou, J., Laser ablation of simple systems: What can we learn from ion-beam interactions with solids. Gordon research conference in laser interactions with materials, Andover, NH (US), 11-16 Jun 2000. Unpublished.

Schou, J., Particle bombardment of the lightest, most volatile and complicated targets in vacuum, the solid hydrogens. Meeting at University of Southern Denmark, Institute of Physics, Odense (DK), 19 Sep 2000. Unpublished. Abstract available.

Schou, J., Sputtering of artificial interplanetary and stellar materials produced by laser ablation. Meeting on surface science in astrophysics and planetary physics, University of Oslo, Oslo (NO), 1 Dec 2000. Unpublished.

Schou, J.; Børgesen, P.; Pedrys, R., Sputtering of thin films of H_2, HD and D_2 by keV electron bombardment. 3. International conference on cryocrystals and quantum crystals, Szklarska Poreba (PL), 28 Jul - 4 Aug 2000. Unpublished. Abstract available.

Schou, J.; Pedrys, R., Sputtering of frozen CO by hydrogen ions. Photolysis and radiolysis of outer solar system ices (PROSSI) workshop, Laurel, MD (US), 27-29 Mar 2000. Unpublished. Abstract available.

Schou, J.; Stenum, B.; Pedrys, R., Sputtering of solid deuterium by He-ions. 13. International workshop on inelastic ion-surface collisions, San Carlos de Bariloche (AR), 20-24 Nov 2000. Unpublished.

Toftmann, B.; Schou, J.; Hansen, T.N.; Lunney, J., Electron temperatures and densities in a laser ablation plume. Gordon research conference in laser interactions with materials, Andover, NH (US), 11-16 Jun 2000. Unpublished.

Vidal, R.; Baragiola, R.; Bahr, D.; Schou, J., Sputter production of water and oxygen atmospheres at icy satellites: Temperature effects. Photolysis and radiolysis of outer solar system ices (PROSSI) workshop, Laurel, MD (US), 27-29 Mar 2000. Unpublished. Abstract available.

5.1.7 Internal reports, including patent applications

Imam, H.; Lindvold, L., CRIS project. Final report. (Forskningscenter Risø. Afdelingen for Optik og Fluid Dynamik, Roskilde, 1999) 29 p.

Juul Jensen, S.; Petersen, P.M.; Pedersen, C.; Raunkjær, M.; Ballegaard, H.P.; Pedersen, E.F., Test af gitterlaser til termisk eksponering i DMX-maskine hos Purup-Eskofot. Risø-Dok-651 (2000) vp.

Lindvold, L., The silver diffusion transfer process. (Forskningscenter Risø. Afdelingen for Optik og Fluid Dynamik, Roskilde, 1999) 2 p.

Pedersen, H.C.; Hovarth, R.; Lindvold, L.; Larsen, N.B., Reverse symmetry. UK patentansøgning 0026346.7.

Petersen, P.M.; Pedersen, C., Laser system with external optical feedback and use of such. DK patentansøgning PA 2000 01321.

Petersen, P.M.; Pedersen, C., Laser system with external optical feedback and use of such. DK patentansøgning PA 2000 01323.

Petersen, P.M.; Pedersen, C.; Juul Jensen, S., Gitterlaserprojekt. Statusrapport 1 til følgegruppe. Risø-Dok-644 (1999) 10 p.

Petersen, P.M.; Pedersen, C.; Juul Jensen, S., Gitterlaserprojekt. Statusrapport 2 til følgegruppe. Risø-Dok-645 (1999) 13 p.

Petersen, P.M.; Pedersen, C.; Juul Jensen, S., Gitterlaserprojekt. Statusrapport 3 til følgegruppe. Risø-Dok-646 (2000) 13 p.

Petersen, P.M.; Pedersen, C.; Juul Jensen, S., Gitterlaserprojekt. Midtvejsrapport til styregruppe. Risø-Dok-647 (2000) 18 p.

Petersen, P.M.; Pedersen, C.; Juul Jensen, S., Gitterlaserprojekt. Statusrapport 4 til følgegruppen. Risø-Dok-648 (2000) 14 p.

Petersen, P.M.; Pedersen, C.; Juul Jensen, S., Gitterlaserprojekt. Statusrapport 5 til følgegruppen. Risø-Dok-649 (2000) 15 p.

Petersen, P.M.; Pedersen, C.; Juul Jensen, S., Gitterlaserprojekt. Statusrapport 6 til følgegruppen. Risø-Dok-650 (2000) vp.

Petersen, P.M.; Pedersen, C.; Juul Jensen, S., Slutrapport for forprojekt til gitterlaserprojektet. Risø-Dok-652 (2000) 34 p.

5.2 Optical diagnostics and information processing

5.2.1 International publications

Andersen, P.E.; Hanson, S.G.; Jacques, S.L., Photoacoustic imaging of buried objects using an all-optical detection scheme. In: Laser-tissue interaction. Jacques, S.L. (ed.), (International Society for Optical Engineering, Bellingham, WA, 2000) (Selected SPIE Papers on CD-ROM, v. 9).

Frandsen, S.; Hansen, R.S.; Kristensen, L.; Miller, G.; Kjaer Hansen, J.; Sangill, O.; Lading, P., Laser anemometry for control and performance testing of wind turbines. 12-monthly progress report for the period 1 July 1999 to 1 July 2000. (2000) 54 p.

Glückstad, J.; Mogensen, P.C., Reconfigurable ternary-phase array illuminator based on the generalised phase contrast method. *Opt. Commun.* (2000) v. 173 p. 169-175.

Jacques, S.L.; Andersen, P.E.; Hanson, S.G.; Lindvold, L.R., Non-contact detection of laser-induced acoustic waves from buried absorbing objects using a dual-beam common-path interferometer. In: Laser-tissue interaction. Jacques, S.L. (ed.), (International Society for Optical Engineering, Bellingham, WA, 2000) (Selected SPIE Papers on CD-ROM, v. 9).

Jørgensen, T.M.; Linneberg, C., Subspace projections - an approach to variable selection and modeling. In: Putten, P. van der; Someren, M. van (eds.), CoIL challenge 2000: The insurance company case. LIACS-TR-2000-09 (2000) Paper no. 26 www.wi.leidenuniv.nl/~putten/library/cc2000/report2.html.

Limeres, J.; Carrascosa, M.; Petersen, P.M.; Andersen, P.E., Nonlinear cross talk between gratings recorded in $BaTiO_3$ by mutually incoherent beam pairs. *J. Appl. Phys.* (2000) v. 88 p. 5527-5533.

Linneberg, C.; Höskuldsson, A., Combined principal component preprocessing and n-tuple neural networks for improved classification. *J. Chemometr.* (2000) v. 14 p. 573-583.

Mogensen, P.C.; Glückstad, J., Dynamic array generation and pattern formation for optical tweezers. *Opt. Commun.* (2000) v. 175 p. 75-81.

Mogensen, P.C.; Glückstad, J., A phase-based optical encryption system with polarisation encoding. *Opt. Commun.* (2000) v. 173 p. 177-183.

Mogensen, P.C.; Glückstad, J., Phase-only optical encryption. *Opt. Lett.* (2000) v. 25 p. 566-568.

Thrane, L.; Yura, H.T.; Andersen, P.E., Analysis of optical coherence tomography systems based on the extended Huygens-Fresnel principle. *J. Opt. Soc. Am. A* (2000) v. 17 p. 484-490.

Yura, H.T.; Thrane, L.; Andersen, P.E., Closed-form solution for the Wigner phase-space distribution function for diffuse reflection and small-angle scattering in a random medium. *J. Opt. Soc. Am. A* (2000) v. 17 p. 2464-2474.

5.2.2 Danish publications

Mogensen, P.C.; Eriksen, R.L.; Glückstad, J., Programmable phase optics. Progress report 3, 1st December 1999 - 31st May 2000. (2000) 20 p.

Mogensen, P.C.; Eriksen, R.L.; Glückstad, J., Programmable phase optics. Progress report 4, 1st June 2000 - 30th November 2000. (2000) 24 p.

Sundstrøm, M., I skyggen af Newtons æbletræ. *Kvant* (2000) (no.1) p. 20-21; bagsiden.

5.2.3 Conference lectures

Andersen, F., Temperaturindikatorer, utraditionelle sensorer og dataloggere. In: Konferanse. Temperatur 2000, Oslo (NO), 7-8 Jun 2000. (2000) 6 p.

Andersen, F., Estimat af total fejl i komplet termoelementkreds. In: Konferanse. Temperatur 2000, Oslo (NO), 7-8 Jun 2000. (2000) 12 p.

Andersen, F., Thermoelectric instability of some metal-sheathed mineral-insulated standard thermocouples related to type, sheath alloy and environment of exposure. In: Konferanse. Temperatur 2000, Oslo (NO), 7-8 Jun 2000. (2000) 7 p.

Andersen, F., Fjernvarmemålere. Måling af temperatur i varmemålere. In: Konferanse. Temperatur 2000, Oslo (NO), 7-8 Jun 2000. (2000) 8 p.

Andersen, F., Building up a laboratory for calibrating temperature instruments. In: Konferanse. Temperatur 2000, Oslo (NO), 7-8 Jun 2000. (2000) 6 p.

Andersen, F., Termometret måler sin egen temperatur!. In: Konferanse. Temperatur 2000, Oslo (NO), 7-8 Jun 2000. (2000) 10 p.

Andersen, P.E.; Thrane, L.; Yura, H.T.; Tycho, A.; Jørgensen, T.M., Modeling the optical coherence tomography geometry using the extended Huygens-Fresnel principle and Monte Carlo simulations (invited paper). In: Proceedings. Laser-tissue interaction 11: Photochemical, photothermal, and photomechanical, San Jose, CA (US), 22-27 Jan 2000. Duncan, D.D.; Hollinger, J.O.; Jacques, S.L. (eds.), (International Society for Optical Engineering, Bellingham, WA, 2000) (Proceedings of SPIE, v. 3914; Progress in biomedical optics and imaging, v. 1, no. 8) p. 394-406.

Clausen, S., Laser flow measurements in flames. In: Combustion laser diagnostics in the area of development and application of laser techniques for combustion diagnostics. One day seminar, Lund (SE), 27 Apr 2000. (2000) 5 p.

Clausen, S., Målenøjagtighed og fejlkilder ved berøringsløs temperaturmåling. In: Konferanse. Temperatur 2000, Oslo (NO), 7-8 Jun 2000. (2000) 8 p.

Clausen, S., Berøringsløs temperaturmåling af varme gasser. In: Konferanse. Temperatur 2000, Oslo (NO), 7-8 Jun 2000. (2000) 9 p.

Glückstad, J., Optical encryption using phase-only spatial light modulation (invited paper). In: Meeting of the Information Optics Group. Satellite event to Northern optics 2000, Uppsala (SE), 8 Jun 2000. (2000) 5 p.

Glückstad, J.; Mogensen, P.C., Optimising the common path interferometer: A theoretical framework. In: Interferometry in speckle light. Theory and applications. Proceedings. International conference, Lausanne (CH), 25-28 Sep 2000. (Springer-Verlag, Berlin, 2000) p. 543-550.

Glückstad, J.; Mogensen, P.C., Optimised imaging and display of phase objects. In: Proceedings. 2. International conference on optical design and fabrication (ODF 2000), Tokyo (JP), 15-17 Nov 2000. (Optical Society of Japan, Tokyo, 2000) p. 133-136.

Hansen, R.S.; Yura, H.T.; Hanson, S.G.; Rose, B., Three-dimensional speckles: Static and dynamic properties. In: Proceedings. 4. International conference on correlation optics, Chernivtsy (UA), 11-14 May 1999. Angelsky, O.V. (ed.), (The International Society for Optical Engineering, Bellingham, WA, 2000) (SPIE proceedings series, 3904) p. 140-149.

Kaiser, N.E., Nøjagtige temperaturmålinger med Pt 100 følere. In: Konferanse. Temperatur 2000, Oslo (NO), 7-8 Jun 2000. (2000) 11 p.

Kaiser, N.E., Feilkilder ved bruk av resistanstermpmeter. In: Konferanse. Temperatur 2000, Oslo (NO), 7-8 Jun 2000. (2000) 9 p.

Kaiser, N.E., Kalibrering av termometre i tørrblokkalibrator. In: Konferanse. Temperatur 2000, Oslo (NO), 7-8 Jun 2000. (2000) 8 p.

Mogensen, P.C.; Glückstad, J., Practical implementation of phase-only optical encryption system. In: Optical security and counterfeit deterrence techniques 3. Electronic imaging 2000, San Jose, CA (US), 27-28 Jan 2000. Renesse, R.L. van; Vliegenthart, W.A. (eds.), (International Society for Optical Engineering, Bellingham, WA, 2000) (Proceedings of SPIE, v. 3973) p. 284-293.

Mogensen, P.C.; Glückstad, J., The application of spatial light modulators to optical encryption systems. In: Proceedings. 4. International conference and exhibition on optoelectronics, optical sensors and measuring techniques (OPTO 2000), Erfurt (DE), 9-11 May 2000. (AMA Service GmbH, Wunstorf, 2000) p. 227-232.

Mogensen, P.C.; Glückstad, J., Dynamic array generation using phase-only spatial light modulators. In: Technical digest. Diffractive optics and micro-optics meeting, Quebec City (CA), 18-22 Jun 2000. (Optical Society of America, Washington, DC, 2000) p. 84-86.

Nørgaard Andersen, T.; Jessen, N.C.; Arendt-Nielsen, L., Determination of the temperature distribution in skin using a finite element model. In: Proceedings. Laser-tissue interaction 11: Photochemical, photothermal, and photomechanical, San Jose, CA (US), 22-27 Jan 2000. Duncan, D.D.; Hollinger, J.O.; Jacques, S.L. (eds.), (International Society for Optical Engineering, Bellingham, WA, 2000) (Proceedings of SPIE, v. 3914; Progress in biomedical optics and imaging, v. 1, no. 8) p. 54-65.

Popov, I.A.; Veselov, L.M.; Hanson, S.G.; Gluzmann, A., Comparative study of accuracy of Doppler and grating velocimeters. In: Proceedings. 4. International conference on vibration measurements by laser techniques: Advances and applications, Ancona (IT), 21-23 Jun 2000. Tomasini, E.P. (ed.), (The International Society for Optical Engineering, Bellingham, WA, 2000) (SPIE proceedings series, 4072) p. 222-227.

Thrane, L.; Yura, H.T.; Andersen, P.E., Optical coherence tomography: New analytical model and the shower curtain effect. In: Optical technologies in biophysics and medicine. Saratov Fall meeting '99, Saratov (RU), 5-8 Oct 1999. Tuchin, V.V.; Zimnyakov, D.A.; Pravdin, A.B. (eds.), (International Society for Optical Engineering, Bellingham, WA, 2000) (Proceedings of SPIE, v. 4001) p. 202-208.

Thrane, L.; Yura, H.T.; Andersen, P.E., Calculation of the maximum obtainable probing depth of optical coherence tomography in tissue. In: Proceedings. Coherence domain optical methods in biomedical science and clinical applications 4, San Jose, CA (US), 24-26 Jan 2000. Tuchin, V.V.; Izatt, J.A.; Fujimoto, J.G. (eds.), (International Society for Optical Engineering, Bellingham, WA, 2000) (Proceedings of SPIE, v. 3915; Progress in biomedical optics and imaging, v. 1, no. 9) p. 2-11.

Tycho, A.; Jørgensen, T.M.; Thrane, L., Investigating the focusing problem in OCT: Comparison of Monte Carlo simulations, the extended Huygens-Fresnel principle and experiments. In: Proceedings. Coherence domain optical methods in biomedical science and clinical applications 4, San Jose, CA (US), 24-26 Jan 2000. Tuchin, V.V.; Izatt, J.A.; Fujimoto, J.G. (eds.), (International Society for Optical Engineering, Bellingham, WA, 2000) (Proceedings of SPIE, v. 3915; Progress in biomedical optics and imaging, v. 1, no. 9) p. 25-35.

5.2.4 Publications for a broader readership

Clausen, S., Lyset afslører detaljer i forbrændingsprocessen. *Byggeteknik Energi og Miljø* (2000) (no.10.april) p. 1 (2. sekt.).

Dam-Hansen, C.; Pedersen, H.C., Replication of microoptics. *DOPS-Nyt* (2000) v. 15 (no.4) p. 18-21.

Hansen, R.S.; Hanson, S.G., Optical design for sensor applications. *DOPS-Nyt* (2000) v. 15 (no.4) p. 13-17.

Hanson, S.G.; Hansen, R.S.; Pedersen, S.P.; Rose, B., Optical sensor systems based on determining angular displacements. *DOPS-Nyt* (2000) v. 15 (no.4) p. 26-29.

Sundstrøm, M., I skyggen af Newtons æbletræ. Rejsebeskrivelse. *DOPS-Nyt* (2000) v. 15 (no.1) p. 20-22.

5.2.5 Unpublished Danish lectures

Andersen, P.E., Non-invasive tissue studies by optical coherence tomography. Symposium: Exploring the potentials for using physics in the study of biological structures, processes and interactions, Risø (DK), 26 Oct 2000. Unpublished.

Andersen, P.E., Opto-acoustics in biomedical optics. BIOP symposium: Biomedical optics and new laser systems, Risø (DK), 21 Nov 2000. Unpublished.

Andersen, P.E.; Bjerring, P., IR thermography in skin disease. Meeting on infrared thermography. Modern developments. Dansk Selskab for Klinisk Fysiologi og Nuklearmedicin, Frederiksberg (DK), 22 Feb 2000. Unpublished.

Clausen, S., Berøringsfri FTIR måling. FT-IR seminar, Brøndby (DK), 15 Jun 2000. Unpublished.

Eriksen, R.L., Laser tweezers. BIOP symposium: Biomedical optics and new laser systems, Risø (DK), 21 Nov 2000. Unpublished.

Glückstad, J., Generalized phase contrast. BIOP symposium: Biomedical optics and new laser systems, Risø (DK), 21 Nov 2000. Unpublished.

Hanson, S.G., Miniature-lasere og deres anvendelser. Foredrag på H.C. Ørsted Instituttet, Ungdommens Naturvidenskabelige Forening, København (DK), 20 Jan 2000. Unpublished.

Jensen, P.S., Fourier-transform infrared spectroscopy on biological materials. BIOP symposium: Biomedical optics and new laser systems, Risø (DK), 21 Nov 2000. Unpublished.

Samsøe, E., Development of a new diode laser system for photodynamic therapy. BIOP symposium: Biomedical optics and new laser systems, Risø (DK), 21 Nov 2000. Unpublished.

Sundstrøm, M., Øjet og de fysiologiske farver. Folkeuniversitetet i Roskilde, Roskilde (DK), Jan 2000. Unpublished.

Sundstrøm, M., Øjet og de fysiologiske farver. Folkeuniversitetet i København, København (DK), Mar 2000. Unpublished.

5.2.6 Unpublished international lectures

Andersen, P.E., Modelling the optical coherence tomography geometry using the extended Hyugens-Frasnel principle and Monte Carlo simulations. St. Petersburg 3. International workshop: Semiconductor and solid state laser in medicine, St. Petersburg (RU), 25-27 May 2000. Unpublished.

Andersen, P.E., Biomedical optics at Risø. Meeting at Universidad Autónoma de Madrid, Facultad de Ciencias, Departamento de Física de Materiales, Madrid (ES), 25 Sep 2000. Unpublished.

Clausen, S., Flow, temperature and radiation measurements. Nordic course: Measurement techniques in solids combustion; methods and experiences, Lyngby (DK), 29-31 May 2000. Unpublished. Abstract available.

Glückstad, J.; Mogensen, P.C., Optimising common path interferometers: A complete approach. In: Program and summaries of contributions. Northern optics 2000, Uppsala (SE), 6-8 Jun 2000. Biedermann, K.; Olin, U. (eds.), (Swedish Optical Society, Stockholm, 2000) p. 105.

Hansen, R.S., Laser anemometry for control and performance measurements on wind turbines. EC wind energy research projects contractors' meeting 2000: Advances in wind energy RTDF - from FP4 towards FP5, Athens (GR), 3-5 May 2000. Unpublished. Abstract available.

Hansen, R.S.; Lading, L.; Miller, G., Optical mixing in coherent LIDARs: Comparing three schemes (invited lecture). IEEE International conference on applications of photonic technology (ICAPT 2000), Quebec City (CA), 12-16 Jun 2000. Unpublished. Abstract available.

Hanson, S.G., The complex ABCD-formalism for beam propagation through optical systems including apertures. Lecture given at International Center for Advanced Studies (INCAS), Nizhny Novgorod (RU), 11 Apr 2000. Unpublished.

Hanson, S.G., Theory for beam propagation through random media: A description based on the ABCD-method. Lecture given at International Center for Advanced Studies (INCAS), Nizhny Novgorod (RU), 13 Apr 2000. Unpublished.

Hanson, S.G., Theory for static and dynamic speckles in complex ABCD systems. Lecture given at International Center for Advanced Studies (INCAS), Nizhny Novgorod (RU), 13 Apr 2000. Unpublished.

Hanson, S.G., Basic sensors for measuring linear displacements and velocities. Lecture given at International Center for Advanced Studies (INCAS), Nizhny Novgorod (RU), 14 Apr 2000. Unpublished.

Hanson, S.G., Sensors for measuring angular deflections and rotational speed. Lecture given at International Center for Advanced Studies (INCAS), Nizhny Novgorod (RU), 15 Apr 2000. Unpublished.

Hanson, S.G., A simple system for measuring 2-D rotations. Lecture given at International Center for Advanced Studies (INCAS), Nizhny Novgorod (RU), 17 Apr 2000. Unpublished.

Hanson, S.G.; Hansen, R.S.; Rose, B., Measurements of twist, rotation and angular position of solid objects (invited lecture). IEEE International conference on applications of photonic technology (ICAPT 2000), Quebec City (CA), 12-16 Jun 2000. Unpublished.

Hanson, S.G.; Rose, B.; Hansen, R.S., Compact optical sensors for measurement of rotations. In: Program and summaries of contributions. Northern optics 2000, Uppsala (SE), 6-8 Jun 2000. Biedermann, K.; Olin, U. (eds.), (Swedish Optical Society, Stockholm, 2000) p. 109.

Kitchen, S.R.; Dam-Hansen, C.; Hanson, S.G., Optical displacement sensor based on common-path interferometry for industrial purposes. In: Program and summaries of contributions. Northern optics 2000, Uppsala (SE), 6-8 Jun 2000. Biedermann, K.; Olin, U. (eds.), (Swedish Optical Society, Stockholm, 2000) p. 134.

Mogensen, P.C.; Glückstad, J., Dynamic array generation for optical tweezers. In: Program and summaries of contributions. Northern optics 2000, Uppsala (SE), 6-8 Jun 2000. Biedermann, K.; Olin, U. (eds.), (Swedish Optical Society, Stockholm, 2000) p. 57.

5.2.7 Internal reports, including patent applications

Andersen, P.E.; Tycho, A.; Bjarklev, A., Optical amplification in coherence reflectometry. DK patentansøgning PA 2000 01318.

Glückstad, J., Method and an apparatus for generating a phase-modulated wavefront of electromagnetic radiation. US provisional patent application.

Glückstad, J.; Mogensen, P.C., Polarisation encryption/decryption module. DK patentansøgning PA 2000 01367.

Hanson, S.G.; Hansen, B.H.; Hansen, R.S., Målesystemer til mikrofonhus og membran. Risø-Dok-630 (2000) vp.

Hanson, S.G.; Hansen, R.S., A computer input device with optical detection means. DK patentansøgning .

5.3 **Plasma and fluid dynamics**

5.3.1 International publications

Bergé, L.; Juul Rasmussen, J., Self-focusing and collapse of light beams in nonlinear dispersive media. In: Nonlinear science at the dawn of the 21st century. Christiansen, P.L.; Sørensen, M.P.; Scott, A.C. (eds.), (Springer-Verlag, Berlin, 2000) (Lecture notes in physics, 542) p. 213-228.

Bergé, L.; Mezentsev, V.K.; Juul Rasmussen, J.; Christiansen, P.L.; Gaididei, Y.B., Self-guiding light in layered nonlinear media. *Opt. Lett.* (2000) v. 25 p. 1037-1039.

Bergeron, K.; Coutsias, E.A.; Lynov, J.P.; Nielsen, A.H., Dynamical properties of forced shear layers in an annular geometry. *J. Fluid Mech.* (2000) v. 402 p. 255-289.

Clercx, H.J.H.; Nielsen, A.H., Vortex statistics for turbulence in a container with rigid boundaries. *Phys. Rev. Lett.* (2000) v. 85 p. 752-755.

Dinesen, P.G.; Hesthaven, J.S.; Lynov, J.P., A pseudospectral collocation time-domain method for diffractive optics. *Appl. Num. Math.* (2000) v. 33 p. 199-206.

Dinesen, P.G.; Hesthaven, J.S., Fast and accurate modeling of waveguide grating couplers. *J. Opt. Soc. Am. A* (2000) v. 17 p. 1565-1572.

Konijnenberg, J.A. van de; Naulin, V.; Juul Rasmussen, J.; Stenum, B.; Heijst, G.J.F. van, Linear spin-up in a sliced cylinder. *Geophys. Astrophys. Fluid Dynamics* (2000) v. 92 p. 85-114.

Lodahl, P.; Bache, M.; Saffman, M., Modification of pattern formation in doubly resonant second-harmonic generation by competing parametric oscillation. *Opt. Lett.* (2000) v. 25 p. 654-656.

Lodahl, P.; Bache, M.; Saffman, M., Spiral intensity patterns in the internally pumped optical parametric oscillator. *Phys. Rev. Lett.* (2000) v. 85 p. 4506-4509.

Lodahl, P.; Saffman, M., Nonlinear analysis of pattern formation in singly resonant second-harmonic generation. *Opt. Commun.* (2000) v. 184 p. 493-505.

Lushnikov, P.M.; Saffman, M., Collapse in a forced three-dimensional nonlinear Schrodinger equation. *Phys. Rev. E* (2000) v. 62 p. 5793-5796.

Lynov, J.P.; Bergeron, K.; Coutsias, E.A.; Nielsen, A.H., An accurate and efficient spectral method for studies of the dynamical properties of forced, circular shear layers. *Appl. Num. Math.* (2000) v. 33 p. 175-181.

Ruban, V.P., Interaction of a vortex ring with the free surface of an ideal fluid. *Phys. Rev. E* (2000) v. 62 p. 4950-4958.

Ruban, V.P., Slow flows of a relativistic perfect fluid in a static gravitational field. *Phys. Rev. D* (2000) v. 62 p. 127504.1-127504.4.

Søndergaard, T.; Dridi, K.H., Energy flow in photonic crystal waveguides. *Phys. Rev. B* (2000) v. 61 p. 15688-15696.

5.3.2 Danish publications

Dannemand Andersen, P.; Michelsen, P.K.; Nissen, L., Dansk energiforskning i et internationalt perspektiv. Risø-R-1194(DA) (2000) 19p. www.risoe.dk/rispubl/andreafd/ris-r-1194.htm.

Lodahl, P., Spatio-temporal structures in cavity enhanced $\chi^{(2)}$ frequency conversion processes. Risø-R-1210(EN) (2000) 162 p. (ph.d. thesis) www.risoe.dk/rispubl/ofd/ris-r-1210.htm.

5.3.3 Conference lectures

Dinesen, P.G.; Hesthaven, J.S.; Lynov, J.-P., Rigorous three-dimensional analysis of surface-relief gratings using a spectral collocation method. In: Diffractive/holographic technologies and spatial light modulators 7. Optoelectronics 2000, San Jose, CA (US), 22-28 Jan 2000. Cindrich, I.; Lee, S.H.; Sutherland, R.L. (eds.), (International Society for Optical Engineering, Bellingham, WA, 2000) (Proceedings of SPIE, v. 3951) p. 2-10.

Dinesen, P.G.; Hesthaven, J.S.; Lynov, J.-P., Rigorous analysis of focusing grating couplers using a time-domain spectral collocation method. In: Diffractive/holographic technologies and spatial light modulators 7. Optoelectronics 2000, San Jose, CA (US), 22-28 Jan 2000. Cindrich, I.; Lee, S.H.; Sutherland, R.L. (eds.), (International Society for Optical Engineering, Bellingham, WA, 2000) (Proceedings of SPIE, v. 3951) p. 11-19.

Dinesen, P.G.; Hesthaven, J.S., Rigorous 3-D analysis of focusing grating couplers using a spectral collocation method. In: Technical digest. Diffractive optics and micro-optics meeting, Quebec City (CA), 18-22 Jun 2000. (Optical Society of America, Washington, DC, 2000) p. 81-83.

Dinesen, P.G.; Hesthaven, J.S., Analysis of grating couplers using the boundary variation method. In: Technical digest. Diffractive optics and micro-optics meeting, Quebec City (CA), 18-22 Jun 2000. (Optical Society of America, Washington, DC, 2000) p. 84-86.

5.3.4 Publications for a broader readership

Dinesen, P.G.; Hesthaven, J.S.; Lynov, J.-P., Optik på supercomputere - når linseligningen ikke slår til. *DOPS-Nyt* (2000) v. 15 (no.1) p. 6-11.

5.3.5 Unpublished Danish lectures

Basse, N.P.; Zoletnik, S.; Saffman, M.; Endler, M., Density fluctuations during confinement changes in the Wendelstein 7-AS stellarator. In: Programme. Abstracts. List of participants. Danish Physical Society annual meeting 2000, Nyborg (DK), 8-9 Jun 2000. (HCØ Tryk, København, 2000) AF10.

Korsholm, S.B.; Cunningham, G.; Michelsen, P.K.; Juul Rasmussen, J., Density fluctuation measurements in the mega amp spherical tokamak. In: Programme. Abstracts. List of participants. Danish Physical Society annual meeting 2000, Nyborg (DK), 8-9 Jun 2000. (HCØ Tryk, København, 2000) AF06.

Lodahl, P., Spatial instabilities in optical second harmonic generation. Atomic Physics' seminar, Aarhus (DK), 18 May 2000. Unpublished.

Lodahl, P., Spatial instabilities and quantum noise in optical second harmonic generation. Workshop on parametric processes, Risø (DK), 14-15 Jun 2000. Unpublished.

Lodahl, P., Spatial instabilities in optical second harmonic generation. Seminar at the Technical University of Denmark, Lyngby (DK), 6 Jul 2000. Unpublished.

Michelsen, P.K., Fusionsenergi - er det en mulighed. Foredrag for gymnasieklasse fra Tønder Gymnasium, Lyngby (DK), 13 Mar 2000. Unpublished.

Michelsen, P.K., Fusionsenergi - er det en mulighed. Foredrag for gymnasieklasse fra Varde Gymnasium, Lyngby (DK), 11 Oct 2000. Unpublished.

Michelsen, P.K., Kursus i plasmafysik. Forelæsningsrække på Danmarks Tekniske Universitet, Institut for Fysik, Lyngby (DK), Sep - Dec 2000. Unpublished.

Naulin, V., Numerical simulation of plasma turbulence. In: Programme. Abstracts. List of participants. Danish Physical Society annual meeting 2000, Nyborg (DK), 8-9 Jun 2000. (HCØ Tryk, København, 2000) AF08.

5.3.6 Unpublished international lectures

Andersen, A., The bathtub vortex. Workshop on plasma turbulence, anomalous transport, and numerical modeling, Risø (DK), 5-7 Dec 2000. Unpublished.

Andersen, A.; Bohr, T.; Schram Christensen, M.; Nørgaard Nielsen, M.; Richter, J., Bathtub vortices. In: Book of abstracts. 4. EUROMECH fluid mechanics conference, Eindhoven (NL), 19-23 Nov 2000. (Eindhoven University of Technology, Eindhoven, 2000) p. 193.

Basse, N.P.; Zoletnik, S.; Saffman, M.; Endler, M., Density fluctuations during confinement changes in the Wendelstein 7-AS stellarator. In: Abstracts of invited and contributed papers. 27. European Physical Society conference on controlled fusion and plasma physics, Budapest (HU), 12-16 Jun 2000. Szegö, K.; Todd, T.N.; Zoletnik, S. (eds.), (KFKI-Research Institute for Particle and Nuclear Physics, Budapest, 2000) p. 325.

Juul Rasmussen, J., Turbulent equipartition and anomalous transport in electrostatic turbulence. Meeting at Alfvén Laboratory, Royal Institute of Technology, Stockholm (SE), 28 Feb 2000. Unpublished.

Juul Rasmussen, J., Turbulent equipartition and anomalous transport in electrostatic turbulence. Seminar, Institut für Ionenphysik, Innsbruck (AT), 19 May 2000. Unpublished.

Juul Rasmussen, J., Electrostatic waves and turbulence in plasmas. Course at Institut für Ionenphysik, Innsbruck Universität (14 lectures), Innsbruck (AT), May 2000. Unpublished.

Juul Rasmussen, J., Collapse dynamics and soliton stability in the nonlinear Schrödinger equation. Meeting on dynamics of attractive Bose condensates, Laboratoire de Physique Statistique, Ecole Normale Supérieure CECAM, Lyon (FR), 29-31 May 2000. Unpublished.

Juul Rasmussen, J., Introduction, turbulence in fluids and plasmas. Workshop on plasma turbulence, anomalous transport, and numerical modeling, Risø (DK), 5-7 Dec 2000. Unpublished.

Juul Rasmussen, J., Energy localization and collapse dynamics in discrete nonlinear Schrödinger equations. Isaac Newton Institute for Mathematical Sciences and Warwick Mathematics Research Centre joint workshop: Singularities in classical, quantum and magnetic fluids, Warwick (GB), 20-23 Oct 2000. Unpublished. Abstract available.

Juul Rasmussen, J.; Naulin, V., Particle dispersion and density flux in electrostatic drift-wave turbulence. 35. Nordic plasma- and gas discharge symposium, Wadahl (NO), 30 Jan - 2 Feb 2000. Unpublished.

Juul Rasmussen, J.; Naulin, V., Turbulent equipartition and pinch fluxes in pressure driven electrostatic turbulence. International workshop on chaotic transport and complexity, Carry le rouet (FR), 26-30 Jun 2000. Unpublished. Abstract available.

Konijnenberg, J. van de; Naulin, V.; Juul Rasmussen, J.; Stenum, B., Generation of large scale zonal flows over topography by forced turbulence. In: Book of abstracts. 4.

EUROMECH fluid mechanics conference, Eindhoven (NL), 19-23 Nov 2000. (Eindhoven University of Technology, Eindhoven, 2000) p. 39.

Korsholm, S.B., Introduction to fusion energy and fusion research. Visit from Stenhus Gymnasium at Culham Science Centre, Culham (GB), 27 Mar 2000. Unpublished.

Korsholm, S.B., Introduction to fusion energy and fusion research. Visit from Tørring Amtsgymnasium at Culham Science Centre, Culham (GB), 12 Apr 2000. Unpublished.

Korsholm, S.B., Reflectometry measurements of turbulence in MAST. Workshop on plasma turbulence, anomalous transport, and numerical modeling, Risø (DK), 5-7 Dec 2000. Unpublished.

Korsholm, S.B.; Michelsen, P.K.; Naulin, V.; Juul Rasmussen, J., Reynolds stress and shear flow generation. In: Abstracts of invited and contributed papers. 27. European Physical Society conference on controlled fusion and plasma physics, Budapest (HU), 12-16 Jun 2000. Szegö, K.; Todd, T.N.; Zoletnik, S. (eds.), (KFKI-Research Institute for Particle and Nuclear Physics, Budapest, 2000) p. 375.

Lomholt, S.; Maxey, M.R.; Stenum, B., Force coupling method for computing particle dynamics in fluid flows. ERCOFTAC conference on particle-laden flows, Kappel (CH), 3-5 Jul 2000. Unpublished.

Michelsen, P.K., Status of the fusion research. Workshop on plasma turbulence, anomalous transport, and numerical modeling, Risø (DK), 5-7 Dec 2000. Unpublished.

Naulin, V., Transport barrier and flux statistics in a turbulent equipartition model (invited paper). 13. US Transport Task Force workshop, Burlington, VT (US), 26-29 Apr 2000. Unpublished.

Naulin, V., Transport und Dispersion idealer Teilchen in 2-dimensionaler Turbulenz. Meeting at IPP Greifswald, Greifswald (DE), 22 Feb 2000. Unpublished.

Naulin, V., Formation of flows out of turbulence in fluids and plasmas. Workshop on plasma turbulence, anomalous transport, and numerical modeling, Risø (DK), 5-7 Dec 2000. Unpublished.

Naulin, V., Physics of drift-Alfvén turbulence. Workshop on plasma turbulence, anomalous transport, and numerical modeling, Risø (DK), 5-7 Dec 2000. Unpublished.

Naulin, V., Generation of flows from turbulence. Ringberg IPP Theorie Seminar, Tegernsee (DE), 13-17 Nov 2000. Unpublished.

Naulin, V., Generation of flows from turbulence. Meeting at University of St Andrews, Solar and Magnetospheric Theory Group, St Andrews (GB), 22 Nov 2000. Unpublished.

Naulin, V.; Jessen, T.; Michelsen, P.K.; Nielsen, A.H.; Juul Rasmussen, J., Anomalous diffusion of particles and the relation to transport in vortex dominated turbulence. International congress on plasma physics (ICPP-2000) combined with 42. Annual meeting of the Division of Plasma Physics of the American Physical Society, Quebec City (CA), 23-27 Oct 2000. Unpublished.

Naulin, V.; Juul Rasmussen, J., 3D driftwave turbulence simulations at Risø. 35. Nordic plasma- and gas discharge symposium, Wadahl (NO), 30 Jan - 2 Feb 2000. Unpublished.

Naulin, V.; Juul Rasmussen, J., Transport and particle diffusion in vortex dominated driftwave turbulence. International workshop on chaotic transport and complexity, Carry le rouet (FR), 26-30 Jun 2000. Unpublished. Abstract available Naulin, V.; Nycander, J.; Juul Rasmussen, J., Transport barriers and turbulent equipartition. International congress on plasma physics (ICPP-2000) combined with 42. Annual meeting of the Division of Plasma Physics of the American Physical Society, Quebec City (CA), 23-27 Oct 2000. Unpublished.

Naulin, V.; Scott, B., Benchmarking codes for drift Alfvén turbulence. 7. EU-US Transport Task Force workshop: Transport in fusion plasmas - transport barriers physics, Varenna (IT), 4-7 Sep 2000. Unpublished.

Nielsen, A.H., Vortex dynamics and turbulence in two-dimensional flows. Workshop on plasma turbulence, anomalous transport, and numerical modeling, Risø (DK), 5-7 Dec 2000. Unpublished.

Nielsen, A.H.; Clercx, H.J.H.; Coutsias, E.A., 2D turbulence in a bounded domain. In: Book of abstracts. 4. EUROMECH fluid mechanics conference, Eindhoven (NL), 19-23 Nov 2000. (Eindhoven University of Technology, Eindhoven, 2000) p. 34.

Okkels, F., Shell models for turbulence. Workshop on plasma turbulence, anomalous transport, and numerical modeling, Risø (DK), 5-7 Dec 2000. Unpublished.

Schröder, C.; Klinger, T.; Block, D.; Piel, A.; Bonhomme, G.; Naulin, V., Taming drift wave turbulence: Experiment and simulation. International congress on plasma physics (ICPP-2000) combined with 42. Annual meeting of the Division of Plasma Physics of the American Physical Society, Quebec City (CA), 23-27 Oct 2000. Unpublished.

Stenum, B., Diagnostics of the flow field of a forced monopole. EGS 2000, 25. General assembly, Nice (FR), 25-29 Apr 2000. Unpublished.

Stenum, B., The force-coupling method applied to particle motion in flow channels. 5. Annual meeting of the Nordic ERCOFTAC Pilot Center, Små Dalarö (SE), 3-5 Sep 2000. Unpublished.

5.3.7 Internal reports

Korsholm, S.B.; Cunningham, G., First results of the MAST fluctuation reflectometer. MAST-OPS-Note-00.17 (2000) vp.

Michelsen, P.K.; Morthorst, P.E. (eds.), Slutrapport fra det rådgivende strategipanel for energiteknologi. Risø-I-1600(DA) (2000) 71 p.

6. Personnel

Scientific Staff

Andersen, Peter E.
Bak, Jimmy
Clausen, Sønnik
Dinesen, Palle (from 1 October)
Glückstad, Jesper
Hansen, René Skov (from 1 March)
Hanson, Steen Grüner
Jakobsen, Michael Linde (from 1 April)
Jensen, Sussie Juul (from 1 October)
Jessen, Niels Christian (until 31 July)
Johansen, Per Michael
Jørgensen, Thomas Martini
Kaiser, N.E. (until 31 January)
Kirkegaard, Mogens
Larsen, Henning
Lindvold, Lars R. (until 30 April)
Lynov, Jens-Peter
Michelsen, Poul K.
Naulin, Volker
Nielsen, Anders H.
Pedersen, Henrik Chresten
Petersen, Paul Michael
Ramanujam, P.S.
Rasmussen, Jens Juul
Schou, Jørgen
Stenum, Bjarne

Post Docs

Chi, Mingjun (from 1 November)
Dinesen, Palle (until 30 September)
Hansen, René Skov (until 29 February)
Jensen, Sussie Juul (1 February – 15 March; 15 August – 30 September)
Lomholt, Sune (28 August – 31 October)
Mogensen, Paul Christian
Nielsen, Birgitte Thestrup (from 1 July)
Thrane, Lars (from 1 October)

Industrial Post Docs

Dridi, Kim (from 1 April)
Løbel, Martin
Nielsen, Steen Arnfred

PhD Students

Andersen, Anders
Andersen, Eva Samsøe (from 1 October)
Andersen, Thim Nørgaard (until 31 July)
Bache, Morten
Basse, Nils
Christensen, Bo Toftman (from 1 June)
Eriksen, René Lynge (from 1 March)
Jensen, Peter Snoer
Jensen, Sussie Juul (until 31 January)
Jespersen, Kim G. (from 1 February)
Korsholm, Søren Bang
Lodahl, Peter (until 30 September)
Lomholt, Sune (until 27 August)
Nikolajsen, Thomas (until 31 January)
Okkels, Fridolin
Thrane, Lars (until 31 August)

Industrial PhD Students

Kitchen, Steven R.
Linnebjerg, Christian

Technical Staff

Andersen, Finn
Eilertsen, Erik
Eliasen, Finn (from 1 October)
Hansen, Bengt Hurup (until 31 March)
Jessen, Martin
Nordskov, Arne
Pedersen, Finn (from 1 June)
Petersen, Torben D.
Rasmussen, Erling
Sass, Bjarne
Stubager, Jørgen
Thorsen, Jess

Apprentice

Pedersen, Søren Peo (from 1 February)

Secretaries

Astradsson, Lone
Carlsen, Heidi
Skaarup, Bitten

Students Working for the Master's Degree

Andersen, Eva Samsøe (until 31 July)
Christensen, Bo Toftmann (until 15 April)
Holmelund, Evy (until 8 December)
Sundstrøm, Martin (until 31 August)

Guest Scientists

Backlund, Johan, Chalmers Tekniska Högskola, Sweden
Benilov, Eygene S., University of Limerick, Ireland
Doggett, Brendan, Trinity College, Dublin, Ireland
Helgert, Michael, Friedrich Schiller University Jena, Germany
Hesthaven, Jan, Brown University, Rhode Island, USA
Keredes, Arpad, The Technical University of Budapest, Hungary
Klapshina, Larisa G., Razuvaev Institute of Organometallic Chemistry of RAS, Russia
Podivilov, Evgeny, Institute of Automation and Electrometry, Russia
Popov, Ivan, Research Centre "Vavilov Optical Institute", Russia
Ruban, Victor P., Landau Institute for Theoretical Physics, Russia
Scott, Bruce, IPP-Garching, Germany
Sturman, Boris I., International Institute for Nonlinear Studies, Novosibirsk, Russia
Wyller, John, Agricultural University of Norway, Norway
Yura, Harold T., The Aerospace Corporation, Los Angeles, USA

Short-term Visitors

Anderson, Johan, Chalmers University of Technology, Sweden
Annibaldi, Silvia Valeria, School of Cosmic Physics, Dublin Institute for Advanced Studies, Ireland
Babka, Robert, Czestochowa University, Poland
Baran, Janusz, Czestochowa University, Poland
Bardenshtein, Alexander, Institute of High Current Electronics, Russia
Bergé, Luc, Commissariat à l'Energie Atomique, Centre d'Etudes de Limeil-Valenton, France
Block, Dietmar, Christian Albrechts Universität zu Kiel, Germany
Dudzig, Sebastian, Czestochowa University, Poland
Germaschewski, Kai, University of Düsseldorf, Germany
Girard, Frederic, Trinity College, Dublin, Ireland
Gloria, Falchetto, Centre de Recherches en Physique des Plasmas, Switzerland
Grauer, Rainer, University of Düsseldorf, Germany
Hopkins, Mike, Scientific Systems Ltd., Dublin, Ireland
Ivonin, Igor, Uppsala University, Sweden
Klinger, Thomas, Greifswald University, Germany
Kontar, Eduard P., University of Oslo, Norway
Lunney, James G., Trinity College, Dublin, Ireland
Minkina, Waldemar, Czestochowa University, Poland
Moestam, Robert, Chalmers University of Technology, Sweden
O'Neil, Tom, University of California, USA
Pavlenko, Vladimir, Uppsala University, Sweden
Pécseli, Hans, University of Oslo, Norway
Raymer, Michael G., University of Oregon, USA
Saffman, Mark, University of Wisconsin-Madison, USA
Schröder, Christiane, Greifswald University, Germany
Senchenko, Sergey, University of Uppsala, Sweden

Title and authors

Optics and Fluid Dynamics Department
Annual Progress Report for 2000

Edited by S.G. Hanson, P.M. Johansen, J.P. Lynov and B. Skaarup

ISBN	ISSN
87-550-2794-6 (Internet)	0106-2840; 0906-1797

Department or group	Date
Optics and Fluid Dynamics Department	May 2001

Pages	Tables	Illustrations	References
99	1	66	65

Abstract (max. 2000 characters)

The Optics and Fluid Dynamics Department performs basic and applied research within three scientific programmes: (1) optical materials, (2) optical diagnostics and information processing and (3) plasma and fluid dynamics. The department has core competences in: optical sensors, optical materials, optical storage, biooptics, numerical modelling and information processing, non-linear dynamics and fusion plasma physics. The research is supported by several EU programmes, including EURATOM, by Danish research councils and by industry. A summary of the activities in 2000 is presented.

Descriptors INIS/EDB

DYNAMICS; FLUIDS; LASERS; NONLINEAR OPTICS; NONLINEAR PROBLEMS; NUMERICAL SOLUTION; PLASMA; PROGRESS REPORT; RESEARCH PROGRAMMES; RISOE NATIONAL LABORATORY; THERMONUCLEAR REACTIONS